

VISUAL RECEPTORS

TU-PM-F1 CONCAVALIN A BINDING SITES OF ROD MEMBRANES.

A.J. Adams* and H. Shichi, National Eye Institute, National Institutes of Health, Bethesda, Maryland 20014

Rhodopsin is the major glycoprotein in the disk and plasma membranes of rod photoreceptors. Its binding to concanavalin A (conA) can be used to study the localization and orientation of rhodopsin in these membranes. Although there is general agreement that conA binding sites are on the external surface of the rod outer segment (ROS) plasma membrane, their location in the disk membrane is still uncertain. To resolve the question we have carefully prepared bovine disks: ROS were isolated in a metrizamide gradient and the disks were prepared in 5% Ficoll. Vit. E was present throughout the procedure. In the absence of metrizamide and Ficoll, intact ROS bind conA but the disks do not. The disks, if frozen and thawed, collapse in size and become capable of binding conA. The results indicate that while the conA binding sites of the plasma membrane are on the external surface, those of the disk are on the internal (intradiscal) surface. This is consistent with the view that the disks are formed by the infolding of the plasma membrane. The results also suggest an asymmetric distribution of rhodopsin oligosaccharide moieties in the membranes.

TU-PM-F2 DETERMINATION OF THE RETINAL/PROTEIN RATIOS FOR THE PURPLE MEMBRANE FROM HALOBACTERIUM HALOBIIUM AND HALOBACTERIUM CUTIRUBRUM, G.K. Papadopoulos, T.L. Hsiao, and J.Y. Cassim, Department of Biophysics, The Ohio State University, Columbus, Ohio, 43210

Published values of retinal/protein ratios of purple membranes from halobacteria are confusing. For *H. halobium* values of approximately 1.00 and 0.45 and for *H. cutirubrum* values of 0.45 and 0.43 have been reported. A redetermination of these ratios in our hands has yielded values of 0.98 ± 0.01 and 0.99 ± 0.01 for the membranes of *H. halobium* and *H. cutirubrum* respectively. These values are in accord with expectations that the ratio be the same for the two species since the similarity of their membrane structure has been established. Furthermore, such a value would fulfill the requirement that every apoprotein molecule be complexed with a retinal since the uniqueness and equivalence of the membrane holoprotein, bacteriorhodopsin, has been demonstrated.

TU-PM-F3 ABSORPTION SPECTRA OF THE PURPLE MEMBRANE PHOTOCYCLE INTERMEDIATES: EVIDENCE OF PROTEIN CONFORMATIONAL CHANGE. B. Becher and T.G. Ebrey, University of Illinois, Urbana, Illinois 61801.

The visible and ultraviolet absorption spectra of purple membrane and the K, L, and M photocycle intermediates are reported. Their visible spectra (λ_{\max} =568, 628, 547, and 412 nm) strongly suggest that the Schiff base bond between retinal and the membrane protein is protonated in PM, K, and L but not in M. Their ultraviolet spectra can be attributed to individual amino acids, to retinal, and to environmental effects on the amino acid transitions. Large changes in the near-ultraviolet spectra occur on conversion to L and M and on bleaching in hydroxylamine; their difference spectra have the shape of the protein spectrum itself. Decreasing the polarity of the membrane environment decreases the extinction changes. These results indicate that the equivalent of ca.60% of the tryptophans and tyrosines in the protein move from a hydrophobic (interior) environment to a hydrophilic (exterior) environment on bleaching or on conversion to L or M. These conformational changes may well be involved in proton transport across the purple membrane on illumination.

TU-PM-F4 PROTON MOVEMENT REVERSAL ACCOMPANIES PHOTOPIGMENT REVERSAL IN FROG ROD DISK MEMBRANES (FRDM). Y. Ching and P. A. Liebman, Bell Laboratories, Murray Hill, NJ and Department of Anatomy, University of Pennsylvania, Philadelphia, PA.

Orange flash bleaching of FRDM suspensions yields fast H^+ (milliseconds) uptake followed by slow H^+ release ($t_{1/2} \sim 3$ sec. at RT and PH 6.1) with stoichiometry of $2H^+$ /Bleached rhodopsin. Blue light flashes soon after formation of metarhodopsin II cause fast H^+ release followed by slow H^+ uptake which looks like mirror image of the bleaching effect. Accompanying increase in 500 nm absorption with blue flashes suggests that we may be seeing recovery of proton dissociating groups with rhodopsin regeneration. If all 500 nm increase is due to rhodopsin, the recovery displays the same stoichiometry as the bleach ($2H^+$ /rhod.). We interpret these effects to probe a reversible fast conformational step associated with the chromophore which then leads to a slow conformation change elsewhere in the molecule. Supported by Bell Laboratories and NIH grant EY00012.

TU-PM-F5 FAST CONTINUOUS MONITOR OF ROD PHOSPHODIESTERASE (PDE): ACTIVATION LATENCY. P. A. Liebman and R. Yee University of Pennsylvania, Philadelphia, PA 19104.

A previous Biophysics Abstract (1976) by one of us initially mistook rapid light and cyclic nucleotide (cG) induced Arsenazo III responses in rod disk membrane (RDM) suspensions to detect Ca^{++} release and Mg^{++} binding. cG responses turned out to be attenuated by H^+ buffers and were due to cG hydrolysis. Subsequent rate studies using H^+ dyes or a recording pH meter showed that RDM-PDE was being directly studied (K_m , V_{max} , Mg^{++} , ATP or GTP requirement, pH optimum, cG > cA preference, inhibitor effect, purified enzyme activity all confirmed earlier work). We now find that the frog RDM-PDE system is switched to maximal activity within milliseconds of a light flash and could clear a single rat interdisk space of cG within a fraction of a second. While this speed is in the range for both visual excitation and adaptation, fast turnover and the implied presence of cG-controlled phosphoproteins (that could bind Ca^{++}) raise the possibility that intracellular Ca^{++} might need only act "passively" to seem like a transmitter in visual transduction. Supported by NEI grant EY 00012. R.Y. is a trainee of the Medical Scientist Training Program (GM 02046).

TU-PM-F6 ROD OUTER SEGMENT PHOSPHODIESTERASE: KINETICS & PARAMETERS OF ACTIVATION AND DEACTIVATION. R. Yee and P. A. Liebman, Univ. of Pennsylvania, Philadelphia, PA 19104

The light activated, nucleoside triphosphate dependent phosphodiesterase of the rod outer segment has been studied in disc suspensions by continuous kinetic monitor. In the dark, hydrolytic activity is low and does not increase in proportion to the quantity of membranes assayed whereas light stimulated activity is linear with membranes assayed. Activity ratio (light/dark) is 66 (frog) and 240 (bovine) by direct assay; at physiologic concentrations, activity ratio is 10^4 - 10^5 . Activation can be seen with light bleaches of $1/10^7$, is linear with light intensity and saturates hyperbolically; bleaches of $1/80,000$ yield 50% activation. Kinetic analysis shows that activation is zero-order and that in vitro deactivation (spontaneous) is an apparent first-order process associated with loss of GTP. ITP ($0.3 \mu\text{M}$) is 3x less effective in activating phosphodiesterase. Others are $>100\text{x}$ less effective (XTP > ATP > CTP > UTP > β, γ CH_2 -GTP > AMP-PNP > α, β CH_2 -ATP). The results suggest a multiplier mechanism whereby a molecule of bleached rhodopsin serially activates 10 - 100 phosphodiesterase molecules. The high gain of the enzyme suggests a role in visual excitation. Support: NIH grant GM 02046 & EY 00012.

TU-PM-F7 ANALYSIS OF LIGHT-INDUCED CURRENT FLUCTUATIONS IN VENTRAL PHOTORECEPTORS OF LIMULUS. Fulton Wong, * Biological Sciences, Purdue Univ, W. Lafayette, IN and Rockefeller Univ, NY, NY (intr. by Michael G. Rossmann)

The "noisy" response of the ventral photoreceptor to light is composed of many small, discrete, transitory increases of membrane conductance, "bumps." The power spectrum obtained from the light-induced current fluctuations measured under voltage clamp, which reflects the shape and size of the bumps, can be fitted well with an equation of the form

$$\frac{A}{(1 + 4\pi^2 f^2 \tau^2)^m}$$

At a rate of about 3 bumps/sec, the values for m and τ are found to be 3 and 12.45 ± 1.53 ms respectively. The conductance due to a single bump is estimated to be $\approx 10^{-8}\text{S}$. At $> 10^5$ bumps/sec, the conductance increase due to a single bump is $\approx 10^{-11}\text{S}$ and the shape of the power spectrum approaches that of a Lorentzian ($\tau \approx 16$ ms). Lowering the external calcium ion concentration increases the conductance of the bumps but it does not change significantly the shape or the rate of the bumps. If each bump is made up of many channels similar to those found in other excitable membranes, the results presented here suggest a cooperative mechanism for the many channels associated with a single bump.

TU-PM-F8 POST STIMULUS INCREASE OF DISCRETE WAVE FREQUENCY IN LIMULUS PHOTORECEPTORS. M. Hanani* and A. Fein Marine Biological Laboratories, Woods Hole, Mass. 02543.

Intracellular recordings from some invertebrate photoreceptors show two types of discrete potential waves (bumps); those which occur during light (quantum bumps) and spontaneous bumps that occur in the dark. The amplitude of both types diminishes after an adapting light. We investigated the effects of adapting lights on the bumps of the Limulus ventral eye, using both voltage clamped and unclamped photoreceptors. In the dark, after a bright flash, there was a large increase in membrane noise which could be resolved into discrete bumps. Both the increase in the bump frequency and the duration of the increase were graded with intensity over a range of 2.5 log units. At its peak the frequency can increase by about a hundred-fold compared to its dark value. The recovery had a time course of several minutes. The sensitivity to light was measured after a stimulus that increased the bump frequency. Higher bump rate was observed while the cell was still desensitized. Lowering the temperature from 20°C to 13°C decreased the spontaneous bump frequency and also greatly reduced the light induced dark noise.

TU-PM-F9 A DIFFUSION-BASED MODEL OF PHOTORECEPTION.

S. Yasui,* M. C. Andresen,* and A. M. Brown, University of Texas Medical Branch, Galveston, Texas 77550

Photoresponse waveforms have similar shapes in a great variety of photoreceptors but have durations that may differ 1,000 fold. Internal transmitter models based on chemical reactions alone are unlikely to encompass this range of durations and are not completely satisfactory even for small cells in which diffusion distances are short. In large photoreceptors diffusion might dominate the response waveform and we have tested this notion in large photoresponsive neurons of Aplysia. Here photons are absorbed by membrane-bound pigmented cytoplasmic organelles and Ca^{2+} , the putative internal transmitter is released. Ca^{2+} then diffuses to the plasma membrane where it activates a K^+ conductance causing hyperpolarization. Diffusion is slowed by irreversible binding to cytoplasmic sites and Ca^{2+} levels are restored by irreversible uptake processes. Chemical reactions are assumed to be instantaneous with respect to duration of the photoresponse. The model predicts the experimental response waveforms produced by impulses and steps of light with various background intensities.

TU-PM-F10 LIPOSOMES BEARING 11-cis RETINAL CAUSE PERFUSED ISOLATED RAT RETINAS TO REGENERATE VISUAL PIGMENTS.

G.N. Noll and S. Yoshikami, Laboratory of Vision Research, National Eye Institute, NIH, Bethesda, Md. 20014.

A perfused, isolated rat retina can respond electrically to light for many hours, but by itself cannot regenerate the light bleached visual pigment. The addition to the perfusate of unilamellar liposomes made by sonicating a mixture of dioleoyl lecithin and 11-cis retinal in Ringers, starts synthesis of visual pigment in the bleached retina immediately. The regeneration kinetics is zero order initially with 50% regenerated in 14 minutes, when 6600 moles of retinal:mole of opsin were used. The rate decreases as regeneration nears completion. Rhodopsin can also be regenerated in perfused frog retinas by this method. Isorhodopsin is formed from added 9-cis retinal. Unlike frog retinas, rat retinas cannot oxidize added 11-cis retinol for pigment synthesis.

The transfer of retinal does not appear to involve vesicle fusion with the cell membrane since large multilamellar liposomes ($>0.2 \mu\text{m}$) can transfer retinal effectively to retinas treated with metabolic inhibitors.

TU-PM-F11 INTRACELLULAR INJECTION OF H^+ AND HCO_3^- IN BALANUS PHOTORECEPTOR. H. Mack Brown and R.W. Meech*, Dept. of Physiology, Univ. of Utah, Salt Lake City, UT, 84108; ARC Unit of Invertebrate Physiology, Cambridge Univ., England.

A dark-adapted Balanus photoreceptor acidifies approximately 0.2 pH unit during illumination. The functional consequence of this pH change was investigated by intracellular injection of HCO_3^- and H^+ by pressure and inter-barrel iontophoresis. An injection of acid could reduce the receptor potential by as much as 33%. On the other hand, HCO_3^- injection augmented the receptor potential. Replacement of Tris saline (pH 7.5) with CO_2 - HCO_3^- (pH 7.5), produced a slow biphasic change in pH. Upon return to Tris saline, the pH underwent a rapid alkalization that required more than an hour to recover to the control level. During this time the amplitude of the receptor potential varied in a linear fashion with pH. Intracellular pH changes could participate in setting the level of light sensitivity.

TU-PM-F12A NEW COLOR VISION MODEL, INCLUDING COLORBLINDNESS. R. D. McLeod, University of Lowell, Lowell, MA 01854.

The hypothesis that two quasi-monochromatic focal intervals are retinally coincident with rod and cone outer segments implies a theory of color vision. Such a model predicts that full color vision must be possible, using only two narrow and nearly overlapping wavelength intervals. This model predicts Land's early color vision results. It enables the identification of his complementary color generation upon "long" and "short" record reversal with a "Psychophysical Phenomenon" -- "subjectively" generating a "normal" flag against a plain light background after first staring at a "complementary flag": blue and black stripes with black stars upon a yellow field. The model can explain colorblindness of all types.

RED CELL MEMBRANES

TU-PM-F13 DIFFRACTION PATTERNS AND A THEORY OF VISION. Roger D. McLeod, University of Lowell, Lowell, MA 01854

Certain phenomena physically distinguish against vision by inverted incoherent images against the retina. Interference effects can be visually and directly perceived from diverse light sources. This implies that vision is mediated by two quasi-monochromatic wavelength intervals focally coincident with rod and cone ends. Pincushion "illusion" and its complement are optically and analytically explainable as field amplitude excitation at the focal or retinal surface. This contradicts the conventional theory of vision.

TU-PM-G1 TEMPERATURE DEPENDENCE OF RED CELL MEMBRANE ELASTIC CONSTANTS. R. Waugh, and E.A. Evans, Duke University, Durham, North Carolina 27706

Two constants have been defined which completely describe the surface elastic behavior of a membrane. The area compressibility modulus, K , is a measure of the resistance to changes in area; the elastic shear modulus, μ , is a measure of the resistance to in-plane extension at constant area. Values for these moduli at room temperature have been obtained previously: $K(25^\circ) \approx 450$ dyn/cm, and $\mu(25^\circ) \approx 10^{-2}$ dyn/cm. Using micropipettes, the temperature dependence of these moduli over the range $50-45^\circ\text{C}$ has been measured. Both moduli vary approximately linearly over this range. The slopes as determined by linear regression are: $dK/dT = -6.0$ dyn/cm $^\circ\text{C}$ and $d\mu/dT = -6.3 \times 10^{-3}$ dyn/cm $^\circ\text{C}$. The fact that the elastic moduli decrease with increasing temperature indicates that the entropy of the system increases with both extension and area dilation, and that the main mechanism of elastic energy storage is energetic; e.g. hyperelastic extension (at constant surface density) produces an increase in internal energy density per unit extension of 2.5×10^{-2} ergs/cm 2 and an increase in configurational entropy density of 6.3×10^{-5} ergs/ $^\circ\text{C}$ -cm 2 .

TU-PM-F14 CARBOHYDRATE CONTENT OF FROG ROD OUTER SEGMENTS R.E. Drzymala and P.A. Lieberman, University of Pennsylvania, Philadelphia, Pennsylvania 19104

After sulfonation of its vicinal hydroxyl groups by peroxidation and subsequent bisulfite addition, polysaccharide backbone binds toluidine blue (ABT staining) with a concurrent metachromatic shift of the dye's (monomer) absorption peak from 620 nm to 575 nm (dimer interaction at vicinal sulfonate groups) or 540 nm (dye multimer interaction). Spectrophotometry of ABT stained aqueous hyaluronic acid (HA) shows a broad absorption which obeys Beer's law for dye concentration between 0 and 3×10^{-3} M giving molar absorptivity of 2023 ± 278 at 540 nm. Microspectrophotometry of ABT stained frog rod outer segments (FROS) showed a spectrum similar to stained aqueous HA with an absorbance value corresponding to 0.5 M bound dye at saturation. Given two dye molecules bound per sugar residue and rhodopsin concentration 3 mM in FROS, the above indicates 80 sugars per rhodopsin are contained in these cells. Both dichroism and birefringence indicate weak transverse dye orientation which may belie net axial polysaccharide chain order. We thank Prof. Gy. Romhányi, Pecs, Hungary for providing slides of ABT stained FROS. Supported by: NIH grants EY00012 & EY07035.

TU-PM-G2 THERMOELASTICITY OF RED CELL MEMBRANE. E.A. Evans and R. Waugh, Duke University, Durham, N.C. 27706

Thermoelastic experiments provide data for decomposition of membrane elastic free energy storage into internal energy and configuration entropy contributions. Coupled with the thermal area expansivity, these data also give the reversible heat of expansion, which is a direct assessment of the thermal repulsive forces in the membrane. In equilibrium, the thermal repulsive forces are balanced by the hydrophobic interaction between the aqueous environment and the membrane surface. The necessary measurements are the temperature dependence of the membrane area compressibility modulus plus the fractional change in membrane surface area with temperature (the thermal area expansivity). Recent data on human red blood cells have shown that the area compressibility modulus for the red cell membrane is 600-300 dyn/cm over the range of $0^\circ-50^\circ\text{C}$. The thermal area expansivity has been measured to be $1.2 \times 10^{-3}/^\circ\text{C}$ for the red cell membrane. Therefore the heat of expansion per unit area is given by the limits 200-110 ergs/cm 2 for 0°C to 50°C . The heat of expansion at 50°C is the same value as that anticipated for a lipid bilayer idealized as twice the behavior of a monolayer at an oil-water interface.

TU-PM-G3 ERYTHROCYTE SHAPE AND MEMBRANE ASYMMETRY CHANGES IN RESPONSE TO SERUM ALBUMIN. A.W.L. Jay, Faculty of Medicine, The University of Calgary, Calgary, Alberta, Canada T2N 1N4.

Previous study (Jay, *Biophys. J.* 15: 205, 1975) showed that serum albumin stabilizes erythrocyte geometry and induces stomatocyte shape. This shape change suggests changes in the total curvature and membrane symmetry. In this study, membrane "asymmetry ratio" is calculated as the ratio of the outside-to-inside membrane areas. Profiles of human red cells were analyzed by computer as reported in the previous study. The computer program was modified to generate an outside and an inside membrane surface. The ratio of the two surfaces is calculated. The membrane thickness can be varied. Statistical results show that the normal cell shape has an "asymmetry ratio" greater than unity. In the presence of serum albumin, the cell shape changes are associated with a change in "asymmetry ratio". Distributions of "asymmetry ratio" are given. Correlation between "asymmetry ratio" and various geometrical parameters are studied.

Supported by the Canadian and Alberta Heart Foundations.

TU-PM-G4 TOTAL CURVATURE OF BICONCAVE AND CUP-SHAPED HUMAN ERYTHROCYTES. P.B. Canham and A.W.L. Jay. Dept. of Biophysics, Univ. of Western Ontario, London, Canada, and Division of Medical Biophysics, Univ. of Calgary, Calgary, Canada.

Cross-sectional profiles were obtained by making photomicrographs of individual cells hanging on edge, as described by Ponder (1). Biconcave and cup-shaped erythrocytes have been treated as surfaces of revolution. The curvatures of cells were calculated by summing the squares of the principal curvatures over the surface of each cell. Cup-shaped cells were interpreted to have a metastable shape, a shape which is more prevalent in Ringer with albumin (e.g. for one subject the curvature of cup cells was 4.3 ± 0.5 (S.D.) compared to 3.6 ± 0.4 (S.D.) for biconcave cells). Flat-sided cells have more total curvature than cup or biconcave cells.

(1) Ponder, E. (1930). *Q. Jl. exp. Physiol.* 20: 29.

Supported by the Canadian, Alberta and Ontario Heart Foundations.

TU-PM-G5 INHIBITION OF MEMBRANE STIFFENING IN HUMAN ERYTHROCYTES. G. E. Siefring, Jr.,* L. Lowe-Krentz,* K. N. Parameswaran,* and L. Lorand,* Dept. Biochem. & Molec. Biol., Northwestern Univ., Evanston, Ill. and B. Smith* and P. LaCelle,* Dept. Rad. Biol. & Biophys., U. Rochester, Rochester, N.Y. (Intr. by I. M. Klotz)

Increase of intracellular $[Ca^{2+}]$ to ca. 0.3 mM (10-20 μ M ionophore A23187) in red cells produces γ -glu-e-lys crosslinks in membrane protein polymers ($M_w > 10^6$). Crosslinking affects internal membrane proteins (4.1, spectrin and 3) and is mediated by Ca^{2+} -regulated transglutaminase (Lorand et al., *PNAS*, 73, 4479, 1976). Primary amines (cystamine, aminoacetonitrile, glycine methylester or histamine), competing against ϵ -lysine crosslinking groups, inhibit polymerization of membrane proteins in intact red cells. Amines also prevent the Ca^{2+} -induced shape change to echinocyte from becoming irreversible (tested for aminoacetonitrile using SEM) and inhibit the loss of membrane deformability (tested for histamine using the "micropipette" method). Thus loss of membrane deformability and irreversible fixing of shape changes in red cells, due to accumulation of Ca^{2+} , seem to be related to the enzymic formation of γ -glu-e-lys crosslinks in membrane protein polymers.

TU-PM-G6 EFFECT OF pH AND OSMOLARITY ON NORMAL AND HS ERYTHROCYTE MEMBRANES. B. Smith*, and P. LaCelle. U. Rochester, Rochester, NY 14642

Acid pH and hypertonicity may influence red cell rheology by effects on both the extrinsic parameter of relative sphericity and membrane protein interactions. This study examines the contribution of altered membrane elasticity to rheology of normal erythrocytes and hereditary spherocytes (HS) in low pH and hyperosmolar conditions. Hypertonicity reduces cell volume to allow comparison of membrane effects in relatively spherical HS cells with control membranes. Portions of normal and HS membranes in hypertonic and acidic buffers were stressed by aspiration in 1.0 μ m pipettes at standard forces. HS membrane response is 56% of control at 300 mosm vs 57% of control with both in 600 mosm buffer; 65% of control with HS in 600 mosm and control in 300 mosm. Normal and HS erythrocytes demonstrate abrupt reduction in membrane deformability below pH 5.0, corresponding to the pH of spectrin aggregation. HS extensibility, 56% of control at pH 7.4 approaches control below pH 5.0. Thus membrane extensibility is affected by low pH in normal and HS erythrocytes and the HS membrane defect, evident at pH 7.4, is not dominant at low pH when maximal spectrin aggregation occurs.

TU-PM-G7 ISOTONICITY AND RED CELL-MEMBRANE DEFORMABILITY. H.C. Mel and D.G. Jung, Div. of Med. Physics and Donner Lab., LBL, Univ. of Calif., Berkeley, CA 94720.

The common view of isotonicity for a cell is as the "physiological" condition of osmotic solute-water balance between intra- and extra-cellular aqueous media. The typical response of red cell (RBC) properties (e.g. volume, form, solute concentration) to changes in solution osmotic pressure is continuous and monotonic in character. In contrast, the cellular property of deformability has been found by several methods to be substantially reduced in extreme high or low tonicities, though little clear or unambiguous information has been available for the near-isotonic region. We have applied to this problem the relatively new technique "resistive pulse spectroscopy," RPS (Mel and Yee, *Blood Cells* 1, 191, 1975), with the following result: a maximum occurs in the curve of RPS-deformability vs. osmotic pressure in the region between 270 and 290 mosm, the region closest to isotonic. Thus, another view of isotonicity is that it is the condition which insures an optimum in the rheological property of deformability—a property essential for the RBC normal survival and function, including smooth passage through the limiting spaces of the microcirculation. (Supported, in part, by DOE).

TU-PM-G8 DEFORMABILITY OF HUMAN FETAL ERYTHROCYTES (RBCs) IN A PRESSURE (P)-FLOW (Q) CELL FILTRATION SYSTEM. J. Kurantsin-Mills* and L.S. Lessin* (Intr. by Marie M. Cassidy) Depts. of Physiol. & Med., The George Washington Univ. Med. Cntr., Washington, D.C. 20037

To simulate RBC deformation in capillaries and assess adult/fetal RBC deformability (1/Rr) we have utilized a cell filtration system (CFS) (*Blood Cells* 3, 241, 1977) to determine 1/Rr at flow rates (Q) of 0.035 to 14.1 ml/min. Resistance to flow of 0.2% cell suspension (Rs) and medium (Rm)=P/Q and relative resistance, Rr=Rs/Rm. Among other factors, Rr depends on Q, filter pore size & complex shear conditions in the CFS. Using 3 μ m Nuclepore filters in the CFS, fetal cells show 2-5 fold greater Rr at Q=0.35, 0.71, 1.77 & 3.53 ml/min than adult cells. With 5 μ m filters, the Rr's are similar. Plots of Rr vs Q simulate viscometric curves. ATP depletion increases Rr 2-3 fold, and also cellular Ca^{++} . Crosslinking membrane neighbor proteins with glutaraldehyde (0.5mM) or diamide (5mM), as evidenced by SDS-gel electrophoresis, increases Rr 2-fold at low Q. Scanning electron microscopy of cells fixed in flow reveals the dynamics of cell deformation. The mechanisms underlying the difference in 1/Rr of the two cell types may be related to membrane protein interactions.

TU-PM-G9 NON-EQUILIBRIUM COOPERATIVE MODEL WITH APPLICATION TO BIOMEMBRANE RUPTURE. J. E. Krizan, U. of Vermont and A. R. Williams, U. of Manchester.*

A mean field non-equilibrium approximation for the Ising model with an external field is described.¹ Defining a critical shear for the case of biomembrane rupture under stress the two-state transition model describes well the behavior of the critical shear threshold as a function of temperature in comparison with experimental curves, for different time trials. An important assumption is that the shear threshold is proportional to the order parameter, on the given time scale (relaxation times of the order of minutes) an asymptotic non-zero critical stress is defined; however, it is conceivable that (solid-like) creep behavior over much longer times could reveal possible limitations of this assumption.

*Supported partially by NIH PHS RO1 08209.

¹J. E. Krizan and A. R. Williams, *Colloid Phen.* **2**, 229 (1977).

TU-PM-G10 BOUNDARY EFFECTS IN CAPPING OF MEMBRANE RECEPTORS. N. Gershon, Johns Hopkins U., Baltimore, MD 21218

Crosslinking of membranes surface receptors may lead to their segregation into patches and then into a single large aggregate at one pole of the cell. In the case that the membrane is a supersaturated solution of the receptors, the crosslinking agent might form stable patches which can grow by the precipitation of the remaining dissolved receptors. Comparison with experimental data, numerical estimates, interactions of receptors with the cytoskeleton and possible effects of capping inhibitors are discussed.

TU-PM-G12 CHLORTETRACYCLINE FLUORESCENCE AS A PROBE OF MEMBRANE BOUND CALCIUM. A. S. Schneider, R. Herz,* and M. Sonenberg, Sloan-Kettering Inst., New York, N.Y. 10021

Chlortetracycline (CTC) is a highly sensitive fluorescent probe of membrane bound calcium and is known to accumulate in tumors and bone. CTC can also provide a topographical probe of cell surface calcium and possibly phospholipid sites. We have characterized the interaction of the CTC-Ca chelate with human red cell membranes in terms of: 1) the specific membrane sites monitored by the probe, 2) the sensitivity of the fluorescent response to cation concentration, 3) the CTC-Ca chelate binding to the membrane and the role of Ca as binding linkage, 4) the effect of membrane modification by neuraminidase, trypsin, and phospholipase C on CTC-Ca binding and fluorescence and 5) circular dichroism of CTC as a function of cations, membranes and polarity of the environment. The results indicate that the membrane Ca sites monitored by the probe are lipid phosphate head groups and suggest a mechanism of transport of the tetracycline antibiotics across plasma membrane into the cell. (Supported in part by NSF grant PCM76 04079, NIH grants CA15773, CA18759, CA08748. A.S.S. is a recipient of an Established Investigatorship from the American Heart Association)

TU-PM-G13 PROTEIN-LIGAND-ERYTHROCYTE STOICHIOMETRY FROM PONDER'S METHOD. R. E. Lovrien, G. Hart*, and R. A. Anderson*, Biochemistry Department, University of Minnesota, St. Paul, MN 55108

The easily monitored erythrocyte reaction, Discocyte \pm Echinocyte, is driven right by echinocytic ligands, and driven left by ligand binding proteins. The morphology conversion may be used as an indicator in the titration of proteins vs echinocytic ligands, which was first described by Ponder (*Hemolysis and Related Phenomena* p. 39, (1948)). For aliphatic anions and serum albumin, the stoichiometries in our work were found to be 5 to 12 ligands/protein molecule. The foregoing, wherein protein-cell interactions are relatively unimportant, with reactions which are rapid and completely reversible, are called "Ponder titrations of the first kind". A quite different class of reactions, which may be called "Ponder titrations of the second kind", involve the cell surface specific proteins, lectins. They confer a remarkable stabilization of the discocyte against echinocytic ligands, and yield information concerning cell surface coverage fractions, normal vs. dysfunctional membranes, and certain rate phenomena. Ponder titrations are easy to carry out, require only μ liter volumes of materials, and quite simple equipment.

TU-PM-G11 HUMAN RED CELL (RBC) MEMBRANE ALTERATIONS PRODUCED BY VIBRIO CHOLERAE NEURAMINIDASE (VCN). F. Nordt, R. J. Knox and G. V. F. Seaman, Dept. Neurology, UOHS, Portland, OR 97201

It is generally assumed that VCN treatment only removes sialic acid (NANA) from RBC surfaces. We have observed that incubation of RBC for 1 hr @ 37°C with 1.5-360 Behringwerke Units (BU) of VCN/ 10^{10} RBC releases 80-100% of the NANA for >14 BU VCN/ 10^{10} RBC with concomitant decreases in electrophoretic mobility (u). Formaldehyde (HCHO) treatment of desialylated RBC increases their u from <0.1 to ~ 0.4 $\mu\text{m sec}^{-1}$ V^{-1} cm at pH 7.4 in 0.15 M NaCl. The pH vs. u profile for HCHO-desialylated RBC displays an isoelectric point at higher pH than control HCHO-RBC and the appearance of an upward inflection in the pH 10-11 region is suggestive of positive surface groups. Thus after desialylation with VCN, the RBC are no longer polyanionic as expected for simple NANA removal. VCN adsorption is not a plausible explanation since 14 BU/ 10^{10} RBC corresponds to only ~ 200 molecules per RBC. Recovery of VCN from the bulk medium and the unexpected u properties of VCN treated RBC indicates that removal of NANA is not the only result of VCN treatment. Thus caution should be exercised in interpreting membrane studies involving VCN digestion. NIH Grant HL 18284

TU-PM-G14 CYTOCHALASIN B BINDING PROTEINS IN HUMAN ERYTHROCYTE MEMBRANES: MODULATION OF GLUCOSE SENSITIVITY BY SITE INTERACTION. H. Pinkofsky*, M. Cowden, and C. Jung, Department of Biophysical Sciences, SUNY, Buffalo, New York 14215.

We have previously described three different cytochalasin B binding sites in human erythrocyte membranes, a D-glucose-sensitive site (site I), a cytochalasin E-sensitive site (site II), and a site (site III) insensitive to both D-glucose and cytochalasin E (Jung and Rampal, *J. Biol. Chem.* **252**, 5456, 1977). The displacement of cytochalasin B in the presence of D-glucose plus cytochalasin E greatly exceeds the sum of their independent displacements, indicating that when site II is liganded site III becomes glucose-sensitive. The ghosts extracted with EDTA or 2,3-dimethylmaleic anhydride retain only site I and III activities, both of which are displaceable by D-glucose alone indicating that the removal of site II confers glucose-sensitivity to site III. These results are consistent with a model that sites II and III exist in a close association through which unliganded site II maintains the glucose-insensitivity of site III, and once site II is liganded or removed by extraction this association is disrupted and site III becomes glucose sensitive. (Supported by NIH and VA Med. Research Funds)

TU-PM-G15 ACETYLCHOLINESTERASE (AChE) AND GLUTAMIC OXALO-ACETIC TRANSAMINASE (GOT) AS MARKERS OF RED CELL AGE? B. Voyda,* R.J. Knox, J. Lochner* and G.V.F. Seaman, Department of Neurology, UOHC, Portland, Oregon 97201

The reported decrease in activity of red cell enzymes such as AChE and GOT with increasing cell age has led to their use as markers of erythrocyte age. However, the enzyme levels are influenced by leukocytes, platelets and reticulocytes. By removal of varying amounts of buffy coat it has been established that the leukocyte activity was insufficient to influence red cell AChE or GOT values. Removal of leukocytes and platelets by cotton wool columns resulted in increased enzyme activities apparently due to the preferential loss of old red cells as evidenced by the lack of response of GOT activity to pyridoxal phosphate. Density fractionated human erythrocytes still contain significant numbers of reticulocytes even in the dense RBC fractions. Currently the reticulocyte count and RNA content of red cell density fractions are being correlated with the levels of AChE and GOT in order to establish the contribution of reticulocytes to the apparent dependence of AChE and GOT activity on red cell age. Supported by NIH, Grant HL 18284.

TU-PM-G16 ERYTHROCYTE MEMBRANE AREA TRANSIENT INCREASE IN RESPONSE TO THIOUREA. A.T. Dypvik* and A.W.L. Jay, Faculty of Medicine, The University of Calgary, Calgary, Alberta, Canada T2N 1N4.

Thiourea increases the membrane area by an average of 22% during hemolysis (Jay, J. Physiol. 262: 447, 1976). The immediate crenation of red cells in response to addition of thiourea suggests that this increase occurs during the initial stages of thiourea penetration. In this study, the geometry of cells equilibrated in isotonic Ringer solution containing thiourea is analyzed. The cells crenated immediately but readily resumed the biconcave shape. Measurements show no increase in membrane area, suggesting that the area increase previously observed was transient. To study this transient area increase, cells were drawn into glass micropipettes of 2 μ m diameter (Jay, Biophys. J. 17: 164A, 1976). The cells assumed cylindrical symmetry, providing a calculation of area. Isotonic Ringer solution containing thiourea was added to the cell sample. Continued measurement of cells gave a statistical time-dependent measurement of area changes. Maximum area increase was observed within 100 s after addition of thiourea. Supported by the Canadian and Alberta Heart Foundations.

TU-PM-G17 QUATERNARY STRUCTURE OF THE HUMAN RED BLOOD CELL ANION TRANSPORT SYSTEM STUDIED WITH FLUORESCENCE ENERGY TRANSFER. A. J. Jesaitis, S. Dissing* and P. A. G. Fortes, Biology Dept., Univ. of California, San Diego, La Jolla, Ca. 92093.

The anion transport protein in purified membrane vesicles from human red cells (Wolosin et al, JBC 252:2419, '77) is labeled by the SH reagent fluorescein mercuric acetate. Maximum labeling is 1.3 mol FMA/mol 95K protein. We have measured self-energy transfer between bound FMA by fluorescence polarization (P). With excitation at 450-500 nm P decreases from 0.4, when less than half of the proteins are labeled, to 0.1 at saturation. This depolarization is not observed when the excitation is at the red edge of the absorption band (510-530 nm). Addition of 0.1% SDS changes P to 0.32, regardless of the degree of saturation with FMA and excitation wavelength. These results indicate that the labeled proteins are close enough to allow energy transfer between fluorophores ($R_0=35$ Å), which does not occur with red edge excitation or when the proteins are separated by SDS. We conclude that the 95K protein exists as a dimer or higher oligomer in these membranes. (Supported by USPHS grant HL-20-262, RR-08135, GM-07169 and the Danish Research Council).

TU-PM-G18 DIVERGENT RESPONSES OF YOUNG AND OLD RED CELLS TO HYPERTONIC MEDIA. R.J. Knox, C.F. Zukoski,* and G.V.F. Seaman, Dept. Neurology, UOHC, Portland, OR 97201

Attempts to describe alterations in RBC properties attending *in vivo* ageing led to using density gradients in centrifugal and, recently, electrophoretic (J. Lab. Clin. Med. 90:744, 1977) methods for separating cells of different ages. The apparent discrepancy between our report (Nature 269:719, 1977) of no difference in the electrophoretic mobilities of density fractionated RBC and the reported electrophoretic separation prompted studying the sedimentation rates (SR) of top and bottom 5% density fractions of human RBC in pH 7.4 hypotonic phosphate-buffered saline (184 mosm/Kg) containing 0 to 0.75 M sucrose. The SR's at 25°C diverged at [sucrose] >0.3 M with the top fraction sedimenting more slowly. No cell crenation was observed. This divergent behavior suggests that: a. cell separation on the basis of SR is enhanced by exposure to hyperosmotic media; b. the reported electrophoretic separation resulted from differences in SR rather than electrophoretic mobility; and c. cells of different *in vivo* age respond to different degrees in hyperosmotic media. Supported by NIH, Grant HL 18284.

LIPID BILAYERS II

TU-PM-H1 THEORETICAL MODEL OF BINARY MIXTURE PHOSPHO-LIPID BILAYER SYSTEMS. R.G. Priest and J.P. Sheridan*, Naval Research Laboratory, Washington, D.C. 20375

A dislocation type model for binary mixture phospholipid bilayers is presented. The two phospholipid species are assumed to differ only in alkyl chain length with differences of two, four and six carbons considered explicitly. The model has the analytic feature of reducing, in the infinite chain limit, to a form similar to that proposed by Nagle (J. Chem. Phys. 63, 1255 (1975)). The primary quantities calculated are the boundaries of the fluid-gel two phase region in the temperature-composition phase diagram. Data from single component systems is used to fit parameters in the model. The effect of chain length mismatch is taken into account both implicitly and explicitly. The implicit mechanism is that dependence of transition temperature on chain length in single component systems is reflected in the model parameters. The explicit mechanism is that the energy associated with the unavoidable vacancies in the binary mixture gel phase is included in the model. The experimental form of the phase diagram, as determined by the Raman technique, is in reasonable agreement with the theoretical results.

TU-PM-H2 LOSS OF TRANSMEMBRANE ASYMMETRY IN VESICLES: EFFECT OF PHOSPHOLIPID DEGRADATION PRODUCTS AS PERTURBANTS J.M. Shaw* and T.E. Thompson, Dept. of Biochemistry, University of Virginia, Charlottesville, Va. 22901

A purified exchange protein has been utilized to introduce $-N(CH_3)_3$ phosphatidylcholine (PC) from negatively charged vesicles (8 mol% glucuronosyl diacylglycerol) into the outer monolayer of $-N(CH_3)_3$ PC vesicles. Upon examination of the $-N(CH_3)_3$ PC vesicles by proton NMR in the presence of Pr^{3+} , the $-N(CH_3)_3$ PC signal was found to be present only in the outer monolayer and represented 61 to 73% of the outer monolayer PC. No transbilayer movement occurred during a 3 day period at 25° and the spontaneous movement of cholesterol from charged donor vesicles to the $-N(CH_3)_3$ PC acceptor vesicles did not affect the $-N(CH_3)_3$ PC asymmetry. After 5 days of incubation, the presence of $-N(CH_3)_3$ PC unavailable for interaction with Pr^{3+} was observed as well as the presence of phosphorus-containing breakdown products. Ratios of Pr^{3+} shifted to unshifted $-N(CH_3)_3$ signals were 2.1 for PC vesicles and 6.7 for PC vesicles containing 6 mol% cholesterol. Explanations for these results which include aggregation-fusion &/or rapid transbilayer movement will be discussed (Supported by USPHS grant GM14628 & fellowship GM05190).

TU-PM-H3 MEASUREMENTS OF WATER FLUIDITY IN MULTILAMELLAR DPPC-WATER SYSTEMS. W. K. Chan* and P. S. Pershan, Harvard Univ., Cambridge, MA 02138.

We describe experiments on the relaxation of water concentration inhomogeneities in aligned multilamellar dipalmitoyl lecithin (DPPC)-water samples. The inhomogeneity, induced by laser interferometry, is sinusoidal with wavevector q in the plane of the smectic layers. The relaxation rate Γ is found to follow $\Gamma = Dq^2$ for a wide range of temperatures T and water concentrations c_w . D varies from 8×10^{-7} to 2×10^{-6} cm²/sec. We can relate D to a "free water" layer thickness d as a function of c_w and thus find d to be in excellent agreement with estimates based on X-ray studies. d goes to zero at $c_w = 10\%$ wt., consistent with the presence of a hydration shell. As a function of T , D has an Arrhenius behavior with an activation energy ranging from 0.25 to 0.45 eV, which increases with decreasing c_w . Work supported in part by Joint Services Electronics Program (U.S. Army, Navy and Air Force) under Contract No. N00014-75-0648 and NSF under Grants No. DMR-76-01111 and DMR-76-22452.

*Cornell Univ., Ithaca, N. Y. 14853.

TU-PM-H4 AN INVESTIGATION OF MOLECULAR ORDER IN SYNTHETIC AND NATURALLY OCCURRING MIXED LIPID BILAYERS,

J. P. Sheridan*, J. M. Schnur*, and P. E. Schoen, Naval Research Laboratory, Washington, D.C. 20375

Raman spectroscopy has been applied to the study of the thermotropic behavior of mixtures of synthetic and naturally occurring phospholipids in multilamellar aqueous suspensions. Phase diagrams of a number of binary mixtures of phosphatidylcholines have been constructed from the temperature dependence of the skeletal optical modes of the lipid hydrocarbon chains for various concentrations of the two components. The relative intensities of these vibrational modes can be used to determine the boundaries of the gel-fluid two-phase region and the changes in molecular order throughout it. Good agreement is observed between the Raman derived data and those recently obtained by calorimetry (Mabrey and Sturtevant, P.N.A.S., 73, 3862 (1976)). Considerably more complex mixtures of sphingomyelins extracted from bovine brain cells have also been studied by the Raman technique. Interestingly, the Raman data reveal evidence of changes in molecular order accompanying multiple phase transitions in the vicinity of the biological temperature regime for these naturally occurring lipid mixtures.

TU-PM-H5 CHEMICAL SHIFT DIFFERENCE OF THE α -METHYLENE GROUPS OF THE TWO FATTY ACYL CHAINS OF PHOSPHOLIPIDS IN MEMBRANE MODELS. Mary F. Roberts* and Edward A. Dennis, Department of Chemistry, University of California at San Diego, La Jolla, CA 92093.

The existence of a large chemical shift difference between the α -methylene groups of the two fatty acyl chains of phospholipids in Triton X-100/phospholipid mixed micelles has been demonstrated using ¹H-NMR [Roberts, M.F., and Dennis, E.A. (1977) J. Am. Chem. Soc. 99, 6142]. The chemical shift difference between the two α -methylene groups in this mixed micelle system can now be compared with that for monomeric phospholipid, for pure phospholipid micelles, and for dipalmitoyl phosphatidylcholine in mixed micelles formed with ionic or zwitterionic detergents. The results suggest that phospholipid molecules adopt a unique conformation in all micellar environments. In this conformation, the sn-1 α -methylene protons have indistinguishable chemical shifts and are in a more hydrophobic environment than the strongly differentiated protons of the sn-2 α -methylene group. The conformation and environment of the phospholipid in the micellar structures will be compared with that in other aggregated structures such as bilayers (NSF PCM 76-21552, NIH GM-05,910).

TU-PM-H6 PHYSICAL PROPERTIES OF AN AMPHIPHILIC NEMATIC LIQUID CRYSTAL. D. Armitage, T. Haven, K. Radley* and A. Saupe*, Liquid Crystal Institute and Department of Physics, Kent State University, Kent, Ohio 44242

Nematic mixtures of decylammoniumchloride, ammoniumchloride and water have been investigated with respect to optical, elastic and viscous properties. Refractive index measurements as a function of temperature show that the transition from the lamellar smectic phase to the nematic phase is second order or nearly second order. It indicates that the nematic phase is formed by a fragmentation of the lamellae into micelles of a bilayer structure.

The nematic system can be oriented by surface action and curvature deformations can be induced by magnetic fields. Curvature elastic and viscous properties can thus be studied on thin films. Our results indicate that the Frank-Oseen equations apply.

TU-PM-H7 FORMATION AND PROPERTIES OF CELL-SIZE SINGLE BILAYER VESICLES. J. Antanavage, T. F. Chien, Y. C. Ching, L. Dunlap, P. Mueller, and B. Rudy, Eastern Pennsylvania Psychiatric Institute, Philadelphia, Pa. 19129

Hydration of single or mixed phospholipids or lipid protein mixtures at low ionic strength results in the formation of a population of large, solvent free single bilayer vesicles with included volume of up to 300ul per micromole lipid. Their size ranges from 2 to 300u and they can be sorted according to size by centrifugation. During formation they can include neutral external solutes and 20u latex beads. They adhere to each other in 1-3 mM CaCl₂ and can be made to fuse in the presence of Ca phosphate. When formed in distilled water their internal solution has a conductivity of $2-3 \times 10^{-5}$ S/cm, an osmolarity of 3-4 mOsm and a density of 1.0005-1.001. The osmotic pressure produced by the internal solutes causes a surface stress for a 50u vesicle of 80-110 dynes/cm. Their breaking strength as determined by osmotic pressure differentials is 300 dynes/cm, and their elastic constant 10-30 dynes/cm. They can be sealed to a small hole in a thin partition between two compartments and the smaller portion of the sealed membrane can be selectively broken by an electrical shock leaving a single membrane across the hole. The capacitance and resistance of such membranes are 0.8uF/cm² and 10^{-8} S/cm² in 10 mM NaCl for pure lipid vesicles. Dielectric breakdown occurs near 200mV. A capacitance of 0.8uF was determined by microelectrodes. Gramicidin increases the membrane conductance and monazomycin induces voltage dependent gating thus providing further evidence that the vesicles are bounded by a single bilayer.

TU-PM-H8 PHOSPHOLIPID BILAYER STRUCTURE: EFFECT OF HEAD GROUP TYPE, DEGREE OF CHAIN UNSATURATION, AND CHOLESTEROL CONCENTRATION. T.J. McIntosh, Dept. of Anatomy, Duke University School of Medicine, Durham, North Carolina 27710.

Although phosphatidyl choline (PC) bilayers have been studied for a number of years, most x-ray diffraction structural investigations of synthetic PC have been performed using fully saturated lipids below the thermal phase transition. We have extended these studies to determine the lipid head group conformation and hydrocarbon chain packing as a function of (1) physical state of the lipid, (2) cholesterol concentration, (3) degree of hydrocarbon chain unsaturation, (4) hydration state of the lipid, and (5) lipid head group type. Cholesterol changes the hydrocarbon chain packing and chain tilt and introduces discrete bumps into the high resolution (4Å) electron density profiles. Bilayers formed from unsaturated PC show marked differences in repeat period, chain packing, and electron density profiles compared to saturated PC. In addition, x-ray data for three of the most common membrane phospholipids were compared. Electron density profiles indicate that PC, PS, and PE all have different head group conformations.

TU-PM-H9 "SOLVENT-FREE" PLANAR BILAYER MEMBRANES: A NOVEL METHOD OF FORMATION. Stephen H. White, Department of Physiology, University of California, Irvine 92717.

The solubility of alkyl molecules in black lipid bilayer membranes is inversely proportional to the length of the molecule. A sufficiently long alkyl molecule such as squalene is essentially insoluble in the bilayer. This observation has been utilized to develop a simple method for forming "solvent-free" bilayer films by the method of Mueller et al. [Circulation 26 (1962), 1167] using glycerol monooleate (GMO) as the surface active lipid. The resulting films are stable, large in diameter, and easy to observe. The specific capacitance (C_g) of the bilayers is $0.7771 \pm 0.0048 \mu\text{F}/\text{cm}^2$ at 20°C . This value of C_g compares favorably with theoretical values and with experimental values obtained using other methods of forming "solvent-free" bilayers. Since the membranes are solvent-free, the area/GMO molecule in the bilayer can be easily determined from the measurement of C_g . The value obtained is $37.9 \pm 0.2 \text{Å}^2/\text{molecule}$ which is in excellent agreement with values obtained by other workers using two entirely different (and relatively complicated) techniques.

Supported by the N.S.F. (PCM76-20691 & NIH (NS10837-03))

TU-PM-H10 INTERACTION OF SMALL MOLECULES WITH LIPOSOMES.

M.A. Singer, Department of Medicine, Queen's University, Kingston, Ontario, Canada.

Multilamellar liposomes were formed from either dipalmitoyl or dimyristoyl phosphatidylcholine, dicetyl phosphate and the spin probe 12-doxyl stearate methyl ester. The additives used, which were incorporated into the vesicles during the formation stage, consisted of a group of substituted benzene and adamantane derivatives. Molecules possessing a polar group were more effective in increasing probe motion than those lacking such a group. Increasing the separation between the polar group and the non-polar moiety also makes the molecule more effective. Among the various polar groups, OH was more potent than NH_2 . A molecule having two polar groups was less effective than that bearing only one. In a parallel series of experiments, the effects of some of these same additives on ^{22}Na permeability were studied in liposomes of similar composition. There was a poor correlation with the spin probe studies in that none of the molecules which caused early "melting" of the bilayer shifted the permeability maximum, observed in the region of the T_c , to a lower temperature.

TU-PM-H11 'SOLVENTLESS' BILAYERS FROM BULK SOLUTIONS. Ron Waidebüllig & Gabor Szabo, Dept. of Physiology, UTMB Galveston, TX 77550 USA

Depleting the solvent level in membrane forming solutions has the effect of depleting the residual solvent level within bilayers formed by the painting method. The membrane solvent content, as estimated from measurements of bilayer specific capacitance (C_g), decreases linearly with the solvent concentration (M_a) of the membrane forming lipid/alkane solution. The concentration dependence of BLM capacitance for bilayers made from monoolein/decane is well described ($r=.99$) by the linear regression equation $C_g = -0.97 M_a + 0.90$ whereas the relationship for monoolein/hexadecane is $C_g = -0.48 M_a + 0.76$. The different slopes provide an index of the membrane solvent partition coefficients.

The results serve to reconcile the difference between BLMs formed by the painting and monolayer methods. For monoolein bilayers from 2.3 molar decane $C_g = 0.649 \mu\text{F}/\text{cm}^2$ and solutions of 1.8 molar hexadecane yield values of $0.694 \mu\text{F}/\text{cm}^2$. These values are very near those reported for 'solventless' bilayers formed from monolayers.

Supported by USPHS grant HL 19639

TU-PM-H12 ALIGNMENT OF MONODOMAIN SMECTIC LIPID LIQUID

CRYSTALS: DEFECTS AND INSTABILITIES. S.A. Asher and P.S. Pershan Division of Applied Sciences, Harvard University, Cambridge, Massachusetts 02138

The homeotropic alignment of monodomain smectic liquid crystals of various lipids, including dipalmitoyl and dimyristoyl phosphatidylcholine is discussed. The alignment of the lipids into uniaxial smectic liquid crystals above the T_c of the lipids is accompanied by characteristic changes in the texture of the samples, as monitored by optical microscopy. Various defect structures such as "oily streaks", "batonnets", and focal conic textures are observed. These defects appear similar to those found in thermotropic, smectic liquid crystals and in cholesteric liquid crystals. A stress applied normal to the plane of the layers results in instabilities in the smectic ordering. Depending on the temperature regime the uniaxial medium will either show a polyganol texture or a texture composed of concentric rings which are alternately dark and bright under crossed polars. The relationship of the macroscopic defect structures to the microscopic lipid layer ordering is discussed. Work supported by JSEP Contract No. N00014-75-C-0648 and NSF Grants DMR 76-22452 and DMR 76-01111.

TU-PM-H13 INTERACTIONS OF FOLCH-LEES PROTEOLIPID APOPROTEIN WITH LIPID BILAYERS. H.P. Ting-Beall, James E.

Hall, J. David Robertson and Marjorie Lees*. Depts. of Anatomy & Physiology, Duke U. Med. Ctr., Durham, N.C. 27710 and Eunice Kennedy Shriver Ctr. for Mental Retardation, Inc., Walter E. Fernald State School, Waltham, MA. 02154.

Detergent-free, water-soluble Folch-Lees (F-L) proteolipid apoprotein from bovine CNS myelin induces a voltage-dependent conductance in black lipid membranes (BLM). Na^+ is required for an F-L induced conductance change but the established conductance has very low ionic selectivity. The induced conductance fluctuates and has a minimum amplitude of 10^{-11} to 10^{-10} mho. The relationship between fluctuations and high level conductance is uncertain. The conductance at a fixed voltage depends on the sixth power of the protein concentration. Pronase added to the cis or trans side of the BLM does not affect established conductance. But if BLM is formed in the presence of F-L and pronase, the conductance does not change. We conclude that the protein responsible for the conductance increase is not accessible to proteolytic digestion, presumably because of its association with the membrane. (Supported by NIH Grant #3 P01-NS10299)

TU-PM-H14 LATERAL DIFFUSION IN LIPID BILAYERS ALTERED BY SOLVENT AND PHASE TRANSITIONS. P. F. Fahey, Univ. of Scranton, Scranton, Pa., 18510, and W. W. Webb, Cornell Univ., Ithaca, N.Y. 14853.

Using fluorescence correlation spectroscopy and fluorescence photobleaching recovery, we have measured the diffusion coefficient, D , of a lipid analog 3,3'-dioctadecyl indocarbocyanine in large (30 μ m), solvent-free, lipid vesicles having single bilayers or multilayers and in multilamellar liquid crystals. In these preparations, both bilayers and multilayers of dimyristoyl, dipalmitoyl and egg lecithin, we found $D \sim 10^{-6}$ cm²/sec above the phase transition temperatures. These values agree with those observed in mammalian cells in tissue culture. Below T_c , D decreased by more than two orders of magnitude to $D \leq 10^{-10}$ cm²/sec. In planar bilayer lipid membranes (BLM's) formed either by thinning from dispersions or by pairing of monolayers (Fahey et al., Science 195, 305 (1977)) we have found $D \sim 10^{-6}$ cm²/sec regardless of T relative to the putative T_c . We think that retained solvent is responsible for the anomalous diffusion in BLMs. No effects on D of interaction between bilayers were discernable to $\pm 40\%$ in the multilayer preparations. The technique for formation of large bilayers vesicles will be described.

TU-PM-H15 INTERACTION OF CHARGED PROTEINS, AMPHIPHILIC MOLECULES, AND PHOSPHOLIPID VESICLES WITH PLANAR BILAYER LIPID MEMBRANES, DETECTED BY ANTIBIOTIC PROBES. J.A. Cohen and M.M. Moronne,* Lab of Physiology and Biophysics, Univ. of the Pacific, San Francisco, CA 94115.

The antibiotics Monazomycin, Valinomycin, and Nonactin have been used to detect the interactions of charged proteins (cytochrome c), polypeptides (poly-L-lysine), detergents (sodium dodecylsulfate), and phospholipid vesicles (phosphatidylserine) with planar bilayer lipid membranes (BLMs). The interactions are sensed by monitoring the antibiotic-mediated BLM conductance, which is related to BLM surface-charge density, as additions of adsorbent are made to the aqueous phase. However, due to the possibility of non-electrostatic effects, this method of surface-charge density determination is only semi-quantitative. More quantitative results are achieved by Stern analysis of the BLM conductance titrated with impermeant screening ions. Such analysis of a series of mixed phosphatidylethanolamine-phosphatidylserine BLMs demonstrates the necessity of accounting for intrinsic binding of the screening ions to the BLMs. Comparisons of Monazomycin and Valinomycin/Nonactin results are made, as are the screening/binding properties of Mg^{++} and Ca^{++} .

Supported by NSF (PCM 76-11950) and NIH (HL 16607).

TU-PM-H16 INHIBITION OF IONOPHORIC ACTIVITY OF Ca^{2+} + Mg^{2+} ATPase AND ITS TRYPTIC FRAGMENTS FROM SARCOPLASMIC RETICULUM BY REDUCING AGENTS. Jonathan J. Abramson*, Adil E. Shamoo, (Intr. by D.A. Goldstein). University of Rochester School of Med. & Dent., Rochester, N.Y. 14642.

Tryptic digestion of Ca^{2+} + Mg^{2+} -ATPase from sarcoplasmic reticulum leads to an initial cleavage into two fragments: a 45K dalton fragment and a 55K dalton fragment. Both fragments act as ionophores when incorporated into an oxidized cholesterol bilayer. The 55K dalton fragment is calcium selective, while the 45K dalton fragment is non-selective. Reduction of a disulfide bond in the 45K dalton fragment by using dithiothreitol, mercaptoethanol or titanium(III) citrate, causes inhibition of ionophoric activity. The 55K dalton fragment is unaffected by these reducing agents, while ionophoric activity of the ATPase is inhibited by them. These inhibition studies imply that the two tryptic fragments are in a series arrangement in the membrane. Inhibition of the ionophoric properties of one fragment, by the reduction of an essential disulfide bond, results in inhibition of transport in the intact enzyme.

Supported by U.S. DOE Contract and Assigned Report #UR-3490-1286. Dr. Abramson is a fellow of MDA of America.

P O S T E R S E S S I O N S

LIPID BILAYERS III

TU-POS-A2 MEMBRANE PROTEIN EXTRACTION BY PHOSPHOLIPID VESICLES. W. H. Huestis, S. R. Bouma,* and S. L. Cook,* Stanford, California 94305

Transfer of membrane bound proteins from cell surfaces to phospholipid vesicles has been observed to occur for some types of cells. The nature of the transferred proteins and their rates of transfer are functions of surface charge and fluidity of cell and vesicle membranes. Those proteins whose function can be assessed appear to associate with the vesicle membrane in a native orientation, and can be transferred into cell membranes with retention of function, although in low yield. This phenomenon is a potentially powerful way to modify the composition and function of cell membranes.

TU-POS-A1 NATURE OF THE COMPLEMENT LESION: FORMATION OF MEMBRANE CHANNELS. D. Michaels and M. Mayer*. Baltimore, Md. 21205

BLM have been used to study three features of the complement C5b-9 membrane attack sequence. (1) Membrane sidedness: cis/trans studies show that the sequence is divided into two pairs, C5b,6 + C7 and C5b-8 + C9. The reaction between partners requires their presence on the same side of the bilayer; however, the coupling between pairs can occur from opposite sides. (2) Membrane thickness: as bilayer thickness decreases BLM become more sensitive to complement action. This sensitivity is correlated to membrane insertion by C5b,6 and C9 but not C7 or C8. Thus different components insert in the bilayer to varying depths. (3) Single channels: membrane permeability increases in discrete steps following the addition of complement components, suggestive of membrane channel formation. Further, the size and stability of the channels increase with sequential addition of components C5b,6 (6 Å), C5b,6,7 (12 Å), C5b-8 (16 Å) and C5b-9 (25 Å). Prior to addition of C9, the C5b-8 channel opens and closes continuously. After addition of C9, the channel remains open.

TU-POS-A3 PULSED GRADIENT NMR MEASUREMENTS OF SELF-DIFFUSION IN LIPID BILAYERS*. P. Ukleja,* N. Vaz,* and J. W. Doane, Kent, OH 44242

Intense (3kG/cm) magnetic field gradients with rise times of 200G/cm per microsecond and coherent averaging techniques are used to study self-diffusion of phospholipid molecules in uniformly oriented phospholipid multibilayers. The field gradient coils are wound in a quadrupolar configuration inside the r.f. coil and can thus be rotated to measure diffusion parallel and perpendicular to the planes. The strong and rapid gradient pulses also allow measurements of the diffusion constant over short diffusion times and distances necessary in restricted diffusion studies.

*Supported in part by Grant No. GM 22599-02 from the Institute of General Medical Sciences.

TU-POS-A4 LATERAL DIFFUSION IN PHOSPHOLIPID BILAYERS.

James R. Sheats and Harden M. McConnell, Chemistry Department, Stanford University, Stanford, CA 94305.

A highly versatile technique has been developed for the accurate measurement of lateral diffusion of any nitroxide in all phases of lipid bilayers. Hydrated multilayers with $\sim 0.25\%$ lipid spin label, and a photoactivable alkylcobalt complex¹ in the aqueous phase, are prepared between two optically flat quartz plates, one of which has deposited on it a thin, rectangular mesh pattern of gold. Brief photolysis with collimated 351 nm light (Ar^+ laser) creates a spin-label concentration gradient U_0 ; $U(D,t)$ is then easily computed. D is thus obtained from the decrease in EPR signal due to two photolyses separated by a dark time t . Advantages include:

1) spatial stability of light beam is not required, so D as low as 10^{-14} cm^2/s can be measured; 2) varying grid size allows examination of defect structure; 3) chemistry of the photoreaction is known in detail; 4) very low energy densities are required for photolysis ($\sim 0.1\%$ of that used for fluorescence photobleaching).

1) J. R. Sheats and H. M. McConnell, *J. Amer. Chem. Soc.* **99**, 7091-7092 (1977).

TU-POS-A5 DENSITY STUDIES OF PHOSPHOLIPID BILAYERS.

D.A. Wilkinson and J.F. Nagle, Pittsburgh, Pennsylvania 15313.

The changes in density, or specific volume, that occur as phospholipid dispersions are heated and cooled have been measured using a highly sensitive differential dilatometer. A series of phosphatidyl cholines, from C14 to C18, has been studied; the specific volumes, the coefficients of thermal expansion, and the volume changes occurring at phase transitions have been determined. These can be compared to the corresponding properties of long chain alkanes and polyethylene. Similar measurements have been performed on two phosphatidyl ethanolamines. They differ from their choline analogues in several ways.

TU-POS-A6 KINETICS OF THE AGGREGATION OF PHOSPHOLIPID L VESICLES.

G.A. Gibson, Chemistry Dept., SUNY at Binghamton, Binghamton, NY 13901

A method has been developed that allows observation of the rate of aggregation of phospholipid bilayer vesicles. Distinct aggregation phenomena are analyzed both on stopped flow and slow mixing timescales. This is accomplished by mixing two phospholipid dispersions, one which contains a fluorescent "donor" probe and one which contains a quencher probe. These probes are designed such that quenching will occur over large intermembrane distances by the Förster resonant energy transfer mechanism. Förster transfer might also be observed if the probes were able to dissociate from the vesicles and diffuse through the aqueous phase resulting in randomization of the donor and quencher. This problem has been avoided by the use of derivatized phospholipids. Dansyl-phosphatidylethanolamine is used as the fluorescent "donor" probe. Its fluorescence is excited by the 325 nm line of an He-Cd laser. The quencher probe is rhodamine-B-phosphatidylethanolamine thiourea. Fluorescence is observed at the fluorescent maxima for each probe. This research was supported by New York State Health Research Council Grant # 362.

TU-POS-A7 EQUILIBRIUM FLUCTUATIONS IN PHOSPHOLIPID BILAYERS.

E. Freire and R.L. Biltonen*, Dept. of Biochemistry, University of Virginia, Charlottesville, VA 22903

Scanning calorimetric data allows evaluation of the bilayer partition function without assuming a particular model for the gel-liquid transition. Analysis of this partition function yields information concerning overall thermodynamic parameters as well as molecular averages and distribution functions. These theoretical results in conjunction with experimental calorimetric data on saturated lecithin bilayers indicate that the gel-to-liquid transition proceeds through the formation of liquid clusters. These clusters are not static domains but dynamic entities characterized by rather large fluctuations. These fluctuations in the size of the clusters give rise to localized density and volume fluctuations in the bilayer. The magnitude of these fluctuations is shown to depend on the length of the hydrocarbon chains, the radius of curvature of the bilayer and the presence of small molecular weight compounds, such as anesthetics, in the system. Indirect evidence suggests that these fluctuations could be of importance in transport related phenomena and protein-protein interactions in the membrane.

TU-POS-A8 THE ADSORPTION OF DIVALENT CATIONS TO

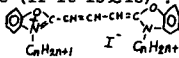
PHOSPHOLIPID BILAYER MEMBRANES. A.C. McLaughlin* and S.G.A. McLaughlin; Brookhaven National Laboratory, Upton N.Y. 11793 and SUNY Stony Brook, N.Y. 11790.

We have combined the use of Phosphorus NMR and electrophoretic mobility measurements to demonstrate that the combination of Henry's law adsorption isotherm, Boltzmann's relation and the Grahame equation from the theory of the diffuse double layer can indeed describe the adsorption of divalent cations to bilayers formed from the zwitterionic lipid phosphatidyl choline. We used Co(II) for the NMR studies for two reasons. First, the ion is paramagnetic and produces large shifts in the ^{31}P NMR signals. Second, the shifts can be calibrated to determine the fraction of phosphate groups bound. The binding deduced from the zeta potential measurements decreased in the sequence Mn, Mg, Ca, Co, Ni, Sr, Ba. The dissociation constants were, assuming a 1:1 stoichiometry .3, 1.0, 1.0, 1.2, 1.2, 2.8, 3.6 M. A comparison of the zeta potential and NMR data, however, indicate that both 2:1 and 1:1 complexes are formed between phosphatidyl choline and Co^{++} .

Supported by grant PCM 76-04363 from the NSF.

TU-POS-A9 CYANINE DYE INDUCED PHOTO-ELECTRIC EFFECTS IN BILAYER MEMBRANES.

J. A. Baker† J. R. Duchek† R. L. Hooper† R. J. Kofman† J. C. Parke† and J. S. Huebner, University of North Florida, Jacksonville, FL 32216.

Transmembrane voltage transients are induced by light flashes when some cyanine dyes are adsorbed into one side of a bilayer membrane. These transient rise and fall times are independent of the flash duration (if it is $< 10 \mu\text{s}$) and the membrane RC time (if it is $\geq 1 \text{s}$)¹. The risetime and amplitude for dyes  varies with n , the membrane lipid composition, aqueous solution salt concentration, and imposed transmembrane voltage. These results are consistent with a photo-ionic mechanism, which considers that the voltage transients result from light induced modifications in the dye molecules' geometry, which by altering the dye solubility in the membrane, induces physical movements of charged dye molecules within the membrane. These effects appear to provide a method of measuring physical properties of selected regions of membranes.

1. J. S. Huebner, *Biochim. Biophys. Acta*, **406** (1975)

178, and J. S. Huebner, *J. Membrane Biol.*, in press.

This work is supported by the NIH through grant GM23250.

TU-POS-A10 COTRANSPORT OF ANIONS AND PROTONS THROUGH LIPID BILAYER MEMBRANES CONTAINING A LONG-CHAIN SECONDARY AMINE
J. Gutknecht, Duke Univ. Marine Lab, Beaufort, NC 28516

Lipid bilayer membranes containing *n*-lauryl (trialkylmethyl)amine show high conductance and high halide selectivity at pH 5.6. In the absence of halide ions, the membranes show H^+ selectivity but relatively low conductance. In 0.1 M NaBr both the membrane conductance (G_m) and the Br^- self-exchange flux (J_{Br}) are proportional to H^+ concentration over the pH range of 7 to 4, and both J_{Br} and G_m saturate at pH < 4. However, J_{Br} is always more than 100 times the flux predicted from G_m and the transference number for Br^- . At pH 7, J_{Br} is proportional to Br^- concentration over the range of 1 to 340 mM, with no saturation kinetics. The results can be explained by a model in which the secondary amine behaves as a monovalent, titratable carrier which exists in three chemical forms (C, CH^+ and CH_2Br). Br^- crosses the membrane primarily as the neutral complex (CH_2Br). The positively charged carrier (CH^+) crosses the membrane slowly compared to CH_2Br , but CH^+ is the principal charge carrier in the membrane. At neutral pH, >99% of the amine is in the nonfunctional form (C), which can be converted to CH^+ or CH_2Br by increasing the H^+ or Br^- concentrations. (Supported in part by USPHS Grant HL 12157.)

TU-POS-A11 OPTICAL STUDIES OF MONODOMAIN PHOSPHOLIPID BILAYER-WATER SYSTEMS CONTAINING Ca^{++} .

C. D'Ambrosio⁺ and L. Powers, Bell Laboratories, Murray Hill, NJ 07974.

The effect of Ca^{++} on phase behavior of L- α -phosphatidylcholine (β - α -dipalmitoyl) bilayers has been investigated as functions of temperature, water content, and Ca^{++} concentration. Monodomain phospholipid bilayers¹ were swelled in $CaCl_2$ solution ($10^{-3}M$ to $10^{-4}M$) and the optical birefringence measured from the conoscopic interference figures as a function of temperature. The Ca^{++} and Cl^- contents were determined at 25°C from their X-ray fluorescence by scanning electron microscopy indicating roughly $Ca^{++}/lipid \sim 10^{-2}$ (with $Cl^-/lipid \sim 10^{-2}$) and $K_{Ca^{++}} \sim 1M^{-1}$. The temperature required to produce monodomain samples at this Ca^{++} content was 30-35°C lower than that required for samples containing only water. The gel transition was also higher in temperature for all water contents ranging from 8°C to 5°C for low to high water content. Optical biaxiality was observed only for water contents less than 10% wt. in a small low temperature region and maximum hydration producing one phase was 25% wt.

⁺Present address is Va. Polytech. Inst., Blacksburg, Va.

¹L. Powers and P. S. Pershan, *Biophys. J.* **20**, (1977), 135.

TU-POS-A12 MONTE CARLO STUDIES OF LIPID LAMELLAE: EFFECTS OF PROTEINS, CHOLESTEROL, CURVATURE, AND LATERAL MOBILITY ON ORDER PARAMETERS. H.L. Scott⁺ and Sheau-lin Cherng^{*}, Oklahoma State University, Stillwater, Oklahoma 74074

We present the results of a Monte Carlo study of the effects of proteins, cholesterol, bilayer curvature, and mobility on the chain order parameters of a lipid bilayer using the Monte Carlo program developed by Scott (BBA 469, 264-271, 1977). Simulations of protein and cholesterol effects were accomplished by insertion of a rigid stationary cylinder into the lipid matrix. We observed boundary lipid around the protein, and we found that the effect of cholesterol depends upon the length of the lipid hydrocarbon chains relative to the depth of penetration of the cholesterol. Our simulations of hydrocarbon chains in curved layers are consistent with experimental results of Chreszczyk et al. (BBA 470, 161-170, 1977). We find that restricting lateral motion of the chains does not measurably alter the order parameters.

⁺Supported in part by the National Science Foundation

TU-POS-A13 THE MODIFICATION OF THERMAL PHASE TRANSITIONS OF PHOSPHOLIPID MULTILAYERS DUE TO VARIATIONS IN CALCIUM CONTENT, W. F. Graddick, and J. B. Stamatoff, Bell Laboratories, Murray Hill, NJ 07974.

That the incorporation of divalent cations in phospholipid multilayers can induce isothermal phase transformations and alter thermal transformations has been well-documented. Here we report the effect of varying concentrations of Ca^{++} on the thermal phase transitions of L-dipalmitoyl Phosphatidylcholine as determined by X-ray diffraction. In addition to the usual lamellar reflections, additional reflections are observed which change in spacing and relative intensities as the calcium concentration is varied. These reflections are similar in nature to those observed by Janiak, et al.¹, which were interpreted as an in-plane ripple. As verified by differential thermal analysis, the onset of the pretransition and main transition also varied with calcium content. The structural implications of the results are discussed.

¹M. J. Janiak, D. M. Small, and G. G. Shipley, *Biochemistry* **15**, 4575 (1976).

TU-POS-A14 8-HYDROXYQUINOLINE: A MOBILE CARRIER IONOPHORE FOR TRIVALENT CATION. Karl J. Hwang, Dept. of Pharmaceutical Sciences, University of Washington, Seattle, Washington 98195

The complex of 8-hydroxyquinoline- In^{+3} diffuses rapidly through the lipid bilayer of DPPC and DPPC:cholesterol liposomes, and can facilitate the transport of In^{+3} ions to the encapsulated chelating agent. Such transport of trivalent cation by 8-hydroxyquinoline is governed by the binding constants of the cations to chelating agents on both sides of the lipid bilayer and by the exchange rate of cations from these chelating agents to 8-hydroxyquinoline. Like the cholesterol, 8-hydroxyquinoline- In^{+3} complexes in liposomes are exchanged readily from one liposome to another. The complexes of 8-hydroxyquinoline- In^{+3} imbedded in lipid bilayer are probably existed in two different forms, namely the lipid-diffusible form and the lipid-nondiffusible form. These two forms are in dynamic equilibrium, and the nondiffusible complexes are located near the region of the polar head groups on both sides of the bilayer. Preliminary studies suggest that it is possible to apply 8-hydroxyquinoline to load liposomes with the gamma-emitting isotope for studying the fate of liposomes *in vivo*, and for preparing radiopharmaceuticals.

TU-POS-A15 ENERGY TRANSFER AND ENERGY LOSSES IN BILAYER LIPID MEMBRANES (LIPOSOMES). G. Strauss and A. Mehreteab^{*}, Department of Chemistry, Douglass College, Rutgers University, New Brunswick, New Jersey 08903.

Singlet-singlet energy transfer between organic molecules incorporated into lipid bilayers was studied for several donor-acceptor pairs, including p-terphenyl/diphenyl octatetraene (DPO) and DPO/chlorophyll a. Transfer efficiency ϕ_{DA} was measured by fluorescence sensitization and found to agree to within 5% with the fluorescence loss ϕ_Q of the donor occasioned by presence of the acceptor. In cyclohexane solutions of the same donor-acceptor pairs ϕ_{DA} was much smaller than ϕ_Q . The difference represents energy lost principally by internal conversion. One of the important functions of the lipid bilayer thus is the suppression of such losses. The observed dependence of ϕ_{DA} in liposomes on the mean donor-acceptor distance was compared with theoretical curves, showing that energy transfer occurs by dipole-dipole interaction and not by a diffusion-controlled process.

TU-POS-A16 THERMOTROPISM IN MIXED LIPID SYSTEMS. S.P.

Verma*, and D.F.H. Wallach, Tufts-New England Medical Center, Boston, MA 02111.

We studied the effect of unsaturated/saturated fatty acids (18 carbons) on the thermal transitions of DML, DPL, DSL and egg lecithin (molar ratio 0.59) by Raman spectroscopy. Plots of I_{2880}/I_{2850} (CH-stretching features) vs temperatures show multi-transitions, while the plots of either I_{2930}/I_{2850} , or I_{2960}/I_{2850} , or position or half-width of the 2880 cm^{-1} band, indicate only a single broad transition, shifted by few °C from the main lipid transition, in the presence of saturated/unsaturated fatty acids. The multi-transitions probably represent multiple phases. This heterogeneity in lipid mixing may be due to differences in chain length and incorporation of *cis*-double bond/s. The location of double bond/s in the middle of the chain (*cis*-form) creates more space between interacting chains than saturated chains of similar length. Quantitative characterization of plots of $\ln(I_{2880}/I_{2850})$ vs $1/T \times 10^3$ suggest the slope is proportional to the size of the lipid clusters (cooperative units).

Supported by Grant 5P02 CA12178 - NIH

INSTRUMENTATION TECHNIQUES I

TU-POS-A17 THE INTERACTION OF UNILAMELLAR VESICLES OF DIMYRISTOYLPHOSPHATIDYLCHOLINE (DMPC) WITH HIGH DENSITY LIPOPROTEINS (HDL). W.A. Bradley*, M.F. Rohde*, R.D. Knapp*, H.J. Pownall, R.L. Jackson* and A.M. Gotto, Jr.*, Baylor College of Medicine and The Methodist Hospital, Houston, Texas 77030 (Intr. by J.D. Morrisett)

The interaction of unilamellar DMPC vesicles with human HDL at 24° C has been characterized by physical and chromatographic methods. Batch microcalorimetry indicates that an exothermic process occurs upon mixing DMPC with HDL at the weight ratio of 1.7:1; the process is complete within 10 min. Gel filtration demonstrates that a particle intermediate in size between the DMPC vesicle (250 Å) and the HDL (~100 Å) is present and that free protein is absent. The isolated particle is shown to be homogeneous by sedimentation and flotation ultracentrifugation at d 1.063 g/ml and 1.21 g/ml, respectively. The partial specific volume of the complex is 0.912 cc/g. Sedimentation equilibrium yields a molecular weight of 293,000 consistent with the gel filtration data. Approximately 53% of the phospholipid of the complex is titrated by a paramagnetic quenching reagent, $\text{Mn}(\text{EDTA})_2$, as measured by ^{31}P -NMR. Models for the complex and the mode of vesicle-lipoprotein interaction will be considered. (Supported by funds from HL-17269).

TU-POS-B1 VOLTAGE NOISE OF H^+ TRANSPORT IN NEUROSPORA. J. Warncke* and C.L. Slayman. Yale School of Medicine, New Haven, CT 06510.

Recent success of noise analysis on artificial and excitable membranes has prompted us to look at noise in a system dominated by ion pumps rather than ion diffusion regimes. Convenient for this purpose is the plasma membrane of *Neurospora*, whose major current flows are a pumped efflux of protons ($20\mu\text{A}/\text{cm}^2$, at -180 mV) and a passive reentry of protons ($16\text{--}18\mu\text{A}/\text{cm}^2$). ATP withdrawal, by cyanide poisoning, reduces pump current by 75%. For noise measurements, amplified voltage signals from two electrodes were filtered (cut off above 25Hz), digitized, and stored in a PDP8 computer. After subtraction of mean-value drift and checking for stationarity, the noise power spectra at both electrodes were calculated using the Fast Fourier Transform or, when necessary, the electrode cross-correlation function. Subtraction of the spectrum during cyanide from that of normal hypha yielded Lorentzian noise with a corner frequency of 13Hz and an amplitude of $10^{-9}\text{ V}^2\cdot\text{sec}$. Lower limits for unit cycle time and flux per cycle were calculated to be 20 msec and 5000 ions, suggesting the noise to arise from either channel-type transport or switched carriers operating in bursts of several thousand cycles (reentry current?).

TU-POS-A18 1/f NOISE IN BLACK LIPID MEMBRANES

INDUCED BY IONIC CHANNELS CREATED BY A CHEMICALLY DIMERIZED GRAMICIDIN A. R.Sauvé and E.Bamberg. Dept. Biol. Univ. Konstanz. 775 Konst. Germany

Malonyl-bis-desformylgramicidin, a dimerized form of gramicidin A, has been recently shown to create long lasting, monovalent cations selective channels when incorporated into B.L.M. (mean lifetime in the order of minutes). A noise analysis of this system was undertaken, the results of which clearly indicated that, under voltage clamp condition, the current spectral density of the fluctuations could be expressed as $4\text{ kT}/R + \alpha I^2/N_f$ where R is the membrane dc resistance, I the membrane average current, f the frequency, α a constant, equal to $1.2 \cdot 10^{-2}$ for a PC 16:4 + cholesterol membrane in contact with a 1M KCl salt solution and N_f the total number of channels. The $1/f$ component could be observed over 3 decades and was found to be independent of the kind of lipid used to form the membranes. Results on the salt concentration and temperature dependency of α will be presented.

TU-POS-B2 A POSITION SENSITIVE X-RAY DETECTOR FOR EQUATORIAL AND MERIDIONAL REFLECTIONS. P. Sand* and C. Crist* (Intr. by R. Podolsky), National Institutes of Health, Bethesda, Maryland 20014

The linear single-wire position-sensitive proportional counter is very useful in recording the X-ray intensity along one direction. In order to obtain intensity data in a second direction, while still retaining the advantages of a single-wire detector, a two-wire position sensitive proportional counter was built. The position of an incoming X-ray is determined by electronic measurement of the difference between rise times of the pulses at the ends of the wires. The spatial resolution of the detector is approximately 0.15 mm fwhm which is comparable to that of other single-wire detectors. The counter was used to record the diffraction pattern arising from living frog sartorius muscle. The (1,0) and (1,1) equatorial reflections as well as the 14.3 nm meridional reflection were clearly resolved.

TU-POS-B3 ADAPTATION OF COMMERCIAL OPTICAL STOPPED-FLOW APPARATUS TO THERMAL MEASUREMENTS. M. Maly*, P. D. Smith B. Balko*, and R. L. Berger Laboratory of Technical Development, NHLBI, Bethesda, Maryland 20014

Modification of the Aminco-Morrow stopped-flow apparatus was made to perform thermal measurements. The mixing chamber of the system was slightly altered to allow the insertion of a thermistor; this arrangement permits thermal measurement of chemical reactions in the ms range. Response time of the thermistor is 2.5 ms, extended thermal stability of the unit is poor, and heat generated by turbulent mixing is several times greater than that for the fast stopped-flow μ -calorimeter (1). Nevertheless, good kinetic curves were obtained by simultaneous thermal and optical absorption measurements of the reaction NaHCO_3 with HCl. Data reconstruction computer programs devised for use with the fast stopped-flow μ -calorimetry system are applicable to the modified system. This device gives a new perspective to the study of chemical kinetics for many laboratories. It presents the opportunity for measuring reactions both thermally and optically, by making a simple modification of a commercially available instrument.

1. R.L.Berger, B. Balko, Biophys. J. 17, 103a, 1977.

TU-POS-B4 RADIATION THERAPY PLANNING WITH COMPUTERIZED TOMOGRAPHY. A.C. Scheer*, R.S. Ledley, and H.K. Huang, Georgetown Univ. Med. Ctr., Washington, D.C.

Four main problems have been encountered in current radiotherapy treatment planning: first, an accurate contour of the patient's body surface at the cross-sectional level of the tumor must be drawn; second, the tumor must be accurately located and outlined in relation to the normal structures within the body cross section; third, corrections for tissues of different densities found in the area to be irradiated must be carried out; and fourth summations of the dose delivered by multiple fields must be calculated.

With computerized tomography, using the ACTA Scanner Model 0100, these four problems can be resolved in a way not previously available in radiotherapy treatment planning. The CT image provides an accurate body contour, showing the internal structures in their proper relation to each other. The tumor and its extension are accurately demonstrated. Corrections for tissue heterogeneities can be accomplished either by arbitrary assignment of densities to tissues or by direct scanning with a therapy source. The computer can be programmed to demonstrate summations of doses delivered from multiple fields.

TU-POS-B5 STANDARDIZATION AND APPLICATION OF THE SINGLE BREATH TEST OF THE DIFFUSING CAPACITY OF THE LUNGS FOR CARBON MONOXIDE (D_{LCO}) Edith Rosenberg and Roscoe Young* Howard University, College of Medicine, Washington, D.C.

We believe that a pulmonary function test that is over 65 years old may turn out to be the noninvasive test for the early detection of emphysema as distinct from other causes of chronic obstructive lung disease. Failure to fully understand this test has in the past prevented its standardization. We are showing that Krogh's K (D_L/V_A) calculated from the D_{LCO} is a measure of the gas transfer capability to the alveolar capillary membrane independent of regional inhomogeneities in the lungs. We demonstrate lack of influence of regional variation of K, (D_L/V_A), on the test by showing that when the test is done under standard conditions CO uptake by pulmonary capillary blood from the alveolar gas follows a single exponential path. We also show that although K decreases as lung volume during breath-holding increases it tends to become constant near total lung capacity.

TU-POS-B6 A NEW MICROELECTRODE FOR RECORDING EXTRACELLULAR ACTIVITY OF SINGLE OLFACTORY RECEPTORS. R. Gesteland, G. Adamek*, R. Yancey*, and J. Weier*, Northwestern University, Evanston, Illinois 60201.

Extracellular action potentials of single, small, closely-packed neurons such as olfactory receptors can be recorded with a 3 μ tip diameter micropipette filled by vacuum boiling with a solution of 3M NaCl and 1.5% by weight gelatin. Advantages of these electrodes over the platinum black plated Dowben and Rose electrodes presently used are: 1, two-times increase in signal amplitude; 2, equally low noise; 3, easy preparation; 4, no degeneration in extended storage; 5, lower amplitude interfering signals from neighboring cells; and 6, frequency response flat to d-c, eliminating the waveform distortion caused by capacity coupling. Quantitative comparison between the two electrode types in amphibian and mammalian olfactory preparations and in other regions of the amphibian brain show the new electrode to be consistently superior. It is particularly useful for investigation of changes in extracellular action potential waveform with invasion of the neuron soma. Supported in part by NSF Grant No. BNS 75-02339.

TU-POS-B7 ELECTROPHORETIC SEPARATION OF T AND B MOUSE SPLEEN LYMPHOCYTES FROM VARIOUS STRAINS. C.D. Platsoucas and N. Catsimopoulos, Biophysics Laboratory, M.I.T., Cambridge, MA 02139

T and B mouse spleen lymphocytes were separated by density gradient electrophoresis, on the basis of their surface charge. In a large number of strains examined, the high mobility cells were predominantly T lymphocytes, whereas the low mobility were B cells. Significant differences were found in the electrophoretic distribution profiles of the C57BL/6j and (BALB/cXC57BL/6j) F_1 and all the following: B $_6$ -C-H-2/cBy (congenic to C57BL/6j), BALB/c, CBA/H/6j, C57BL/10Sn, CBA/J, C3H and DBA/2. The C57BL/6j and the (BALB/cXC57BL/6j) F_1 cells appear more heterogeneous than the others which give only two major peaks. Moreover, the high mobility areas are less populated in the C57BL/6j and the (BALB/cXC57BL/6j) F_1 animals than in all the others. The above differences are consistent with cells prepared by different methods. It is concluded that the surface charge of the cells is genetically determined and that the density gradient electrophoresis technique can be employed for the separation of T and B lymphocytes from different mouse strains.

TU-POS-B8 SPIN TRAPPING IN BIOLOGICAL SYSTEMS. OBSERVATIONS OF FREE RADICALS PRODUCED DURING NITROSOAMINE CARCINOGEN INTERACTION WITH RAT LIVER MICROSOMES OR NUCLEI AND DURING L-DOPA (L-3-4, DIHYDROXYPHENYLALANINE) AUTO-OXIDATION. Robert A. Floyd, Oklahoma Medical Research Foundation, Oklahoma City, OK 73104

Using the spin trap 5,5-dimethylpyrroline-l-oxide we have demonstrated that the nitrosoamine carcinogen, l-nitrosopiperidine, upon incubation with rat liver microsomes and nuclei produces two trapped free radical species. One trapped species is the hydroxyl free radical whereas the other is a free radical of unknown structure of the carcinogen itself. Oxygen was required to produce the hydroxyl free radical but its presence decreased the yield of the carcinogen radical. Both cyanide and α -tocopherol acetate caused a decrease in the yield of the carcinogen free radical.

Autooxidizing L-DOPA yielded one discernible trapped radical having $A_{\text{max}} \approx 15.5$ gauss and $A_{\text{max}} \approx 18.6$ gauss. (This work was supported in part by NIH Grant No. CA-18591)

TU-POS-B9 CLASSIFYING CELLS USING RF IMPEDANCE. Robert A. Hoffman, Biophysics and Instrumentation Group, Los Alamos Scientific Laboratory, University of California, Los Alamos, New Mexico 87545.

The radio-frequency (rf) impedance of a suspension of a single cell or cells depends upon the size, shape, and internal structure and composition of the cell. We have developed a flow-system instrument in which the passage of a particle or cell through a small ($\sim 100 \mu\text{m}$ diameter) orifice in a stream of saline produces a change in the complex rf impedance of the orifice. The impedance change is registered either as a change in amplitude and phase of an rf signal or equivalently as the change in in-phase and quadrature components of the signal. The first prototype of this instrument has detected phase and amplitude changes of test particles such as plastic spheres and mulberry pollen. We will report on the use of a refined version of this instrument for detecting mammalian cells and will discuss a method for classifying cells according to their rf impedance characteristics. (This work was performed under the auspices of the U. S. Energy Research and Development Administration.)

TU-POS-B10 MEASUREMENT OF THE ATP CONTENT OF SINGLE RED CELLS F.H.Kirkpatrick, C.Gabel*#, A.G.Muhs*, F.Kalk*#, & R.Kostak*# Dep't Radiation Biology & Biophysics, and (#)Institute of Optics, U.Rochester, Rochester NY 14642

Recent improvements in technique allow us to collect over 10^7 photons after lysis, by a laser pulse, of a red cell suspended in a luciferin-luciferase medium. Use of a cooled RCA C31034 photomultiplier and of excess synthetic luciferin have been important. The maximum signal to noise ratio is over 30, allowing accurate observation of the ATP content of cells during metabolic depletion. The relation between average single cell count and bulk cell ATP is strictly linear. Fresh cells have a large spread in their ATP count, but much of this spread may be due to the underlying volume distribution of the red cells. Accelerated ATP depletion at 37° in the presence of metabolic inhibitors decreases the spread, thus excluding certain mechanisms of ATP loss. "Old", i.e. dense, red cells separated from bulk blood have normal ATP contents, implying that ATP depletion may not determine red cell survival *in vivo*. Hereditary spherocytes are low in ATP content and normal in count distribution.

Supported by NIH and ERDA/DOE (Report #UR-3490-1291)

TU-POS-B11A NOVEL RADIOIMMUNE ASSAY. I. Glaever, General Electric R&D Center, Schenectady, NY 12301, and C. R. Keese,* State University of New York, Cobleskill, NY 12043 (Intr. by E. Uzgiris).

A novel method of radioimmune assay to detect antigen-antibody interactions is described. It departs from conventional assays in that the radiiodine is reacted with protein following, rather than before, the antigen-antibody reaction. First a monolayer of antigen is adsorbed on a glass substrate which is then exposed to a solution containing antiserum. Next the slide is removed, washed, and the surface bound protein is tagged with ^{125}I using the chloramine-T method. Finally, after washing again, the antigen-antibody complexes on the substrate are disrupted by exposure to an acid and the amount of ^{125}I removed from the substrate is determined. The level of radioactivity obtained in this manner is a measure of the concentration of antibodies specific for the antigen in the antiserum. Early results using a BSA/anti-BSA system indicate detection of antibody of less than 100 ng/ml in one hour exposure to an antiserum.

TU-POS-B12 EQUILIBRIUM ULTRACENTRIFUGATION OF POLYMERS IN ASSOCIATION-DISSOCIATION EQUILIBRIUM: A NEW METHOD OF DATA REDUCTION. C.L. Stevens, Department of Life Sciences, University of Pittsburgh, Pittsburgh, PA. 15260.

Equilibrium centrifugation is a useful method for determining the stoichiometry and stability constants of associating macromolecules. Very often, important information is to be obtained when solute concentration is low and when only concentration difference is available from the Rayleigh interferogram. There is a function of concentration differences which overcomes these limitations in a straightforward way. The function, referred to as Ξ , can be expanded in a power series in a dimensionless positional parameter, X . The Ξ function has a mathematical form characteristic of the polymerization and takes particularly simple form for monomer-dimer monomer-trimer, monomer-trimer and condensation polymerization. Absolute concentration is obtained as a parameter of the fit. If polymerization is chemically reversible, stability constants are directly obtainable.

TU-POS-B13 PHOTON CORRELATION SPECTROSCOPY OF LIGHT SCATTERED FROM MICROSCOPIC REGIONS. T.J. Herbert and J.D. Acton*, Dept. of Biology, University of Miami, Coral Gables, FL 33124.

Photon correlation spectroscopy is used to study the motion of macromolecules and cellular organelles in individual living cells and in microscopic regions of tissue. Scattered light is collected by the objective of a tissue culture microscope and directed into a photomultiplier tube through a series of lenses and apertures. One aperture, placed at the image plane of the microscope ocular, is used to select a specified region of the scattering volume. A lense is used to image the back focal plane of the objective onto the photomultiplier tube face where a second aperture selects for angular acceptance and coherence area. Analysis of the coherence area shows that we can describe criteria for collection of one coherence area in terms of the numerical aperture of the objective. This system has been applied to the determination of diffusion constants of macromolecules and to such systems as muscle cells, protozoa, and cilia.

(Supported by the Research Corp. and the Pet. Res. Fund of the American Chemical Society.)

TU-POS-B14 SMALL-VOLUME CUVETTE FOR HIGH RESOLUTION THERMAL DENATURATION OF NUCLEIC ACIDS. A. T. Ansevin and D. L. Vizard, M. D. Anderson Hospital and Tumor Institute, Houston, Texas 77030

One of the practical limitations of thermal denaturation experiments is the amount of sample consumed in the analysis. Usual techniques would employ about 10 to 12 μg of DNA for conventional denaturation and around 30 μg per high resolution determination. Sample requirements are especially demanding for experiments on electrophoretically isolated restriction fragments. With a new small-volume cuvette and holder we have now obtained useful high resolution thermal denaturation profiles on 1 μg of DNA or determinations of T_m with about 50 nanograms of DNA. Three samples and a blank fit into the standard sample compartment of a Gilford spectrophotometer. Unique features are: one-piece all quartz cuvettes, 45 μl loading volume, 13 mm optical path, easy cleaning of cuvettes without removal, no significant modification of the spectrophotometer. The chief limitation is an approximately doubled noise level due to slight irreproducibility of positioning of the moving carrier. (Supported by NIH Grant GM 23067.)

TU-POS-B15 RESONANCE RAMAN SPECTRA OF FERRIC CYTOCHROME c: A PROBE OF d TO d TRANSITIONS ON THE IRON. Fran Adar, Dept. Biochem. Biophys., U. of Penna. Phila., PA 19104

Linewidths of resonance Raman bands of ferric and ferrous cytochrome c have been measured and compared. The RR lines of ferric heme are observed to be broadened by shuffling of the hole between the t_{2g} orbitals. Selection rules relating the various electronic excitations to vibrational types are derived. The lower excited state is estimated to be in the vicinity of the 750 cm^{-1} depolarized vibrational mode. The highest of the Krausz' doublets is close to 1300 cm^{-1} above the ground state and is observed to have significant effects on the widths of the inverse polarized modes at 1123 and 1580 cm^{-1} and the polarized mode at 1371 cm^{-1} . These energy levels compared favorably with those derived from electron spin resonance g values (624 and 1298 cm^{-1}). It is proposed that similar comparisons of linewidths of RR bands of certain hemeoproteins (e.g. Co substituted hemoglobin and myoglobin and half-reduced cytochrome oxidase) where EPR signals of photolyzed and deoxy species are dissimilar even though their optical spectra are indistinguishable may be useful in characterizing their electronic structures.

TU-POS-B16 REMOTE CONTROL SYSTEM FOR MICROELECTRODE IMPALEMENT. R. Chilson*, O.W. Oakeley*, M. Lieberman, and E.A. Johnson*. Dept. Physiology, Duke Univ. Med. Ctr., Durham, NC 27710

Transmembrane potentials recorded from small cells (ca. 10 μm diameter), either in isolation or within multicellular preparations, are often unreliable because of difficulties associated with the electrode impalement. A micromanipulator has been developed to precisely control the static position and dynamic motion of the microelectrode. The new design utilizes an electromagnetic transducer in the form of a deflecting parallelogram. Two cantilevers of flexible stainless steel are firmly attached to a supporting structure such that interaction of two magnetic fields (one fixed and one variable) can move the free side of the parallelogram to which a microelectrode is mounted. This system produces a virtually pure axial motion without incorporating sliding elements. Signals from an electronic control unit provide smooth, bipolar changes in the static position of the microelectrode as well as variable velocity thrusting motions of programmable waveforms. The small size allows it to be mounted on a conventional micromanipulator. Supported in part by grants from NIH (HL-12157 and HL-07101).

TU-POS-B17 Rapid Fluorometric Determination of Bilirubin Levels and the Reserve Binding Capacity in the Blood of Newborns.

W. E. Blumberg, J. Eisinger, J. Flores, A. A. Lamola, S. Patel and D. M. Zuckerman, Bell Laboratories, Murray Hill, N. J. 07974.

Binding of (unconjugated) bilirubin (BR) to human blood fractions has been studied using spectrofluorometry, and the results obtained were used to interpret the titration curve of BR in whole blood as determined by front face fluorometry. It is found that BR fluorescence from whole blood reflects only that BR tightly bound to albumin the normal BR transport protein. A significant amount of BR may be bound to erythrocytes as well as to plasma proteins other than albumin, and is essentially non-fluorescent. Detergents can extract BR from all blood sites. Since BR is fluorescent in detergent micelles, total blood BR can be assayed. A significant difference between albumin-bound BR and total blood BR reflects a saturation of the albumin binding or a reduced albumin binding affinity. The reserve albumin binding capacity for BR can be obtained from the incremental fluorescence measured upon adding a saturating quantity of BR to the specimen. All three parameters (albumin-bound BR, total blood BR, and reserve albumin capacity) can be measured simply and within a few minutes on less than 100 μl blood by the use of a dedicated front face fluorometer (hematofluorometer), facilitating effective management of neonatal jaundice (abnormally high bilirubin levels in newborns which can lead to brain damage). Prototypes of the BR-hematofluorometer in two intensive care nurseries have yielded results in excellent agreement with those obtained by present, more laborious methods, which are impractical for routine use.

TU-POS-B18 AN INEXPENSIVE MICROPROCESSOR BASED MULTIPARAMETER LASER FLOW CYTOPHOTOMETRY SYSTEM. J.C.S. Wood*, J. F. Leary*, R. Habbersett*, and P. Todd. The Pennsylvania State University, University Park, PA 16802

A laser flow cytophotometry system was constructed by combining a rebuilt Bio/Physics Systems, Inc. Cytograf and Cytofluorograf, a specially designed fractional rise time and fractional-height pulse width measuring circuit and an IMSAI 8080 microprocessor with teletype and video monitor. Six optical parameters can be produced for every cell: fluorescence intensity at two wavelengths, large angle light scatter intensity, and any three selected pulse-rise or pulse-width related measurements. Simple software in BASIC allows the acquisition of correlated pulse heights and their storage and retrieval in a variety of forms, e.g., a 64x64 channel 2-dimension histogram printed by a standard teletype or dynamic display on a video monitor. Examples of stain-independent cell size measurements, nuclear/cytoplasmic diameter ratio determinations, and other standard cytophotometric parameter evaluations of mixed cell populations will be described. Work supported by USPHS Grant R01-CA-17536 and Contract N01-CB-43984 from the National Cancer Inst.

TU-POS-B19 A NEW METHOD OF STUDYING THE LOW PRESSURES OF MONOMOLECULAR FILM AT AIR/WATER INTERFACE. G. Munger* and R.M. Leblanc, Département de Chimie-Biologie, Université du Québec à Trois-Rivières, P.Q., Canada G9A 5H7

The determination of the properties of gaseous films at air/water interface requires very special techniques as far as the measurements of the surface pressure are concerned. We have designed an apparatus based upon the characteristics of Langmuir trough. The measuring system consists of a lamp, three optics fibers and two high-gain phototransistors. The surface pressures that have been measured (accurately with great ease) range from 0.0010 - 0.1400 \pm 0.0005 $\times 10^{-5}$ newton/cm. One successful application of the apparatus had been the determination of the molecular weight of proteins, particularly the bovine serum albumine, ovalbumine, cytochrome c and bovine rhodopsine.

TRANSPORT SYSTEMS III

TU-POS-C1 ENERGY COUPLING FOR GROWTH-ASSOCIATED ENHANCEMENT OF AIB ACCUMULATION IN HUMAN FIBROBLASTS. M. L. Villereal and J. S. Cook, Univ. Tenn.-Oak Ridge Graduate School of Biomed. Sci., and Cancer and Toxicology Section, Biology Division, ORNL, Oak Ridge, TN 37830 USA.

The accumulation of α -aminoisobutyric acid (AIB) in log-phase HSWP cells is 2.5X that in quiescent cells. It can be shown that, in the presence of the K-ionophore valinomycin (Val): $\ln(AIB_i/AIB_o) = m/k \ln(Na_o/Na_i) + m/k \ln(K_i/K_o)$, where $m/k = Na/AIB$ coupling ratio. Varying K_o in the presence of Val and measuring (AIB_i/AIB_o) gives $m/k = 0.4$ for both log-phase and quiescent cells in 50mM Na and $m/k = 0.6$ for cells in 110mM Na. Apparent (Na_o/Na_i) values, estimated from the above equation, show no growth-associated change in Na concentration ratio. In 110mM Na the estimated cytoplasmic $[Na]$ is 8mM. Plots of $\ln(AIB_i/AIB_o)$ vs. V ($\approx -RT/F \ln K_i/K_o$) are linear and serve to calibrate the AIB ratio as a measure of p.d. Estimates of p.d. (in 50mM Na_o) give $V = -22mV$ for quiescent cells and $-49mV$ for log-phase cells. In summary there is no growth-associated change in apparent Na concentration gradient or Na/AIB coupling ratio; the enhanced AIB accumulation appears to be energized solely by the increased p.d. [Supported by NCI, DOE, and grant #CA 05296.]

TU-POS-C2 SUBSTRATE-DEPENDENT FUNCTION OF AMINO ACID TRANSPORT SYSTEM A IN EXCHANGE. R.H. Matthews, J.H. Im*, G.E. Milo*, and N.J. Lewis*, Ohio State University, Columbus, Ohio 43210.

S37 ascites tumor cells have two transport systems for neutral amino acids designated the A and L systems. These two transport systems had broad overlapping specificities, but appeared to differ in functional characteristics. System L was known to function well in exchange. Previous reports from ourselves and others suggested that system A did not function in exchange. We now find that if methionine is the intracellular amino acid, both systems A and L function in exchange. Uptake of labeled histidine across a broad concentration range yields biphasic double-reciprocal plots, permitting observation of the function of the two transport systems. Preloading of the S37 cells with unlabeled methionine causes both limbs of the biphasic plot to be deflected in slope and in elevation. When the S37 cells are preloaded with labeled methionine and exposed to varying concentrations of unlabeled histidine, a double-reciprocal plot of the augmented efflux is again biphasic. This contrasts with the linear result obtained after preloading with labeled histidine. Supported by DHEW grant CA 17925.

TU-POS-C3 STIMULATION OF ACTIVE TRANSPORT IN CULTURED

HEART CELLS. J.F. Aiton*, C.R. Horres, M. Lieberman, Dept. Physiol., Duke Univ. Med. Ctr., Durham, NC 27710

Muscle enriched cultured heart cells exposed to a K-free solution for 10 min. undergo a rapid decrease in $[K]_i$ and a concomitant increase in $[Na]_i$. Reperfusion with 5.4 mM K produces a transient hyperpolarization in excess of E_K and recovery of the intracellular ion content. Stimulation of Na-K transport during this recovery has been studied by measuring net changes in $[Na]_i$ and $[K]_i$ and the unidirectional ^{42}K influx. The kinetics of Na loss and K gain were consistent with a Na-K pump stoichiometry of 3Na:2K, there being a five-fold stimulation of ^{42}K influx. This is in contrast to the two-fold stimulation of ^{42}K influx measured in non-muscle preparations under similar conditions. Na-K transport was near full activation at 5.4mM $[K]_o$ and half maximal at 2mM $[K]_o$. The stimulation seen after transient Na loading could generate a current of ca. $2.5 \mu Acm^{-2}$ as compared to an estimated steady state value of $0.5 \mu Acm^{-2}$. These results suggest that the Na-K transport system may contribute to the electrical characteristics of myocardial cells. Supported in part by a grant from NIH (HL12157).

TU-POS-C4 MUSCLE CHLORIDE INACTIVATION. P. Vaughan and D. Loo*, Vancouver, Canada.

Inactivation of chloride conductance in *Xenopus* muscle has been studied in two-pulse (conditioning (V_1) and test (V_2), pulses) voltage clamp experiments. In variable- V_1 experiments the dependence of the current at the on set of V_2 ('instantaneous current') was sigmoidally related to V_1 (inactivation relation). The slope of the relation was twice as steep in acid as in alkaline solutions, but was independent of the resting potential. In variable- V_2 experiments the current-voltage relation was linear over a wide range and for different values of V_1 these relationships converged in the outward current region; they also had zero-current potentials that became increasingly negative with respect to the holding potential as V_1 was made more negative.

TU-POS-C5 EFFECT OF INSULIN ON OUBAIN INSENSITIVE Na FLUXES IN FROG SARTORIUS. J. L. RABOVSKY*, R.D. MOORE (Intr. by D.C. Lee). Biophysics Lab. SUNY, Plattsburgh, 12901.

In K-free Ringer containing 10^{-3} M ouabain, insulin increased ^{22}Na efflux by 50% without changing Na_i , suggesting that insulin may be stimulating a Na^+ Na exchange mechanism. This possibility was supported by the finding that in the same conditions, insulin stimulated ^{22}Na influx by 34%. In Na-free, K-free Ringer containing 10^{-3} M ouabain (Na^+ replaced by Mg^{++}), insulin still produced a 77% increase in ^{22}Na efflux. This stimulation of ^{22}Na efflux by insulin was unaffected by the removal of external Ca^{++} and the replacement of Tris buffer by a phosphate buffer, indicating that Tris and Ca^{++} are not required for insulin stimulation of Na^+ efflux in K-free, Na-free Ringer containing ouabain. These results suggest at least two possibilities: 1) insulin stimulates, in addition to Na:Na exchange, a mechanism which exchanges Na^+ for some other external cation, 2) insulin alters the existing Na:Na exchange mechanism so that it can exchange Na_i for some other external cation.

TU-POS-C6 DETERMINATION OF EXTRACELLULAR SPACE OF FROG SKELETAL MUSCLE. B. Graves* & R.D. Moore, Biophysics Laboratory, SUNY, Flattsburgh, 12901.

In frog skeletal muscle, the extracellular space, ECS, was determined by simultaneous wash-out of ^3H -sucrose and ^{14}C -DMO (^{14}C 5,5-dimethyl 1-2,4-oxazolidinedione). The efflux kinetics of ^3H -sucrose was fitted by a curve-peel technique to a sum of exponentials. For a good fit, three exponentials were required, the mean \pm S.E. of the three time constants, t_1 , for 25 experiments was: 105 ± 0.08 min, 5.61 ± 0.29 min, and 79.0 ± 10.0 min. Because of its long time constant, and comparatively small size, the third component is considered to be due to sucrose effluxing from the cytoplasm. Thus, the sum of the first and 2nd components was chosen to represent the ECS. When compared to the ECS determined by a similar analysis of the wash-out of DMO, a plot of ECS as determined by DMO versus ECS as determined by sucrose, gave a slope (0.905 ± 0.21) not significantly ($P > 0.5$) different from 1.0 over a range of ECS between 13% and 55% muscle wet weight.

ECS determined by either method varied markedly with the size of the muscle following approximately the relation: $\% \text{ECS} = 1400 \text{ mg}/\text{muscle wet weight in mg}$.

TU-POS-C7 ASSAY OF MYOPLASMIC ATP IN BARNACLE MUSCLE FIBERS BY THE FIREFLY METHOD. E.E. Bittar & T. Keh*, Dept. of Physiology, Univ. of Wisc., Madison, Wisc. 53706

Luminescence is detected in a black Perspex box with an RCA 6342A PM tube the output of which is recorded by a Watanabe pen recorder. Luciferase-luciferin (DuPont) in 3mM-Hepes solution, pH 7.2 is introduced into the myoplasm of a cannulated fiber by means of a special injector. The injector is operated by a micromanipulator which in turn is driven by an Aminco motor unit. Peak flash occurs within 5 sec of turning on the switch; this is followed by a brief but rapid decline in luminescence, presumably caused by end product inhibition, and by a slower decay phase 1-2 min later. Luminescence is found to be reduced by injecting dehydrochloriferin, Cl^- , PPi or raising pCO_2 . Attempts at internal calibration failed. External calibration, however, using glutamate as a Cl^- substitute resulted in plots of ATP vs $h\nu$ (mV) which were linear in the ATP concentration range of 10^{-5} to 10^{-2} M. Flash height (FH) measured in six fibers (from the same barnacle) averaged 340 ± 10 mV (SEM). A value of 340 corresponded to 9×10^{-4} M-ATP. In six fibers from another specimen FH averaged 436 ± 24 mV. This corresponded to 2×10^{-3} M-ATP. (Supported by NSF and ONR).

TU-POS-C8 ESTIMATION OF THE SIZE OF A K^+ , Na^+ CHANNEL IN SARCOPLASMIC RETICULUM VESICLES. D. McKinley* & G. Meissner* (Intr. by A. Finn), University of North Carolina, Chapel Hill, N. C. 27514

A portion of purified rabbit muscle sarcoplasmic reticulum vesicles are known to be highly permeable to K^+ and Na^+ , indicating the presence of a channel for these ions¹. We have now attempted to estimate the size of this channel using various organic cations. Cation permeabilities were measured by comparing membrane potentials formed in the presence of different ions. Potentials were formed by diluting K gluconate-filled vesicles into Tris gluconate media plus the test cation and were measured using the dye, 3,3'-dipentyl-2,2'-oxacarbocyanine. The channel appeared to discriminate between cations of different size and shape. For example, dimethylaminoethanol permeated the channel, but trimethylaminoethanol and tetramethylammonium did not. Comparison of the van der Waals dimension of the various cations and their permeability indicates that the cross sectional area of the channel may be approximately $5 \times 6 \text{ \AA}$.

(Supported by Established Investigatorship (to GM) of American Heart Association and USPHS Grant #AM18687).

¹D. McKinley and G. Meissner (1977) FEBS LETTERS 82, 47.

TU-POS-C9 K^+ -ATPase AND H^+ TRANSPORT IN GASTRIC MICROSOMES. H.C. Lee*, H. Breitbart* and J.G. Forte. Department of Physiology-Anatomy, Univ. of California, Berkeley 94720.

The Mg^{2+} -dependent, K^+ -stimulated ATPase found in microsomal vesicles from pig gastric mucosa has been studied in relation to observed active H^+ transport into vesicular space. Uptake of fluorescent dyes (acridine orange and 9-aminoacridine) was used to monitor the generated pH gradient. Valinomycin (val) stimulates both the dye uptake and K^+ -ATPase (val- K^+ -ATPase); stimulation requires the presence of permeable anions. Both the val- K^+ -ATPase and dye uptake follow similar dependence on $[\text{K}^+]$. Arrhenius plots show a break $\sim 15^\circ\text{C}$; E_a above and below the break are similar for both cases. A calculated H^+ uptake and the val- K^+ -ATPase have the same pH optimum. SH-reagents (NEM and DTNB) and amine-group reagents inhibit preferentially the val- K^+ -ATPase and also eliminate dye uptake. We conclude that the K^+ -ATPase, as manifest by val stimulation, pumps H^+ in and K^+ out of gastric microsomes. A computer model using Nernst-Planck conditions for passive pathways and simple kinetics for the pump was developed. The model predicts the observed correlations, stimulation and inhibition. (Supported by USPHS grant AM 10141.)

TU-POS-C10 CALCIUM PERMEABILITY OF NORMAL AND DYSTROPHIC MICROSOMES. R. Sabbadini, Dept. of Biology, San Diego State University, San Diego, CA 92182 and G. Inesi, Lab of Physiology and Biophysics, University of the Pacific, San Francisco, CA 94115.

Microsomes isolated from genetically dystrophic chicken muscle are unable to support calcium transport against high intravesicular calcium gradients, while the initial rates of Ca -ATPase and calcium transport are not impaired. We have investigated the possibility that the reduced Ca loading capacity could be due to changes in Ca^{2+} permeability. We devised a technique for measuring Ca^{2+} efflux from vesicles which are first actively loaded with Ca^{2+} and ATP (250uM) and then treated with a nucleotide depletion system containing apyrase (5 units/ml) and .1mM EGTA. Under these conditions, Ca^{2+} efflux is composed primarily of a single component with a $T_{1/2}$ of .5 min. Calculations of Ca^{2+} permeability yield a value of $6 \times 10^{-8} \text{ cm sec}^{-1}$. Ca^{2+} permeability is increased by nucleotide analogues (AMP-PNP), phosphate, and the ionophore X-537A. Moreover, the permeability of dystrophic microsomes is not different from that of normal microsomes and therefore cannot account for the reduced calcium loading capacity.

TU-POS-C11 THE SIGMOID DOSE-RESPONSE RELATION FOR GLUCOSE INDUCED INSULIN SECRETION FROM PANCREATIC ISLETS. J.A. DeSimone and S. Price*, Dept. of Physiology, Medical College of Virginia, Richmond, Virginia 23298.

Glucose stimulated insulin release from pancreatic islets typically shows a sigmoid dose-response curve which saturates at high glucose. This has been interpreted as evidence for a cooperative mechanism and Hill's equation has been used to fit it. With square waves of glucose in the medium a Hill's constant of 3.1 was found, with $K_m = 9 \text{ mM}$. Studies on β -cells or fragments show no evidence of a sigmoid and give K_m about 2 mM. We present a reaction-diffusion theory which accounts for the data. We model the islet as a tissue sphere with an outer layer of α -cells around a core of β -cells. Glucose diffuses into the islet and is consumed by all cells. It is assumed to stimulate insulin release by Michaelis-Menten kinetics. The observed sigmoid results from glucose attenuation by diffusion and metabolism. A cubic relation is predicted for insulin release as glucose in the medium approaches zero, as is a global K_m of 10 mM and a local K_m of 2.4 mM. Each prediction is confirmed. We conclude that much or all of the sigmoidal response can be explained by islet geometry, metabolism and diffusion.

RHODOPSIN AND VISUAL RECEPTORS

TU-POS-D1 RESONANCE RAMAN SPECTROSCOPY OF RHODOPSIN AND BACTERIORHODOPSIN CHROMOPHORE ANALOGS. R. Cookingham, A. Lemley, and A. Lewis (Intr. by B. Siegel), Cornell Univ., Ithaca, N.Y. 14853.

Resonance Raman spectroscopy has been used to study chemically modified retinal analogs involving chain substitutions, ring substitutions or Schiff base linkages. In addition, retinal fragments and fully deuterated retinals were investigated, and infrared spectra of the four isomers of retinal were obtained. Reasonable assignments for all the vibrational features observed in the spectra were made by combining the above information together with normal coordinate calculations and an investigation of the temperature dependence of the 11-cis-retinal spectra. In some instances our results were applied to interpret the spectral features of the Schiff bases of retinal and the spectra of visual pigments and bacteriorhodopsin. Low frequency resonance Raman spectra are also reported for all of the isomers of retinal, for the protonated and unprotonated Schiff bases of trans retinal, for 8-ionone and for trans-3-dehydroretinal. The data obtained agree well with the theoretical predictions of Warshel and Karplus¹. (1) A. Warshel and M. Karplus, *J. Am. Chem. Soc.* **96**, 5677 (1974).

TU-POS-D2 X-RAY DIFFRACTION ANALYSIS OF α -HELIX IN RHODOPSIN. S.M. Gruner, D. Barry*, Geo. T. Reynolds, Physics Dept., Princeton Univ., Princeton, N.J. 08540; J. K. Blasie, Biochem. & Biophy. Dept., Univ. of Pa., Phila., Pa. 19174.

Diffuse X-ray reflections ascribable to α -helix in rhodopsin in isolated, water-washed and re-oriented frog rod photoreceptor discs were first observed on X-ray film by Santillan (1975, Ph.D. Thesis, Univ. of Pa.). Considering the instability of the specimens, the long film exposure times required rendered quantitative interpretation of the data difficult. Using a 2-dimensional intensified-TV X-ray detector we have been able to collect the data in 1/50 the time required by film. The reflections consist of one predominantly equatorial at $\sim 1/10 \text{ \AA}^{-1}$ and one predominantly meridional at $\sim 1/5 \text{ \AA}^{-1}$. These data will be analyzed as to: mosaic spread correlations with that of the stacked disc lamellar reflections; orientation distribution of the polypeptide helices in the membrane; tertiary conformation, average length, side-to-side correlations, and average number of helices; changes in the reflections upon membrane bleaching.

Supported by ERDA Contract EY-76-S-02 & NIH Grant EY00673

TU-POS-D3 ¹³C NMR STUDY OF THE CHROMOPHORE OF RHODOPSIN J.W. Shriver, G.D. Mateescu*, R.S. Fager, and E.W. Abrahamson, Chemistry Department, Case Western Reserve University, Cleveland, Ohio 44106

An enriched visual pigment has been synthesized by incorporating 11-cis-[14-¹³C]retinal into opsin. Subsequent purification and delipidation by affinity ¹³C chromatography of the rhodopsin permits obtaining ¹³C NMR spectra without interfering resonances due to unsaturated fatty acid chains. The resonance of the enriched position has a chemical shift significantly downfield (10 ppm) from that expected for a protonated Schiff base of 11-cis-retinal. Theoretical and experimental results imply that a protonated Schiff base chromophore could not have the observed chemical shift and a λ_{max} of 498 nm. C14 is an excellent position for a probe which would be indicative of a protonated Schiff base since its shift is relatively insensitive to counterion placement along the retinylidene chain due to the nearness of the nitrogen. These results would appear to contradict earlier conclusions drawn from chemical and resonance Raman experiments.

TU-POS-D4 COLLECTIVE DIELECTRIC BEHAVIOR OF ROD OUTER SEGMENTS. D.S. Kirkpatrick*, J.E. McGinness*, W.D. Moorhead*, H.M. Garza*, and P.H. Proctor*¹; (1) Dept of Ophthalmol., Baylor College of Med, Houston, TX; (2) Dept of Physics, Univ of Texas Cancer Center, Houston, TX; Dept of Physics, Youngstown State Univ, Youngstown, OH.

Concentrated suspensions of rod outer segments demonstrated a "slow" dielectric process with a relaxation time, $\tau \approx 10^{-8}$ s. Dielectric measurements were made in the time domain. The dielectric constant, ϵ , of the slow process 1, varied with the hydration level of the suspension, reaching a maximum greater than 1000 (too large to be explained by linear combinations of water and membrane with ϵ of 78 and 2, respectively, 2, varied strongly with temperature, but in a manner opposite to water or salt solution, and 3, correlated with conductivity and ionic strength of the suspending solution. Interfacial polarizations, eg., Maxwell-Wagner, were inconsistent with our data. We suggest a collective or many-body interaction between water, ions, and membrane macromolecules to explain the magnitude of ϵ , its dependence upon hydration and temperature, and its correlation with conductivity. The sensitivity of ϵ to temperature and ion concentration suggests ϵ as a modulator of ionic mobility near membrane surfaces. Supported by The Retina Research Foundation.

TU-POS-D5 REFRACTIVE INDEX GRADIENTS IN FROG ROD OUTER SEGMENT DISC MEMBRANES. M. W. Kaplan, Neurol. Sci. Instit., Good Samaritan Hospital, Portland, OR 97210

The basal 1/3 to 1/2 of R. pipiens rod outer segments (ROS) have a negative axial gradient of birefringence (Δn) in the basal to distal direction. Plots of Δn as a function of the refractive index of imbibing glycerol-containing solutions yield values for the intrinsic Δn component, form Δn component, disc membrane refractive index ($n[m]$), disc membrane volume fraction ($f[m]$), and cytoplasmic solids content (ρ) along the ROS axis. The basal Δn gradient is principally a gradient of the intrinsic Δn component. The form Δn component is approximately the same along the ROS axis. Effects upon the form Δn due to a uniformly decreasing $f[m]$ (from .28 to .22) are compensated by effects due to an increasing $n[m]$ (from 1.492 to 1.508). No significant changes in ρ were found. Measurements of rhodopsin concentration and dichroism along the ROS axis showed no correlation with other measured parameters. The change in $n[m]$ is approximately proportional to the age of the disc membrane, and may thus reflect factors regulating disc membrane turnover. (Supported by NIH grant EY01779 and the Oregon Lions Sight Foundation).

TU-POS-D6 LIGHT-INDUCED LIGHT-SCATTERING CHANGES FROM ROD OUTER SEGMENTS (ROS) C.L. Wey* and R.A. Cone, Dept. of Biophysics, Johns Hopkins Univ., Baltimore, MD 21218

Flash illumination of an excised frog retina produces a small change in the amount of light scattered by the ROS. This light-scattering response can also be observed in suspensions of isolated ROS, fragmented ROS, and sonicated vesicles from ROS. In such suspensions, the rise-time of the response is about 0.3 sec, and the maximum extinction increase is about 0.6%, when measured in the IR (650-1000nm). The rise-time varies only slightly with temperature ($Q_{10}=1.2$). The response is sensitive to both Ca^{++} and Mg^{++} , but not to several cation ionophores. The response amplitude increases with flash energy but plateaus when the flash bleaches only 10% of the rhodopsin. (Hoffmann, Uhl, and Hoffmann have observed a similar response from cattle ROS.) Further bleaching flashes fail to elicit a response unless the sample is allowed to dark-adapt for about 10 min. This implies the response cannot be produced independently by each rhodopsin molecule, and this "cooperativity" together with the time course of the response and its recovery in darkness suggest the response reflects some aspect of the visual excitation mechanism.

TU-POS-D7 NEUTRON SMALL ANGLE SCATTERING STUDY OF RHODOPSIN-DEUTERATED DETERGENT MICELLES. H.B. Osborne, M. Chabre Biophysique Mol. et Cell. DRF, CEN Grenoble F 38041 and C.Sardet², Stat.Zool.Marine, Villefranche s/M, F.06230.

Monodisperse solutions of rhodopsin monomers in non-ionic detergent can be prepared. When the scattering density for neutrons of the solvent is made equal to that of the detergent by changing its D_2O content, the detergent contribution is totally cancelled and scattering from rhodopsin alone is measured, only if the detergent part of the micelle has a homogeneous scattering density. Such detergent micelles were obtained by using mixtures of hydrogenated and deuterated alkylpolyoxyethylene detergents which are contrast matched in highly deuterated water. The radius of gyration of rhodopsin (R_G) was 16 ± 1 Å in 79% D_2O and 20 ± 1 Å in 99% D_2O . Measurements on rhodopsin-DDAO complexes gave an upper limit of 21 ± 2 Å for R_G in 5% D_2O . From this data and those of a parallel hydrogen isotope exchange study it appears that rhodopsin is slightly elongated (axial ratio 2:1). The central region (60% of volume) embedded in the detergent is very hydrophobic in nature. This excludes the possibility of an aqueous transmembraneous channel. (supported by : ILL Grenoble, CNRS (ER 199) and DGRST).

TU-POS-D8 DIFFERENTIAL SCANNING CALORIMETRY OF ROD OUTER SEGMENT MEMBRANES AND EXTRACTED PHOSPHOLIPIDS.

George P. Miljanich, Susan V. Mabrey¹, Michael F. Brown, Julian M. Sturtevant*² and Edward A. Dratz, Div. of Natural Sciences, Univ. of Calif., Santa Cruz, CA 95064 and ¹Dept. of Chem., Yale Univ., New Haven, CT 06520

Bovine rod outer segment (ROS) membranes exhibit one reversible endothermic phase transition between 0° and 80°C centered at ~7°. A transition at ~40° is not observed as was preliminarily reported here two years ago. Two irreversible transitions are observed in partially bleached ROS which correspond to the thermal denaturation of opsin at 55° and rhodopsin at 72°. Aqueous dispersions of total extracted ROS phosphatidyl ethanolamine (PE) also exhibit large reversible transitions at ~7°. Aqueous dispersions of pure ROS phosphatidyl serine (PS) and a 3:1 mixture of PE:PS have no detectable transition above 0°. These observations together with our unpublished results on membrane lipid asymmetry suggest that PE and PS are laterally separated in the ROS membrane. Dispersions of ROS phosphatidyl choline (PC) possess a large transition centered at 18°, while dispersions of PC containing 5% by weight cholesterol have similar thermal behavior but with much diminished enthalpy.

TU-POS-D9 THE PHOTOCHEMISTRY OF RHODOPSIN, ISORHODOPSIN, AND THE PURPLE MEMBRANE AT 77°K. J.B. Hurley* T.G. Ebrey, M. Ottolenghi², and B. Honig, Univ. of Illinois, and Hebrew University.

The photoconversions of rhodopsin and isorhodopsin to bathorhodopsin and the purple membrane protein (PM) to its bathoproduct (K) were studied at 77K to gain insight into the nature of these processes. We found that while rhodopsin shows wavelength and temperature-independent photochemistry down to 77K, the quantum efficiency of isorhodopsin decreased from 0.22 at RT to between 0.10 and 0.15 at 77K depending on wavelength. These results are consistent with efficient population of a minimum in the excited state potential surface common to rhodopsin and bathorhodopsin by rotation about the 11-12 bond. There seems to be a small rotational barrier in the excited state for the 9-10 bond. At 77K photosteady state mixtures of PM and K show anomalous quantum efficiencies which we attributed to energy transfer (ET) from PM's to K's within the same trimer cluster. When ET was accounted for, we found $\phi_{PM \rightarrow K} = 0.33$ and $\phi_{K \rightarrow PM} = 0.67$ at 77K (temperature and wavelength independence). From these experiments and others, we conclude that for both pigments the primary effect of light is to change the geometry of the chromophore.

TU-POS-D10 LIPID PEROXIDATION IN RETINAL ROD OUTER SEGMENTS

(ROS). W.L. Stone, C.C. Farnsworth*, E.A. Dratz

U. of Cal., Div. of Nat. Sci., Santa Cruz, CA 95064

ROS membranes are rich in polyunsaturated fatty acids (PUFA) that are highly susceptible to peroxidation catalyzed by micromolar levels of iron. CaEDTA (or transferin) and the maintenance of anaerobiosis are effective in preventing this peroxidation. CaEDTA, in contrast to EDTA, will not remove the endogenous Ca(II) or Mg(II) ions necessary for membrane stability. By employing these antioxidant conditions we have measured higher levels of PUFA for rat, frog and bovine ROS membranes than reported by others. The susceptibility of ROS membranes to oxidative loss of PUFA is dependent upon the levels of endogenous α -tocopherol (α -TOC). ROS membranes containing less than 0.2-0.3 μ g of α -TOC per mg of rhodopsin undergo oxidative loss of PUFA during isolation and manipulations unless antioxidant precautions are taken. The α -TOC content of bovine ROS preparations are found to range from 0 to 0.8 μ g/mg rhodopsin. Other workers have reported that antioxidant conditions favor maintenance of the functional response of ROS to light (Wormington & Cone, submitted to J. Gen. Phys., 1977; Bownds & Brodie, 1975, J. Gen. Phys. 55, 407, 1975; supported by NIH EY 01521).

TU-POS-D11 DOES RHODOPSIN CHANGE ITS STATE OF AGGREGATION

DURING VISUAL EXCITATION? N.W. Downer & R.A. Cone, Biophysics Dept., Johns Hopkins Univ., Baltimore, MD 21218

Excitation of vertebrate photoreceptor cells may involve the association of a single photoactivated rhodopsin(R^*) with other rhodopsin molecules, possibly to form a membrane channel for transmitter release. To look for changes in photopigment aggregation during visual excitation, we have used photoinduced transient dichroism at 568 nm in bullfrog retinas to observe the rotational diffusion rate of rhodopsin following both an initial flash which bleached ~25% of the rhodopsin and a second flash delivered at various times after the initial flash. For delays of 10, 25, 50, 100 & 600 msec after an initial bleaching flash, decay of transient dichroism($t_{1/2} = 4$ msec at 10°C) was indistinguishable from that following the initial control flashes. Since a single R^* is sufficient for excitation, any physiologically active photopigment aggregate would necessarily involve unbleached rhodopsin. The absence of a detectable change in rotational diffusion of rhodopsin in these experiments argues against the role of such an aggregate in excitation. Control experiments indicate that our methods are sensitive to small changes in photopigment aggregation.

TU-POS-D12 LIGHT-STIMULATED ATPASE OF RETINAL ROS.

S. Thacher* (Intr. by S.C. Tu) Harvard Biological Laboratories, Cambridge, Mass. 02138

Retinal rod outer segments (ROS) of the toad, *Bufo Marinus*, have light-stimulated ATPase and GTPase activities. Broken or intact ROS separated on a metrizamide gradient, lysed in low ionic strength buffer, show the same light-enhanced activity. The enzyme is half stimulated by bleaching ~10% of rhodopsin in orange or blue light. The K_m 's for GTP and ATP are .2mM and .03mM. The reaction is specific for the gamma phosphate. The same enzyme may catalyze both since .1mM AMP-PNP halves the ATPase and GTPase (.5mM substrate) and .1mM GMP-PNP has little effect. Stimulation by bleaching requires Mg^{++} , is unaffected by Na^+ , K^+ , or Cl^- , or by inhibitors of the mitochondrial ATPase. EGTA increases light stimulation as much as two fold and added Ca^{++} lessens it. The activity was $.9 \pm .25$ μ moles/mg rhodopsin/hour and increased a factor of $2.1 \pm .3$ in light. Added all-trans does not mimic light. The light effect occurs in low Triton X-100 (5 parts to 1 part rhodopsin) and after lysis of ROS in 1mM EDTA. Another light-activated GTPase is distinct (Wheeler et al., *Nature* 269, 822, 1977).

TU-POS-D13 RAPID LIGHT INDUCED ATP - DEPENDENT PROCESSES IN BOVINE ROD OUTER SEGMENTS. R. Uhl*, T. Borys*, and E.W. Abrahamson, Univ. of Guelph, Guelph, Ont. Canada.

It has been known for several years that in the presence of ATP and Mg^{2+} rhodopsin becomes phosphorylated upon illumination. The time course of this phosphorylation, however, is much too slow for a reaction possibly involved in the transduction process. We here report the existence of a different ATP and Mg^{2+} requiring process in ROS, which is considerably faster: A light stimulated swelling of the ROS disks, completed about 200-300msec. after flash illumination and with a half-lifetime of 40msec. at room temperature. Without ATP or Mg^{2+} no such swelling is observed. The effect has the action spectrum of rhodopsin bleaching, a very narrow pH optimum at pH 7.3 and can be abolished by 1.5 mM Ca^{2+} . The rapid swelling is monitored as a light induced light scattering decrease, using the flash photolysis light scattering technique previously introduced by us. (Hofmann et al. *Biophys. Struct. Mechanism* 2, p. 61-77, 1976), (Uhl et al. *BBA* 469, p. 113-122, 1977). Several possible molecular origins of the observed disk swelling and their meaning for transduction will be discussed.

TU-POS-D14 RECOVERY FROM ADAPTING LIGHT IN LIMULUS PHOTORECEPTORS. A. Fein, and J.S. Charlton*, Marine Biological Laboratory, Woods Hole, Mass. 02543.

The recovery that occurs at the offset of a light stimulus was investigated in superfused *Limulus* ventral photoreceptors. Lowering the extracellular Na^+ concentration prolonged the recovery of the photoreceptor following cessation of illumination. The return of both the sensitivity and the membrane potential to their resting values were prolonged. Both the effects of lowering extracellular Na^+ were reversed by simultaneously lowering extracellular Ca^{++} . In these photoreceptors, membrane voltage noise is observed during steady illumination and is believed to result from the summation of discrete waves of depolarization. For some photoreceptors bathed in low Na^+ saline the voltage noise persists for tens of seconds after stimulus offset. These findings suggest that in low extracellular Na^+ discrete waves of depolarization continue to be produced after cessation of the light stimulus.

TU-POS-D15 EFFECTS OF EXTERNAL Ca ON THE PHOTORESPONSE OF A NUDIBRANCH MOLLUSC. J.A. Schmidt*, Y. Grossman*, and D.L. Alkon, NINCDS, NIH, MBL, Woods Hole, MA.

The effect of Ca-blocking agents and changes in extracellular calcium, $[Ca]_o$, on the photoreponse of *Hermisenda crassicornis* photoreceptors was measured. Photoreceptors were impaled with single microelectrodes and responses of dark adapted cells to 20 ms flashes (500±10 nm) were recorded during continuous perfusion. Reduction of $[Ca]_o$ reversibly increased the latency and the Na-dependent amplitude of the photoreponse in solutions containing both normal and reduced $[Na]_o$, while an increase in $[Ca]_o$ reversed these effects. The organic Ca-blocking agent D-600 (2.1 mM), in the presence of 10 mM Ca, mimicked the effect of lowered extracellular Ca. Lowering $[Na]_o$ caused the hyperpolarization which follows the early depolarizing transient to become larger. The hyperpolarization was larger in high $[Ca]_o$, smaller in low $[Ca]_o$, eliminated by D-600 and had a $[K]_o$ -dependent reversal potential. These findings indicate that a component of the photoreponse is a light-induced influx of Ca through the cell surface. The transient increase in $[Ca]_i$ appears to modulate a K conductance that produces the hyperpolarization. This conductance may also partially short circuit the inward Na current of the early transient.

TU-POS-D16 MONITORING FLUORESCENCE FROM INTACT TASTE PAPILLAE. APPLICATIONS TO THE BIOPHYSICS OF TASTE RECEPTION. J.G. Brand and D.L. Bayley*, Monell Chemical Senses Center, U. of Pa., Philadelphia, Pa. 19104.

The mechanisms that underlie gustatory chemoreception at the peripheral level are, to a large extent, a matter of speculation. We are using front face (surface) fluorescence techniques to examine some aspects of chemical reception in an intact taste papillae preparation (circumvallate papillae) from bovine tongues.

Emission of both intrinsic fluorescence [from total tryptophan plus tyrosine and from reduced pyridine nucleotides] and fluorescence from extrinsic sources, such as that from applied probes or dyes, can be observed originating on the taste bud-rich lateral epithelial surface of bovine circumvallate papillae. A flow cuvette arrangement permits rapid exchange of media bathing the isolated intact papillae. We observed that many fluorescent dyes are taken up by these papillae only in the region of the taste bud apex and not by the surrounding keratinized epithelium. Localization of the dyes on the tissue and their reports of intrinsic data consistent with other experiments suggest that changes observed upon monitoring dyes during chemical stimulus addition are taste-related.

TU-POS-D17 COMPARISON OF STIMULUS TRANSMISSION THROUGH THE LATERAL AND MEDIAL GENICULATE NUCLEI C. Torda, N.Y. Center PA Training, New York, N.Y., 10028.

Intrathalamic processing of visual and auditory stimuli were compared to ascertain the nature of basic differences and similarities. Bioelectric processes of single neurons randomly selected from the lateral and medial geniculate nuclei, the optic radiation and the corticothalamic fibers were measured during (a) spontaneous activity, (b) stimulation of neurons ascending to the thalamus, and (c) iontophoretic administration of acetylcholine, GABA, amino acids, serotonin or catecholamines. Under specific circumstances statistically significant differences occurred in the method of stimulus processing of the lateral and medial geniculate nuclei. This conclusion was reached by quantitative comparison of the results obtained from the lateral and medial geniculate neurons. To illustrate: serotonin and acetylcholine affect the excitability of the lateral and medial geniculate neurons in a quantitatively different manner. Furthermore, the global responses of lateral and medial geniculate neurons differ during the various phases of the sleep cycle, suggesting the presence of somewhat different regulatory processes, at least partly extralaminar of origin.

TU-POS-D18 CELL INTERACTIONS IN RETINOTECTAL MAPPING. J.H. Rho, Biophysics Dept., Johns Hopkins U., Balto., MD 21218

Surgical rearrangement of *Xenopus* optic tectum (rotating or translocating tectal grafts) was used by many labs. to assay for target properties (TP) in tectum and to argue against optic-fiber (OF) self-sorting and in favor of OF-TP affinities in retinotectal mapping. My electrophysiologic data (on 180°-rotations, 'pancaking' of grafts inside-out, mediolateral exchanges, and rotation/translocation of multiple grafts) confirm, for rotations and in some frogs in the more complex rearrangements, the two types of previously reported results: Place-specific reinnervation (PSR) of graft by OF appropriate to the implantation site but inappropriate to the graft; and Graft specific reinnervation (GSR) in which OF appropriate to graft tissue track down their old connection sites in the new (inappropriate) location. I also find, in the complex procedures, cases of GSR & PSR of the same graft; cases in which the subset of OF mapping to the graft is based on PSR yet within the subset OF map according to the orientation of graft tissue; and cases in which PSR grafts, translocated a second time, receive GSR. That both OF-TP affinities and OF self-sorting operate in map assembly now seems inescapable. (Support by NIH NS12606)

TU-POS-E2 RAT LIVER P-420 CATALYZED ACTIVATION OF THE CARCINOGEN N-HYDROXY-2-ACETYLAMINOFLUORENE. D.L. Reigh*, J.S. Guerra* and R.A. Floyd. (Intr. by J.J. Killion). Oklahoma Medical Research Foundation, Okla. City, OK 73104

The carcinogen N-hydroxy-2-acetylaminofluorene is activated in vitro to the more potent carcinogens N-acetoxy-2-acetylaminofluorene and 2-nitrosofluorene by various model peroxidase systems via a nitroxyl free radical intermediate. P-450 "particles" were prepared from rat liver microsomes by limited trypsin digestion. "High spin" P-420 was prepared by incubation of "particles" with Lubrol WX and p-hydroxymercuribenzoate "Low spin" P-420 was prepared by incubation of "particles" with sodium deoxycholate. Electron spin resonance spectroscopy demonstrated nitroxyl radical formation catalyzed by both P-420 spin types from N-hydroxy-2-acetylaminofluorene and linoleic acid hydroperoxide. These results further implicate the microsomal cytochrome system in "peroxidase-like" one-electron transfers and suggest a possible carcinogen activation pathway for N-hydroxy-2-acetylaminofluorene. (This work was supported in part by NIH Fellowship CA-06048)

TU-POS-E3 HYDROLYSIS OF p-NITROPHENYL ACETATE IN AQUEOUS ORGANIC MIXTURES: CATALYSIS BY IMIDAZOLE AND POLY(HIS-ALA-GLU). H.J. Goren and T. Fletcher*, University of Calgary, Calgary, Alberta, T2N 1N4, Canada, M. Fridkin* and E. Katchalski-Katzir*, Weizmann Institute of Science, Rehovot, Israel.

The hydrolysis of p-nitrophenyl acetate was followed spectrophotometrically between pH 6 and 9. The ester, dissolved in dioxane, ethanol or trifluoroethanol, was added to 0.1 M phosphate or Tris buffer containing imidazole or poly(His-Ala-Glu). With EtOH and F₃EtOH the rate of hydrolysis of p-nitrophenyl acetate increases up to 10 and 20%(v/v), respectively, and decreases thereafter. Imidazole catalysis of ester hydrolysis, however, decreases with increasing organic solvent content. Solution free imidazole is 3 to 4 times a better catalyst than polymeric imidazole, poly(His-Ala-Glu), in low organic/water mixtures. In 40%(v/v) F₃EtOH the two forms of imidazole have equal catalytic activity. The ability for the organic solvents to promote hydrogen bonding may explain both the observed increases and decreases in rates of ester hydrolysis. Indirect evidence for ester synthesis on the polymer backbone is available. (Supported by MRC of Canada MA 5521)

ENZYME MECHANISMS II

TU-POS-E1 INTERACTIONS OF NAD AND NADH WITH 3-PHOSPHOGLYCERYL-GLYCERALDEHYDE-3-PHOSPHATE DEHYDROGENASE. D. Eby* and M.E. Kirtley, Univ. Maryland Sch. of Med., Baltimore, Maryland 21201.

The interactions of NAD and NADH with acylated glyceraldehyde-3-phosphate dehydrogenase were examined kinetically. Stopped-flow studies gave no evidence of cooperativity in the interaction of NADH with the acylated enzyme. Studies of the interaction of NAD with partially acylated enzyme suggest that this coenzyme is an allosteric effector promoting the deacylation not only of the subunits to which it binds but also of neighboring subunits. Dissociation constants for both NAD and NADH with partially acylated glyceraldehyde-3-phosphate dehydrogenase, used as a stable analog of the acylenzyme, were determined by ultrafiltration and gave no indication of cooperativity in the binding of either coenzyme. The interaction of NAD with enzyme alkylated with 4-iodoacetamido-1-naphthol, a half-of-the sites agent, results in partial recovery of dehydrogenase activity. Under physiological conditions the interactions of NAD and NADH with the acylenzyme is significant since the acylenzyme probably has a regulatory role in the control of NAD/NADH concentrations. Supported by NIH Grant GM 20294

TU-POS-E4 ARRANGEMENT OF P-ENOLPYRUVATE AND CRADP ON PYRUVATE KINASE. R.K. Gupta and J.L. Benovic* (Intr. by A. Nath), Inst. for Cancer Research, Philadelphia, Pa. 19111.

CrADP, a non labile paramagnetic analog of MgADP, inhibits the phosphoryl transfer reaction of pyruvate kinase competitively vs. MgADP and noncompetitively vs. P-enolpyruvate (PEP) but activates the enzyme-catalyzed enolization of pyruvate in the presence of Mg²⁺ and K⁺ indicating that CrADP replaces MgADP at the active site of the enzyme. From the paramagnetic effects of CrADP on the relaxation rates (1/T₁) of the ³¹P and ¹H nuclei of PEP in the E·Mg·ADP·Cr·PEP complex, using the τ_s of $\sim 3.5 \times 10^{-10}$ s from the frequency dependence of 1/T₁ of water protons, Cr to P distance of 5.9 ± 0.4 Å and Cr to H distances of 8.4 ± 1.0 Å were obtained indicating molecular contact between a phosphoryl oxygen of PEP and the hydration sphere of the ADP-bound metal. The Cr to P distance indicates the absence of direct coordination of the phosphoryl group of PEP by the ADP-bound metal but supports molecular contact between PEP and MgADP on the enzyme, consistent with an S_N2 mechanism. Since after phosphorylation of ADP, the metal ion is coordinated to the transferred phosphoryl group, the overall migration of the latter during phosphoryl transfer is ~ 3 Å toward the nucleotide bound metal. (Supported by NIH grant AM19454 and RCDA AM00231).

TU-POS-E5 NEAR-INFRARED SPECTROSCOPIC STUDY OF ENZYME-SUBSTRATE INTERACTION. N. Ressler and D. VanderMeulen, Pathology and Biochemistry, University of Ill. Med. Cntr., Chicago, IL 60612

Enzyme-substrate interaction was studied by near-infrared (NIR) absorption spectroscopy, which provides information about excluded volume and water of hydration in the overtone-combination band region (ca. 1-2 μ). Difference spectra were obtained by comparing the spectrum of RNA + RNase vs. RNA + buffer with that of RNase vs. buffer. After mixing RNA + RNase, time-dependent changes were seen: (1) increase in excluded volume, observed at 1.4-1.5 μ and 1.9-2.0 μ , and (2) an increase in the 1.5-1.8 μ region, ascribed to the H⁺ continuum. The latter is supported by pH and D₂O measurements. Difference spectra can help distinguish excluded volume changes from those due to water of hydration. Data suggesting that changes in water of hydration can be detected by NIR difference spectra during other enzyme-substrate reactions will be presented.

TU-POS-E6 METAL COORDINATION OF ATP IN REACTIONS

CATALYZED BY DNA POLYMERASE, PRPP SYNTHETASE, AND PYRUVATE KINASE. T.M. Li, A.S. Mildvan and R.L. Switzer*, Institute for Cancer Research, Philadelphia, Pa. 19111, and Dept. of Biochemistry, U. of Illinois, Urbana, Ill. 61801

Using NMR methods and the stable metal complexes [β, γ Co³⁺(NH₃)₄ATP] and [α, β, γ Cr³⁺ATP], the metal coordination of ATP in enzyme-catalyzed substitutions at each of its three phosphorus atoms has been studied. Substitution at the α -P (DNA polymerase) occurs with metal coordination of the leaving group only. Substitution at the β -P (PRPP synthetase) occurs with metal coordination of the attacked phosphoryl group only. Substitution at the γ -P (pyruvate kinase) occurs with metal coordination of both the leaving group and the attacked phosphoryl group. In all cases the metal coordinates the γ -P, while with PRPP synthetase and kinases β -coordination is also seen. In the PRPP synthetase reaction CD studies with [Co³⁺(NH₃)₄ATP] reveal an inversion at the chiral β -P-atom. These results and molecular contact distances between the bound substrates indicate associative (S_N2) displacements on the β and γ phosphorus atoms of ATP.

TU-POS-E7 pH DEPENDENCE OF THE THERMODYNAMIC PARAMETERS FOR THE BINDING OF SUBSTRATE ANALOGS TO E. COLI ASPARTATE TRANSCARBAMYLASE. N. Allewell, G. Hofmann, A. Zaugg, Middletown, Ct. 06457.

A model implicating two ionizable groups in substrate binding which predicts that the pH dependence of $\Delta\bar{v}_{H^+}$, the net change in the state of protonation of protein and ligand upon complex formation, will be qualitatively different for the native enzyme and catalytic subunit has been proposed (1). To test this model, we have examined the pH dependence of $\Delta\bar{v}_{H^+}$ for the binding of N-phosphonacetyl-L-aspartate (PALA), carbamyl phosphate (CP), and succinate to the native enzyme and catalytic subunit. The data for PALA were obtained by direct titration, those for CP and succinate by flow microcalorimetry from the dependence of ΔH_{obs} on the enthalpies of ionization of a series of buffers. Together with information on the pH dependence of $\Delta G^{\circ}_{binding}$ and the Hill coefficients, evaluated by difference spectroscopy, these data allow inferences to be drawn about the identity of the ionizable groups which participate in the binding of substrates. (Supported by NIH (AM-17335).)

(1) Mosberg, H.I., Beard, C.B., and Schmidt, P.G. (1977) *Biophys. Chem.*, **6**, 1-8.

TU-POS-E8 ADENINE N-OXIDE NUCLEOTIDES AS SUBSTRATE ANALOGS OF PHOSPHOTRANSFERASES. H.H. Mantsch and O. Barzu*, Division of Chemistry, National Research Council Canada, Ottawa, K1A 0R6.

Due to the central role of adenine nucleotides as metabolic control agents, adenine nucleotide analogs are becoming important tools for probing enzyme structure and function. We report here on the participation of such derivatives in the phosphotransferase activity of liver mitochondria. The N-oxide adenine nucleotides are good substrates for mitochondrial phosphotransferases located in the intermembrane space, however they are not recognized by the translocase system and can not be used as substrates by the respiratory chain enzymes in oxidative phosphorylation. The ATP N-oxide analog for instance is an excellent substrate for rabbit muscle phosphofructokinase, but has lost its capability to act as allosteric effector for the same enzymatic system. UV, IR and NMR data are used as evidence for function:structure correlations.

TU-POS-E9 MITOCHONDRIAL INTERMEDIATE PHOSPHATE-WATER OXYGEN EXCHANGE: FREQUENCY DISTRIBUTIONS OF MULTIPLY-LABELLED P_i FORMED BY HYDROLYSIS IN HIGH-ENRICHMENT O-18 WATER. R. A. Mitchell, C. M. Lamos*, and J. A. Russo. Biochemistry Dept., Wayne State Univ., Detroit, MI 48201

ATP maintained at 2 or .05 mM by a regenerating system was hydrolyzed in 90 atom % O-18 water using submitochondrial vesicles as catalyst. P_i released was analyzed as the trimethylsilyl derivative and the frequency distributions of species containing 1,2,3, or 4 oxygen from H₂O / P_i were measured. After correcting for Si-30 spillover and adjusting to 100 atom % water, the peak intensities were .65, .27, .07, .01 (ave. O:P=1.44) for 2 mM ATP and .4, .34, .19, .06 (ave. O:P=1.91) for .05 mM ATP. All 4 oxygen can be labelled but if incorporation occurs via cycles of hydrolysis/esterification, the low O:P at 2 mM ATP signifies marked kinetic restriction, possibly on bound P_i rotation, or on exchange between bound and bulk water. Introduction of F (0 < F < 1) where the limiting values represent respectively complete and no kinetic restriction, permits calculation of species distribution for successive cycles before P_i release. For 2 mM ATP the observed distributions correspond approx. to 3 cycles with F=0.2. Supported by GM19562 & Mich. Heart Assoc.

TU-POS-E10 STUDIES ON THE KINETICS OF BINDING OF ACETYL PYRIDINE ADH TO CHICKEN HEART LACTATE DEHYDROGENASE. P.D. Smith, R.L. Berger Lab. Technical Development, NHLBI Bethesda, MD 20014, J. Everse*, Dept. of Biochem, Texas Tech Univ., School of Medicine, Lubbock, TX 79409

The binding of reduced coenzyme AcPyADH to purified chicken heart lactate dehydrogenase has been studied using fluorescence techniques with the Aminco Morrow and Berger high speed stopped-flow apparatus.

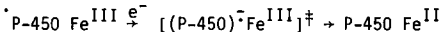
The fluorescence enhancement of the AcPyADH which occurs on binding of the coenzyme to the LDH appears to follow first order kinetics with a rate constant of 50 + 10 s⁻¹ at 20°C pH 7.0. This result is qualitatively in agreement with our earlier stated result (1). In the experiments reported the AcPyADH concentration was varied between 1 and 10 μ M with an enzyme concentration of 1 μ M (4 μ M sites), thus completely saturating the enzyme (2). Pig LDH gave similar results.

Investigation of the nature of protein fluorescence (excited at 280nm) is currently being studied. Preliminary work has suggested that this is the second order process with a rate constant of 8 x 10⁷ M⁻¹ s⁻¹.

1) J. Everse, R.L. Berger, N.O. Kaplan; FEBS Lett **73**, 120 (1977)
2) J.J. Holbrook, H. Gutfreund; FEBS Lett **31**, 157 (1973)

TU-POS-E11 ENZYMATIC PORPHYRIN REDUCTION. R.P. Mason and F.J. Peterson*. VA Hospital and University of Minnesota, Minneapolis, Minnesota 55417.

Our investigations of the reduction of nitro and azo compounds by NADPH and microsomes show that many of these compounds accept a single electron from the flavo-enzyme cytochrome P-450 reductase (NADPH-cytochrome c reductase) just as the endogenous electron acceptor P-450 does. We have found that anaerobic microsomal incubations containing NADPH and uroporphyrin I have electron spin resonance spectra consistent with the enzymatic formation of a porphyrin anion free radical. In addition, we have found that these incubations reduce uroporphyrin I to the dihydro porphyrin, as is shown by the appearance of an absorption maximum at 737 nm. These enzymatic reactions occur in the dark and are not a consequence of photoreduction. These results suggest that the porphyrin ring of cytochrome P-450 or cytochrome c may act as a conduit in the reduction of these ferrihemo-proteins.



The species $(P-450)^-\text{Fe}^{\text{III}}$ is not simply a resonance form of reduced P-450, but is a proposed transition state of the electron-transfer process.

TU-POS-E12 SUICIDAL INACTIVATION OF DNA POLYMERASE BY 2'-3'-EPOXY-ATP. M.M. Abboud*, W.J. Sim*, L.A. Loeb* and A.S. Mildvan, Institute for Cancer Research, Philadelphia, Pa. 19111

Epoxy-ATP is a suicidal inactivator of *E. coli* DNA polymerase I by the following criteria: Inactivation is complete, is first order in enzyme activity, and shows saturation kinetics with an apparent K_D of $30 \pm 10 \mu\text{M}$ for epoxy ATP which is comparable to the K_M of the substrate dATP. The $t_{1/2}$ for inactivation is 1.3 min. Inactivation requires Mg^{2+} and the complementary template. The enzyme is protected by dATP but not by an excess of template. Gel filtration of the reaction mixture after inactivation with [^3H]epoxy ATP results in the co-migration of *E. coli* DNA polymerase I, epoxy ATP, and the DNA template. The binding stoichiometry approaches 1 mole of [^3H]epoxy nucleotide per mole of inactivated enzyme. Hence epoxy ATP initially may serve as a substrate for the polymerase reaction, elongating the DNA chain by a nucleotidyl unit, and subsequently may alkylate an essential base at the primer terminus binding site of the enzyme. Epoxy ATP also inactivates human and viral DNA polymerases but not *E. coli* RNA polymerase or rabbit muscle pyruvate kinase.

TU-POS-E13 REVERSIBLE UNFOLDING OF THE α SUBUNIT OF TRYPTOPHAN SYNTHETASE. C. R. Matthews and M. M. Crisanti*, Chem. Dept., Penn State U., University Park, PA 16802

The reversible unfolding of the α subunit of tryptophan synthetase from *E. coli* has been studied by measuring the change in UV absorption at 286 nm. Equilibrium studies of the unfolding induced by guanidine hydrochloride (Gdn·HCl) or urea at pH 7.2, 25°C, show that the unfolding transition induced by both denaturants is biphasic. A sharp, highly cooperative transition that accounts for approximately two-thirds of the total change in absorption occurs with a midpoint at 0.9 M Gdn·HCl or 2.6 M urea. A second, less cooperative transition then occurs with a midpoint at 1.9 M Gdn·HCl or 3.7 M urea. The unfolding is reversible when measured by optical absorption and by enzymatic activity. Preliminary experiments involving concentration studies and measurement of molecular weight across the transition region by ultracentrifugation indicate that the biphasic nature of the unfolding transition is not due to dimerization. We tentatively conclude that the unfolding of the α subunit proceeds through a stable intermediate. The existence of over two dozen missense mutations of this protein should aid in the characterization of this intermediate. This work was supported by PHS grant GM 23303-02.

TU-POS-E14 CIRCULAR DICHROISM OF GLUTAMATE DEHYDROGENASE-NADH COMPLEXES. L. Zeiri* and E. Reisler, Polymer Department, The Weizmann Institute of Science, Rehovot, Israel and Department of Chemistry and Molecular Biology Institute, UCLA, Los Angeles, California 90024.

CD measurements of bovine liver glutamate dehydrogenase complexes with NADH were undertaken to determine the role of protein aggregation in NADH binding. Recently contested observations of Koberstein and Sund (FEBS Letters 19, 149 (1971) on the existence of two distinct cotton effects of opposite sign and different magnitude, each one associated with a separate NADH binding site/subunit were confirmed with the native protein and its crosslinked monomeric form. Titration of the first NADH binding site/subunit (the "catalytic" site) revealed significant dependence of the molar ellipticity of the bound coenzyme on the state of protein aggregation. It is suggested that this site is located at or near the monomer-monomer interface. In spite of this, the substrate induced changes in the binding of NADH to the catalytic site are only partially mediated through shifts in the state of the protein aggregation. The binding of NADH to the second, weak binding ("regulatory") site leads to inversion of the CD signal. The molar ellipticity of the coenzyme bound to this site is not affected by aggregation.

MUSCLE PROTEINS IV

TU-POS-F1 PROTEOLYTIC FRAGMENTS FROM THE LOBSTER MYOSIN MOLECULE. C.R. Zobei, SUNYAB, Buffalo, N.Y. 14226.

Fragments produced by proteolysis of lobster abdominal muscle myosin with trypsin, $\alpha\text{-chymotrypsin}$ and papain have been investigated by SDS-gel electrophoresis. Monodisperse populations of long rods are produced by $\alpha\text{-chymotrypsin}$ and papain digestion of rabbit myosin, corresponding digestion of lobster myosin yields multi-component species. The low ionic strength insoluble fraction from tryptic digestion of lobster myosin is polydisperse, whereas rabbit LMM is monodisperse. Comparative tryptic digestion of rabbit and lobster myosin long rods shows that the latter have five susceptible cleavage sites in the subfragment-2 region while rabbit rods have only one: both rods appear to have three cleavage sites in the LMM region. Fragments produced by tryptic digestion of rabbit myosin papain long rods have been identified by comparison with fragments isolated from papain digests of rabbit LMM and tryptic digests of rabbit LMM. The results suggest significant differences in stability between the subfragment-2 regions in rabbit and lobster myosin as well as relative differences in stability between the subfragment-2 and LMM region within the individual molecules.

TU-POS-F2 PROPERTIES OF LARGE α -TROPOMYOSIN FRAGMENTS PREPARED BY SELECTIVE ENZYMIC AND CHEMICAL CLEAVAGES. M. Pato* and L.B. Smillie, MRC Group on Protein Structure & Function, Department of Biochemistry, University of Alberta, Edmonton, Canada T6G 2H7.

Several large fragments of rabbit skeletal α -tropomyosin (Tm) have been prepared by selective enzymic and chemical methods. Limited tryptic and chymotryptic digestion resulted in single peptide bond cleavages at positions 133-134 and 169-170 respectively. Prolonged digestion with trypsin produced peptides 13-125, 183-284, 183-244. Non-polymerizable Tm was prepared by treatment with carboxypeptidase. The action of DTNB and KCN cleaved peptide bond 189-190 while CNBr treatment yielded fragments 11-127 and 142-281. Circular dichroism studies showed that the NH₂-terminal fragments have higher helical content and greater thermal stability than fragments from the COOH-terminal half of the molecule. COOH-terminal fragments bind with a significantly higher affinity to troponin-T immobilized on Sepharose 4B than NH₂-terminal fragments. Non-polymerizable Tm is bound with lower affinity than intact Tm. None of the fragments except carboxypeptidase-treated Tm bind to F-actin. (Supported by the Medical Research Council of Canada.)

TU-POS-F3 POLYMERIZATION OF ACTIN: EFFECT OF PREPARATIVE METHOD ON KI INDUCED DEPOLYMERIZATION. Michael Gallagher*, Julie I. Rushbrook*, Thomas C. Detwiler, Alfred Stracher, Dept Biochem, SUNY Downstate Med Center, NY.

It is well established that F-actin prepared from rabbit muscle following acetone treatment is depolymerized by 0.5M KI. However, using natural actomyosin preparations we found that one form of platelet actin (Cold Spr Hrb, Cell Motility 3:475, 1976), and chicken gizzard actin remain polymeric in 0.5M KI, 1mM CaATP. Therefore, polymerization properties of natural actomyosin from rabbit muscle was investigated in the presence of 0.5M KI. Under these conditions the bulk of the actin was polymeric. The results indicate that KI should not be used on actomyosin preparations with the prior assumption that actin will be depolymerized. The effect of the preparative method (acetone/natural) and the effect of tropomyosin or myosin on the actin polymerization properties were investigated as possible explanations for the varying behavior of the two rabbit muscle preparations. (Supported by GM19626)

TU-POS-F4 TITRATION OF PARAMYOSIN AT LOW AND AT HIGH IONIC STRENGTH. S. Krause and L. B. Cooley, Dept. of Chemistry, Rensselaer Polytechnic Institute, Troy, N.Y., 12181

Titration data were obtained at both low ionic strength, 0.001 M KCl, and at high ionic strength, 0.3 M KCl, on paramyosin extracted from Mercenaria mercenaria by several different methods. The low ionic strength titration curves of the different paramyosin preparations were similar to each other but indicated the slight difference between the number of groups titrating in the pH 3.2 to 3.3 region for the different preparations predicted earlier; DeLaney and Krause, *Macromolecules*, 9, 455 (1976). High ionic strength titration curves of the paramyosin preparations were quite different depending on whether the titration was performed with base (pH 2 to 11) or with acid (pH 12 to 3.5). In the titrations with acid, for example, over 70 groups were titrated abruptly near pH 8.5; this does not occur in the titrations with base. The various titration data are probably connected with phosphate groups that are attached to native paramyosin and that are slowly removed from the macromolecule at high pH.

TU-POS-F5 IMMUNOLOGIC CROSS-REACTIVITY AMONG SKELETAL MUSCLE MYOSINS. M. J. Elfvin, R. J. C. Levine, and H. S. King* The Medical College of Pennsylvania, Philadelphia, Pennsylvania, 19129.

Antibodies specific for *Limulus* myosin were used to stain glycerinated myofibrils prepared from skeletal muscles of *Balanus nubilis* and *Homarus americanus* by the indirect immunofluorescence technique. Fluorescence was seen in the A-bands of both the barnacle and lobster myofibrils. Absorption of the primary antibody with an excess of either *Limulus* myosin or *Limulus* actomyosin abolished the specific staining. Anti-myosin stained throughout the A-bands, with the exception of the H-zone, in long sarcomeres, but was restricted to the lateral regions of the A-bands in short sarcomeres. This staining pattern is similar to that produced using anti-*Limulus* LMM on *Limulus* fibrils and may indicate similarity of the LMM region of the myosin molecules from different species.

Supported by USPHS grants: GM21956 and HL15835 to The Pennsylvania Muscle Institute. R.L. has RCDA: NS70476.

TU-POS-F6 THE ATPase ACTIVITY OF SUBFRAGMENT-1 FROM HYPERTROPHIED HEARTS. R.Z. Litten*, J.E. Brayden*, and N.R. Alpert. Univ. of Vermont, Burlington, VT 05401

Myosin and subfragment-1 (S-1) were prepared from rabbit hearts hypertrophied secondary to pulmonary artery constriction. The Ca²⁺-stimulated ATPase activity was reduced while the (K⁺)EDTA-stimulated ATPase activity was unchanged in both the myosin and S-1 from hypertrophied hearts. When hypertrophy myosin was mixed with an equal quantity of control myosin, the Ca²⁺-stimulated ATPase activity of the mixed protein fell halfway between control and hypertrophy values. Similar results were obtained with control and hypertrophy S-1. The actin-stimulated ATPase activity of hypertrophy S-1 was slightly depressed but unlike hypertrophy myosin this depression was not significant when compared to normal S-1. This suggests that papain cleavage may have removed part of the conformational difference that exists between control and hypertrophy myosins.

This work was supported by a grant from National Institutes of Health (T32 HL07073).

TU-POS-F7 ON THE ENTHALPY OF ATP BINDING TO MYOSIN. C.A. Swenson and P.A. Ritchie* Department of Biochemistry, University of Iowa, Iowa City, Iowa 52242

The enthalpy of ATP binding to myosin is important to our understanding of the basic mechanism of energy transduction and heat production in striated muscle. When combined with existing values of the equilibrium constant, a full set of thermodynamic parameters can be obtained for the process. We have made measurements of the heat production when ATP interacts with myosin in a heat burst calorimeter at low mole ratios of ATP to myosin (0.5 - 2.0). Heat production is partitioned into two phases: a fast phase which includes binding and hydrolysis on the enzyme surface and a slow phase which includes product release. An estimate of the binding enthalpy was made by correcting the fast phase for hydrolysis. The enthalpy of ATP binding will be compared to that measured for other nucleotides. Implications for energy transduction will be noted.

TU-POS-F8 CALCIUM BINDING PROPERTIES OF SKELETAL & CARDIAC TN-C. M.T. Hincke,* W.C. McCubbin,* and C.M. Kay, Dept. of Biochemistry, University of Alberta, Edmonton, Alberta Canada T6G 2H7.

Calcium titration of the conformational change in cardiac and skeletal TN-C was followed by CD and difference spectroscopy over a pH range of 5.2 - 7.4. Computer analysis of the CD data reveal contributions from both the high and low affinity sites which are pH dependent in each protein. The finding of a substantial CD contribution from the low affinity sites (~30% of the high affinity contribution at pH 6.94) suggests that skeletal TN-C with Ca^{2+} bound at the low affinity sites is in a different conformation from that when just the high affinity sites are occupied. These effects appear to arise through protonation of classes of carboxyl groups with high pKa values which regulate Ca^{2+} affinity and the expression of the Ca^{2+} induced conformational change. The low affinity sites of skeletal TN-C play a larger role than those of cardiac TN-C in the total conformational change, reflecting the inability of site 1 in the cardiac protein to bind Ca^{2+} . The difference spectroscopy measurements confirm this finding and reveal subtle differences in the structure of the high affinity Ca^{2+} binding sites between the two proteins. (Supported by the Canadian M.R.C.)

TU-POS-F9 NMR STUDIES OF THE MYOSIN S-1 ATPase. J.H. Baldo, J.W. Shriver, P.E. Hansen* and B.D. Sykes, Department of Biochemistry, University of Alberta, Edmonton, Alberta, Canada.

Various intermediates in the hydrolysis of ATP by myosin subfragment-1 (S-1) are being studied by ^{31}P and ^{19}F NMR. A fluorine derivative of ATP, 2-fluoro-ATP (2FATP) has been synthesized and appears to behave identically to ATP as judged by its rate of hydrolysis by S-1. In an attempt to see bound ATP, Na^+ 2FATP and Na^+ ATP are being investigated. Preliminary results indicate peaks in the ^{19}F spectra which are broadened and shifted (nearly 2 ppm) from free FATP and attributed to bound FATP. Resonances in addition to those of free ATP appear in the ^{31}P NMR spectra and may indicate multiple bound forms. AMP-PNP, a non-hydrolyzable analog of ATP, has been used to mimic the bound form of ATP. In the absence of Mg^{2+} the most prominent difference between the free and bound forms in the ^{31}P NMR spectrum is a 1 ppm upfield shift of the β -peak. In the presence of Mg^{2+} there is no significant difference between ^{31}P peaks of the free and bound species.

TU-POS-F10 SOLID-PHASE SYNTHESIS OF FRAGMENTS OF TROPONIN I WHICH INHIBIT THE ATPase ACTIVITY OF ACTOMYOSIN. J. Talbot* and R.S. Hodges, Dept. of Biochem., University of Alberta, Edmonton, Alberta.

A 22-residue CNBr fragment of rabbit skeletal Tn-I 96-117 possesses 70% of the inhibitory activity on a molar basis compared to whole Tn-I to inhibit the actomyosin ATPase. Rabbit cardiac Tn-I shows approximately one third of the inhibitory activity of skeletal Tn-I when assayed in the skeletal actomyosin-tropomyosin system. No examination of the inhibition of the corresponding cardiac Tn-I CNBr fragment is possible due to the replacement of the Met residues at positions corresponding to 95 and 117 of the skeletal Tn-I. The major difference between these highly basic peptides is the replacement of Arg 113 of skeletal Tn-I by a Leu residue. While it is entirely possible that the lower inhibition of cardiac Tn-I is due to conformational changes in the inhibitory region induced by other parts of the molecule it is equally possible that this change in the primary sequence of the inhibitory fragment is responsible for the decrease in inhibition. The results of ATPase assays of synthetic peptides in these regions of Tn-I will be discussed in relation to the observed differences in the inhibitory activity between whole cardiac and skeletal troponin I.

TU-POS-F11 EVIDENCE FOR THE PHOSPHORYLATION OF PARAMYOSIN. L. B. Cooley, Dept. of Chemistry, Rensselaer Polytechnic Institute, Troy, N.Y. 12181

Paramyosin isolated from *Mercenaria mercenaria* appears to contain bound inorganic phosphate which is involved in intermolecular interactions. Three to four phosphates per molecule have been found in native paramyosin. Dialyzing paramyosin against 0.01N KOH at 4°C for 24 hours appears to remove one or more phosphates. Partial dephosphorylation may explain the change in solubility of alkali-treated paramyosin and the slight change in the near ultraviolet circular dichroism of alkali treated paramyosin. In addition, partial dephosphorylation may occur during the titrations of paramyosin, explaining why the forward and reverse titrations at high ionic strength are not the same. No change in molecular weight, length, or percent α -helicity was found in alkali treated paramyosin.

TU-POS-F12 EFFECT OF DIVALENT CATIONS AND ACTIN ON LIMULUS MYOSIN ATPase ACTIVITY. V. Sawyna, D. L. Pulliam,* E. S. Elgart, and R. J. C. Levine, The Medical College of Pennsylvania, Philadelphia, Pennsylvania 19129

In order to ascertain the optimal conditions for Limulus myosin (LM) ATPase activity prior to studies examining the effect of paramyosin on this parameter, we have investigated the requirements of LM ATPase for divalent cations. LM both purified by column chromatography and in the presence of increasing proportions of actin was assayed for ATPase activity in either 0.03M or 0.6M KCl, 10mM imidazole buffer, pH 7.4 and varying ratios of Mg^{++} and Ca^{++} . Prior to the experiments, divalent cations were removed by chelation with 1mM EDTA. Our results show that LM ATPase is activated by 10mM Ca^{++} , and such activity is inhibited by further addition of Mg^{++} , whether or not actin is present. In the absence of Mg^{++} , Ca^{++} activated LM ATPase increases with increasing actin concentrations. LM ATPase activity with Mg^{++} alone is low and equal to that seen in the presence of both Ca^{++} and Mg^{++} . (Supported by USPHS grant HL15835 to the Pennsylvania Muscle Institute. D. P. has NIH Postdoctoral fellowship: NS05615. R. L. has RCDA: NS70476).

TU-POS-F13 MYOFIBRIL REASSEMBLY IN CULTURED EMBRYONIC CHICK HEART CELLS. R.R. Kulikowski* and F. J. Manasek, Department of Anatomy, The University of Chicago, Chicago, IL 60637. (Introduced by R.B. Uretz).

When embryonic myocardium is dissociated into single cells in Ca^{2+} -free medium myofibrils are disrupted reversibly. We have examined fibril reassembly by indirect immunofluorescence using anti-skeletal muscle myosin antibody. Newly isolated myocytes have their myosin content as irregular clumps, short rods, or finely dispersed forms. Formation of linear arrays occurs only after myocytes have begun to spread suggesting that stress may be a factor in initiating fibrillogenesis. Several morphologies of linear, myosin-containing structures appear. Unstriated stress fibers can be present, often continuous with banded fibrils, suggesting homology. Fibril reassembly proceeds at different rates within the same cell and can follow different pathways reflecting the morphological forms of myosin available. This study shows that myofibril reassembly can proceed through a variety of intermediate, myosin-containing forms and that striated muscle myosin is not restricted to typical myofibrils in embryonic cardiac muscle. (Supported by HL 13831 and the Chicago Heart Association).

TU-POS-F14 STUDIES ON THE SELF-ASSOCIATION AND AGGREGATION OF CHICKEN GIZZARD FILAMIN. M.S. Lewis, P.J.A. Davies and I. Pastan. Biomedical Eng. and Instr. Branch, DRS and Lab. of Mol. Biol., NCI, Natl. Inst. Health, Bethesda, MD 20014.

Filamin is a high molecular weight actin binding protein present in smooth muscle and non-muscle cells. Chicken gizzard filamin, used in these studies, has a monomer molecular weight of 250,000 in denaturing solvents. In 50 mM potassium phosphate, pH 7.5, 100 mM KCl, 1 mM EDTA, 1 mM DTT at 5°, ultracentrifugal analysis showed solutions of filamin contain dimer ($M = 500,000$) and variable amounts of higher molecular weight aggregates. In the same buffer at 0.6 M KCl, the data best fits a model of a reversible monomer-dimer association with variable amounts of irreversible tetramer present depending upon the history of the preparation. With fresh preparations, at 5°, $\Delta G^\circ = -5.7 \pm 0.1$ kcal/mole for the monomer-dimer association with little tetramer present. Heating of filamin to 10° or prolonged storage at 5° resulted in increased aggregation and a change in ΔG° to -6.7 to -7.0 kcal for the association. We conclude that chicken gizzard filamin is a dimer at physiological salt concentrations but shows marked tendency to aggregate in vitro.

TU-POS-F15 EPR AND FLUORESCENCE DEPOLARIZATION STUDIES ON BOVINE CARDIAC MYOSIN. D.B. Stone, R.A. Mendelson and P.H. Cheung*, Cardiovascular Research Inst., Univ. of Calif., San Francisco, CA 94143

Bovine cardiac myosin (CM) was labeled with a spin label (SL) or a fluorophore (1,5-IAEDANS) having iodoacetamide reactivity. Activation of Ca^{2+} -ATPase and inhibition of K^+ (EDTA)-ATPase occurred to the same extent as observed for rabbit skeletal myosin (SM) indicating specific reaction with SH₁ groups. SL mobility was greater for CM suggesting a more open structure around the SH₁ groups of CM. Binding of ADP produced similar changes in mobility for SL-CM and SL-SM. Formation of M^{**} -ADP·P_i during steady state hydrolysis of ATP and complex formation with actin produced smaller mobility changes in SL-CM than SL-SM suggesting more limited conformational changes in CM. Time resolved fluorescence depolarization of CM was similar to SM: soluble SM showed mobility ($\phi(CM) = \phi(SM)$) which was removed upon synthetic filament formation or actin binding. This suggests that the SH moieties of CM and SM enjoy a comparable degree of segmental flexibility. (Supported by USPHS Program Project Grants HL 06285 and HL 16683 and NSF Grant PCM76-11491.)

TU-POS-F16 ORIGINS OF SPECIALIZED MUSCLE TYPES INVESTIGATED WITH PROTEIN SEQUENCES. W. C. Barker, L. T. Hunt,* S. Hurst-Calderone,* and M. O. Dayhoff, National Biomedical Research Foundation, Georgetown University Medical Center, 3900 Reservoir Road N.W., Washington, D.C. 20007

The specialized muscle types of vertebrates contain sets of homologous proteins that may have arisen by successive duplication of individual genes or by duplication of entire chromosomes or even of the whole genome. Phylogenies derived from the protein sequences may distinguish between these possibilities, provide an estimate of when the important genetic events took place, and trace the history of the development of tissue specialization at the molecular level. Rates of change and phylogenies of muscle proteins derived from currently available sequence data will be presented.

Supported by NIH Grants HD 09547 and GM 38710.

TU-POS-F17 ACTIVATION OF SUBFRAGMENT I ATPASE BY PARTIALLY POLYMERIZED ACTIN. James E. Estes, Lynn A. Selden*, Lewis C. Gershman, Medical and Research Services USVA Hospital, Albany, N. Y. 12208.

Partially polymerized actin populations were examined by viscometry, ability to activate the subfragment 1 (S-1) Mg^{++} -ATPase, and digestibility by subtilisin. The critical actin concentrations (CAC) for polymer formation measured by viscosity were 2, 10 and 35 μM for actin polymerized in 20, 10 and 5 mM KCl, respectively. The CAC values determined by ATPase activation were 1, 9 and 27 μM for these same [KCl]. Since the digestibilities of actin samples below the CAC indicate the presence of both G-actin and F-monomer, neither of the monomeric states of actin appear to significantly activate the S-1 ATPase. The small, consistent difference between the values of the CAC determined by viscosity and by S-1 ATPase activation was also observed in measurements of the activation of heavy meromyosin ATPase by partially polymerized actin. Since S-1 reportedly does not promote the polymerization of actin, the results suggest that during actin polymerization an "oligomeric" intermediate may be formed which has essentially monomeric viscosity, but the digestibility and ATPase-activating ability of F-actin. Supported by the Medical Research Service of the Veterans Administration.

TU-POS-F18 TEMPERATURE DEPENDENCE OF THE EQUILIBRIUM BETWEEN G-ACTIN, F-MONOMER AND F-ACTIN. Lewis C. Gershman, Lynn A. Selden* and James E. Estes, Medical Service and Research Service, USVA Hospital, Albany, N.Y.

Solutions of G-actin at various concentrations were partially polymerized to equilibrium in 10 mM KCl at 5°, 15°, 25° and 35° C. The critical actin concentration (CAC) at each temperature was determined by viscosity and by subfragment 1 Mg^{++} -ATPase activation, and portions of each sample were also digested with subtilisin. The digestibilities of the partially polymerized populations were always intermediate between those of G-actin (in OM KCl) and F-actin (diluted from 100 mM KCl) at the same temperatures. From these data the size of the fractions of G-actin, F-monomer and F-actin in a population of partially polymerized actin could be calculated. With an Arrhenius plot of the $[F\text{-monomer}]/[G\text{-actin}]$ ratio vs $1/T$, it was possible to determine the ΔH for the change in monomer conformation from G-actin to F-monomer. It appears that a major portion of the value for ΔH of about 15 Kcal/mole measured for the complete polymerization reaction is due to the transition in the monomer conformation. Supported by the Medical Research Service of the Veterans Administration.

TU-POS-F19 MYOSIN NUCLEOTIDE CONFORMATIONS FORMED BY $Mg\text{GADP}$ AND $MgADP$. Morris Burke and Helen Rose Russell*, University of Maryland, Baltimore, Maryland 21201

Previous studies have shown that the affinity and stoichiometry of binding $Mg\text{GADP}$ to myosin are identical to that for $MgADP$ and this suggests that the conformational states of the protein with either nucleotide may also be the same. This possibility has been examined by employing chemical probe methods to compare the accessibility and spatial disposition of the essential thiols SH₁ and SH₂ in these two nucleotide induced conformations. Our results indicate that $Mg\text{GADP}$ binding to myosin does not expose SH₂ as effectively as $MgADP$ and is unable to bring these two thiols into close proximity. These results show that the substitution of the 6-amino group of the adenosine ring by the 1,N⁶-etheno moiety significantly alters the binding interactions between the protein and nucleotide even though the binding affinity is not so altered. (Sup. by NSF PCM 76-21464)

TU-POS-F20 INTERACTIONS OF FRAGMENTS OF TROPONIN C (TnC) WITH TnI AND TnT. P.C. Leavis, S. Rosenfeld*, W. Drabikowski*, Z. Grabarek* and J. Gergely, Dept. Muscle Res., Boston Biomed. Res. Inst.; Dept. Neurology, Mass. Gen. Hosp.; and Dept. Biol. Chem., Harvard Med. Sch., Boston, MA; and Nencki Inst. of Exp. Biol., Warsaw, Poland.

The Ca^{2+} -stabilized formation of complexes between fragments of TnC obtained by cleaving with trypsin, thrombin and cyanogen bromide (Leavis et al., in "Calcium Binding Proteins and Calcium Function", ed. Wasserman et al., Elsevier, 1977, p. 281) and either TnI or TnT from rabbit fast skeletal muscle were studied by urea gel electrophoresis, affinity chromatography and fluorescence spectroscopy. Several of the fragments bind to TnI, suggesting two regions of attachment involving residues 46-77 and 89-120 (regions II and III, respectively) of TnC. Similar studies indicate that the binding site of TnC for TnT involves residues 121-159 (region IV). A fluorescent dansyl probe on TnI complexed to TnC fragments is perturbed by Ca^{2+} -binding. This change was previously associated with Ca^{2+} binding to low affinity sites in complexes of intact TnC and TnI (Leavis, Fed. Proc. 35,1746,1976). (Supp. by NIH (HL-05811,HL-5949), NSF and MDAA)

TU-POS-F21 ARTERIAL SMOOTH MUSCLE MYOSIN. D. Frederiksen, Dept. of Biochem., Vanderbilt Univ., Nashville, TN 37232

Several important aspects of the molecular basis for the contractile process in smooth muscle differ from those of striated muscle. Electrophoresis and sedimentation studies indicate that myosin from porcine aortic smooth muscle has a molecular weight of 470000 daltons and consists of 6 subunits, two each of 200000, 19000 and 16000 daltons. Circular dichroism studies indicate that native aortic myosin is 62% α -helix and that the secondary structure of the protein is not significantly altered upon phosphorylation of the 19000 dalton light chain by smooth muscle myosin light chain kinase. In addition the measurements of intrinsic viscosity (2.24 dl/gm) and sedimentation coefficient (5.50 S) indicate that the smooth muscle myosin is significantly more resistant to translation through a viscous solvent than is striated muscle myosin. Therefore, the hydrodynamic model of the smooth muscle protein is better a cylinder than a prolate ellipsoid, or aortic myosin may be a more rigid molecule than its skeletal muscle counterpart. The observed structural differences in myosins from different muscle types are no doubt reflected in the contractile properties of smooth and striated muscle.

TU-POS-F23 CONFORMATIONAL LOCK EFFECT OF Ca^{2+} OR Mg^{2+} BINDING TO THE HIGH AFFINITY SITES OF TROPONIN C: THERMAL STUDIES. B. Nagy, Dept. of Muscle Research, Boston Biomedical Research Institute; and Dept. of Neurology, Harvard Medical School, Boston, MA 02114

Circular dichroism of troponin C (TnC) in 0.05M KCl, 0.01M HEPES, pH 7.4 was determined from 0° to 85° at 5° intervals. In the presence of 5×10^{-4} M EDTA a 50% decrease in $[\theta]_{222}$ occurs at about $T_m = 55^\circ$; the transition is biphasic indicating at least two different thermal stability domains. Ca^{2+} or Mg^{2+} saturation of the binding sites produces a monophasic curve with $T_m = 75^\circ$. In 6M urea without divalent cations TnC is completely unfolded at 0°-10°C but regains some structure with increasing temperature up to 85°. In the presence of Ca^{2+} or Mg^{2+} which binds to the Ca^{2+} - Mg^{2+} sites in 6M urea (Nagy et al., Biophys. J. 15,35a,1975) T_m is the same as without urea, viz. 75°. These results suggest that Ca^{2+} or Mg^{2+} acts as a conformational lock for most of the secondary structure of TnC in both denaturing and non-denaturing solvents. (Supported by grants from NSF (PCM76-84390) and MDAA)

MACROMOLECULES

TU-POS-F22 ABSTRACT WITHDRAWN

TU-POS-G1 VISCOSITY FROM ELECTROSTATIC ORDERING OF GLOBULAR PROTEIN SOLUTIONS. M. B. Weissman, Department of Chemistry, Harvard University, Cambridge, Massachusetts 02138

Solutions of bovine serum albumin with a charge of $Z \sim -20$ were found to exhibit a large electroviscous effect (extra viscosity due to electrostatic interactions) in the absence of excess salt. At 6.4% (w/v) BSA, the extra viscosity was 0.16 cp. This incremental viscosity scaled as the 0.6 power of the BSA concentration, and was thus larger than the ordinary viscosity increment for ζ 2% BSA. The electroviscous effect fell off rapidly for small concentrations of added salt but was insensitive to the mobilities of the salt ions. Partial ordering of the macroion solutions (as revealed by substantial suppression of light-scattering intensities) is implicated as the source of the extra viscosity. Flow through 500 Å pores is retarded by a factor of 2 for a 2% solution of BSA without salt, indicating structure on the 100 Å scale. Preliminary quasi-elastic light-scattering results indicate that the diffusion coefficient may be predicted from the viscosity and light-scattering intensity.

TU-POS-G2 MEASUREMENT OF MAGNETIC ORIENTATION OF VARIOUS MACROMOLECULAR ASSEMBLIES IN SOLUTION. T.W. Houk, Miami University, Oxford, Ohio 45056

In order to determine the possibility of aligning large molecular assemblies in solution using strong magnetic fields, we have investigated the magnetically induced birefringence of myosin, actin, and tubulin and their respective aggregates in solution. These aggregates are accepted *in vitro* models of the thick and thin filaments of vertebrate striated muscle and microtubules respectively. The magnetically induced birefringence of the aggregates consists of two contributions, the intrinsic birefringence (Cotton-Mouton effect) and the induced form birefringence. We have attempted to measure the Cotton-Mouton constants of the associated monomeric molecules and their aggregates as well as determine the degree of orientation of these filaments in magnetic fields of strengths up to 1.2 Teslas.

TU-POS-G3 SEDIMENTATION AND SPECTRAL STUDIES OF THE SELF-ASSOCIATION OF SOME CATIONIC DYES. J. Lary,* and E. Braswell, Storrs, Connecticut 06268

The self-associative properties of methylene blue, acridine orange, and thionine were studied in aqueous solution by equilibrium ultracentrifugation in the presence of a neutrally buoyant salt. In all cases, an indefinite association model was consistent with the data. The equilibrium constants obtained were then used to calculate the spectra of three of the components (monomer, dimer, and trimer) from the visible absorption spectra. The effect of ionic strength, and temperature on the association constants led to the evaluation of various thermodynamic parameters describing the self-association.

TU-POS-G4 THE THREE-DIMENSIONAL STRUCTURE OF BOVINE INTESTINAL CALCIUM BINDING PROTEIN. M. Szebenyi,* K. Obendorf,* R. Sleight* and K. Moffat, Section of Biochemistry, Molecular & Cell Biology, Cornell University, Clark Hall, Ithaca, N.Y. 14853

Bovine intestinal calcium binding protein is a vitamin D-dependent protein which binds 2 moles/mole of calcium, and which is involved in some way in the intestinal translocation of calcium. The sequence of the closely related porcine protein reveals at least one calcium-binding EF-hand of the type proposed by Kretsinger. Calcium and lanthanide binding have been studied by terbium fluorescence enhancement in solution; the maximum in the excitation spectrum occurs at 235 nm. X-ray crystallographic data have been collected on the native protein, and on Au and Nd derivatives, to 2.3 Å resolution. Phases have been determined by isomorphous replacement and anomalous scattering techniques. The preliminary electron density map will be interpreted in the light of the sequence, the EF-hand(s), the fluorescence data, and the NMR data of Levine.

Supported by grants from NSF and NIH to K.M.

TU-POS-G5 THE BETA BULGE: A SMALL UNIT OF NON-REPETITIVE PROTEIN STRUCTURE. J.S. Richardson, E.D. Getzoff*, and D.C. Richardson*, Duke University, Durham, NC 27710.

Antiparallel β sheets commonly contain irregularities, which almost all turn out to be of one recognizable sort. Such a " β bulge" is a region between consecutive β -type hydrogen bonds, which includes two residues on one strand opposite a single residue on the other strand, and which puts the alternation of side chain direction out of register on the two ends of the "bulged" two-residue strand. β bulges are less common than tight turns, but much commoner than any other non- α , non- β structure yet described: 54 examples are listed. The "classic type" β bulge has the first bulged residue in approximately α -helical conformation and the second close to normal β . The "G1 type" β bulge has a strong requirement for glycine in position 1, which has a conformation close to left-handed α . Almost all G1 bulges occur as an interlocking structure in which the glycine also forms position 3 of a type II turn. Probable functional roles of β bulges include providing the strong local twist needed to form a β barrel, and compensating for the disruptive effect of a single-residue insertion or deletion within a β sheet.

TU-POS-G6 EFFECT OF BULK WATER STRUCTURE ON PROTEIN INTERACTIONS. H. B. Halsall, T. Hodges,* C. W. Anderson,* and G. P. Kreishman, Department of Chem., Univ. of Cincinnati, Cincinnati, Ohio 45221.

In previous work we have demonstrated biphasic behavior as a function of temperature in a variety of systems, including the redox potential of cytochrome *c* and purine aggregation. We have interpreted the data to indicate a temperature dependent destructuring of bulk water which has the appearance of a cooperative phenomenon at about physiological temperatures. In a most elegant series of studies of elastin structure, Urry and coworkers (Crit. Revs. Biochem. 1976) have also observed biphasic behavior in the temperature dependence of the chemical shift of the amide protons in water and saline solutions. Here, we report the temperature dependence of the association constant for the binding of progesterone to human α_1 -acid glycoprotein (orosomucoid). A plot of $\ln K$ vs $1/T$ for this system again shows a biphasic transition near physiological temperatures. These data will be discussed in terms of the effects of changes in bulk water structure near physiological temperatures on macromolecular systems.

TU-POS-G7 SUBUNIT INTERACTIONS IN OVINE LUTROPIN (oLH) USING POLARIZATION OF TYROSYL FLUORESCENCE. Kenneth C. Ingham, and Carol Bolotin,* American National Red Cross Blood Research Laboratory, Bethesda, Md. 20014.

Polarization of tyrosyl fluorescence provides a sensitive probe of conformational changes which alter the internal rotational mobility of the phenolic groups. When the subunits of oLH were dissociated, *P* decreased from ~ 0.17 to ~ 0.13 . Titration of the isolated subunits with acid or GdmCl had little or no effect on *P*, suggesting that residual secondary or tertiary structure is either absent, very stable, or its disruption does not alter the rigidity of the tyrosyl environment. The relatively high *P* for oLH- β (0.17) suggests a conformation which is rigid compared to oLH- α (*P*=0.13). *P* for both subunits decreased smoothly with increasing temperature between 20 and 70°C. By contrast, oLH exhibited a thermal transition characterized by a drop in *P* from a value near that of β to a value near that of α . Because α has more tyrosines with a higher average quantum yield, its fluorescence dominates that of the hormone or an equimolar mixture of subunits. Thus, most of the conformational changes which accompany dissociation and recombination occur in the α subunit. (NIH #AM 19719)

TU-POS-G8 INTERACTIONS BETWEEN SUBUNITS OF PROTEIN OLIGOMERS. D. O. Tinker*, Univ. of Toronto, Toronto, Canada M5S 1A8, V. A. Parsegian, National Institutes of Health, Bethesda, Maryland 20014

Using a computer-controlled electronic display, we have examined the contact faces of several dimeric or tetrameric proteins of known structure. These proteins include the Bence-Jones dimer, the Fab fragment of human immunoglobulin, prealbumin, lobster glyceraldehyde dehydrogenase, lactate dehydrogenase, trypsin-trypsin inhibitor, and hemoglobin. Depending on the protein, two classes of stabilizing interaction appear: hydrophobic interactions between complementary surfaces of nonpolar residues (as emphasized by Chothia and Janin, *Nature* 256, 705, (1975)); and electrostatic (ES) attraction between specifically arranged charges or dipoles on such surfaces. Computations suggest that ES forces provide relatively stronger and more specific contacts to allow (a) structural influence of one monomer on another, (b) destruction of contact by means of small conformational changes, (c) separation into monomers made soluble by the presence of polar groups on the peptide surface.

TU-POS-G9 COMPARATIVE STUDY OF THE VOLUME EFFECTS PRODUCED BY THE INTERACTION OF Cu(II) WITH SERUM ALBUMIN AND OVALBUMIN. Sam Katz¹, R.G. Shinaberry¹ and W. Squire²* (1) Biochem. Dept. and (2) Aerospace Eng. Dept., West Virginia Univ. Morgantown, WV 26505

To interpret the volume changes, ΔV , produced by the activation of apometalloenzymes by their specific metal cofactors it is essential to establish the volume effects produced by cation:protein non-specific interaction. To assess the effect of protein composition and structure equilibrium dialysis and dilatometric studies were made of the reaction of Cu(II) with serum albumin and ovalbumin. It was found that the binding and volume effects were strongly dependent on the proteins' structure and the pH of the system; both micro- and macroscopic charge effects are involved. To calculate the volume contributions attributable to the formation of the individual complexes, $\text{Cu(II)}_i\text{P}$ (where i indicates the number of Cu(II) bound to the protein, P) a computer analysis was made to determine the number and types of complexes formed as a function of Cu(II) concentration and equilibrium constants. This enabled us to calculate the values for ΔV for each of the $\text{Cu(II)}_i\text{P}$ complexes generated in the system.

TU-POS-G10 TRANSIENT KINETICS OF THE BINDING OF METHOTREXATE TO E. COLI MB 1428 DIHYDROFOLATE REDUCTASE. J.C. Williams*, M. Poe, and K. Hoogsteen. Merck Institute for Therapeutic Research, Rahway, New Jersey 07065.

The transient kinetics of the ultraviolet absorbance change in methotrexate upon binding to E. coli MB 1428 dihydrofolate reductase and its binary NADPH complex were investigated by monitoring absorbance changes at 340 and 388 nm on an AMINCO-Morrow stopped flow spectrophotometer at $25 \pm 0.1^\circ\text{C}$ and in medium of 0.05M TrisHCl-0.3M NaCl, pH 7.2. For binding to the enzyme 1.5 to 45 μM was studied using equal concentrations of enzyme and ligand, while the ternary methotrexate-enzyme-NADPH complex was studied from 2.0 to 10.6 μM , each species in equimolar ratio. Blank experiments using enzyme alone, methotrexate alone, or enzyme-NADPH gave no signal in the time range investigated (2 msec to 5 sec). Extrapolation of absorbance changes to zero time showed no difference which would indicate a reaction with faster time constant. The data have been analyzed using a one step second order-first order reversible kinetic model. For methotrexate binding to the apoenzyme a forward rate constant of $6.1 \pm 0.9 \times 10^6 \text{ M}^{-1} \text{ sec}^{-1}$ was determined, while the value for methotrexate binding to enzyme previously complexed with NADPH was $1.5 \pm 0.2 \times 10^7 \text{ M}^{-1} \text{ sec}^{-1}$.

TU-POS-G11 ANALYSIS OF TRITON X-100 BINDING TO HUMAN SERUM ALBUMIN USING THE SCATCHARD BINDING MODEL. Wayne W. Sukow, Department of Physics, University of Wisconsin-River Falls, River Falls, WI 54022

The binding of TRITON X-100 to human serum albumin (HSA) was studied at 16°C in pH 7.0, $I = 0.05$ phosphate buffer. Following equilibrium dialysis the TRITON X-100 and HSA concentrations were determined spectrophotometrically. Analysis of the binding isotherms shows the binding is described by a Scatchard Model with six sites. The corresponding equilibrium constant is $7.2 \times 10^5 \text{ M}^{-1}$. This binding mechanism is in sharp contrast to the positive cooperativity observed in the binding of TRITON X-100 to bovine serum albumin under the same conditions (FEBS LET. 42, 36 (1974)). The maximum number of TRITON X-100 molecules bound, at the critical micelle concentration of the detergent is the same for both albumins under these conditions. Also in contrast to the HSA, preliminary work on the binding of TRITON X-100 to sheep serum albumin suggests a binding mechanism which includes positive cooperativity.

Supported by University of Wisconsin-River Falls. Research Grant #0645-5-76.

TU-POS-G12 KINETICS OF LIPID-APOLIPOPROTEIN ASSOCIATION

J.B. Massey*, S.K. Kusserow*, A.M. Gotto, Jr.* and H.J. Pownall, Baylor College of Medicine and The Methodist Hospital, Houston, Texas 77030

The interaction of liposomes of dipalmitoyl and dimyristoyl phosphatidylcholine (DPPC and DMPC respectively) with human serum apolipoprotein A-I (ApoA-I) was studied by chromatographic and kinetic methods. The rate of association of DMPC and ApoA-I as a function of temperature was followed by measuring the rate of disappearance of liposomal turbidity. Below the transition temperature (T_c) the rate of association is slow; the rate is fastest at T_c and decreases to nil at 40°C . The reaction rate of DPPC is very slow even at T_c . Incorporation of cholesterol into DMPC liposomes accelerates the reaction at all temperatures. Complete incorporation of DMPC and ApoA-I into a lipid-protein complex occurred only at T_c . The high rate of interaction of ApoA-I and DMPC at T_c was assigned to increased permeability of the DMPC matrix produced by a high percentage of boundary lipid between coexisting gel and liquid crystalline phases. The slower reaction of DPPC was probably due to its lower permeability even at its T_c . The addition of cholesterol appears to increase the number of defects enhancing the likelihood of association.

TU-POS-G13 DIETARY EFFECTS ON HUMAN LIPOPROTEIN COMPOSITION AND STRUCTURE. W.W. Mantulin, J. Shepherd*, A.M. Gotto, Jr.* and H.J. Pownall, Baylor College of Medicine, Houston Texas 77030

The human plasma lipoproteins HDL (high density), LDL (low density), and VLDL (very low density) from a dietary study of saturated (sat.) and polyunsaturated (unsat.) fats were examined by differential scanning calorimetry (DSC), fluorescence spectroscopy, and chemical analysis. DSC measurements of HDL and VLDL revealed no thermal transitions. The endotherms observed in scans of LDL showed a lower transition temperature (T_c) on the unsat. diet relative to the sat. diet. A negative linear correlation between % fat in the LDL neutral lipids and the T_c was observed. The empirical "microviscosity" (η) parameter for diphenylhexatriene showed that the sat. diet, relative to the unsat. diet, decreased the fluidity of the corresponding lipoprotein particle. In the temperature range 10 – 37°C the flow activation energy ($\eta = A e^{-\Delta E/RT}$) was higher for the sat. diet: (sat. VLDL $\Delta E = 7.98 \text{ kcal/mole}$; unsat. VLDL $\Delta E = 6.50 \text{ kcal/mole}$) (sat. HDL $\Delta E = 8.05 \text{ kcal/mole}$; unsat. HDL $\Delta E = 6.72 \text{ kcal/mole}$) (sat. LDL $\Delta E = 8.58 \text{ kcal/mole}$; unsat. LDL $\Delta E = 7.12 \text{ kcal/mole}$).

TU-POS-G14 INTERACTION OF GLYCOSAMINOGLYCANS AND POLYPEPTIDES. R. Potenzzone, Jr. and A.J. Hopfinger

Department of Macromolecular Science, Case Western Reserve University, Cleveland, Ohio 44106.

Connective tissue is composed of collagen and elastin fibrils embedded in a gel-like matrix, rich in glycosaminoglycans (GAG). The interaction between the negatively charged GAG and the positively charged collagen molecules is believed to be of primary importance in the formation, maintenance and aging of connective tissue. We have studied the interaction of two GAG, chondroitin-6-sulfate (C6S) and chondroitin-4-sulfate (C4S) with a charged lysine tetramer (LYS) and a model of collagen (GLY-PRO-LYS⁺). The molecular Assembly Software System (MASS) was developed for studying these interacting species. Empirical potential energy functions are used by MASS. The predicted assembly is to be correlated to experimentally determined thermal stability measurements of GAG Poly-lysine and GAG collagen systems. These results have been obtained by Blackwell and co-workers and are reviewed by Hopfinger (1977).

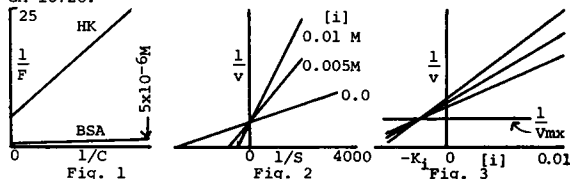
Hopfinger, A.J. (1977) Intermolecular Interactions and Biomolecular Organization, John Wiley and Sons, Inc., New York, Chapter 11, pp. 239-250.

BIOLOGICAL STRUCTURE,

MACROMOLECULES AND POLYPEPTIDES

TU-POS-G15 FLUORESCENT SUGAR ANALOG COMPETITIVE INHIBITOR OF HEXOKINASE. P.A. Lartey* and M. Derechin, Buffalo, NY, 14226

DNS-glucosamine (DNS-G, Lartey and Derechin, 1977, 174 ACS Meeting, Abs. Biol. 106) showed excitation and emission maxima at 330 nm and 500 nm, respectively. Relative fluorescence intensity (F) vs concentration (C) indicated (from 1/F vs 1/C, Fig. 1) F increases at saturating C of 20% and 200% respectively for hexokinase (HK) and albumin (BSA). Plots of 1/v vs 1/[glucose] (Fig. 2) for HK+glucose+DNS-G+Mg.ATP showed competitive inhibition; Dixon plots (Fig. 3) gave $K_i = 3 \times 10^{-3} M$. Results indicate interactions that are specific (i.e., at polar + nonpolar environment of the active site) for HK + DNS-G and nonspecific (mainly non-polar) for BSA + DNS-G. Supported by NIH grant #5 R01 GM 16726.



TU-POS-H1 LOW ANGLE X-RAY DIFFRACTION OF RECONSTITUTED COLLAGEN GELS. E. Eikenberry*, B. Brodsky, CMUJ-Rutgers Medical School, Piscataway, N. J. 08854.

Connective tissues contain different genetic types of collagens (e. g. Type I in skin and tendon; Type II in cartilage; Type III in aorta) as well as non-collagenous components. Purified collagen can be precipitated into gels with the characteristic 670Å staggered arrangement, and we have done low angle x-ray diffraction on such oriented gels. Diffraction patterns from gels of different collagen types should indicate whether genetic type specifies fibril structure. We have obtained low angle diffraction patterns with more than 30 orders of the 670Å axial spacing from reprecipitated Type I collagen. Intensities of these reflections were similar to those observed in the native tendon pattern, indicating that the axial arrangement in tendon is due essentially to the Type I collagen present. There was little sign of lateral ordering of molecules in the gel, but fixation and staining intensified row lines at ca. 42Å, suggesting some order. Work on precipitated gels of Type II and III collagens is in progress.

TU-POS-H2 ELECTRON AND X-RAY DIFFRACTION STUDIES OF GLYCERO-PHOSPHOLIPID CRYSTAL STRUCTURE USING ANALOGS BASED ON CONFIGURATIONAL ISOMERS OF CYCLOPENTANE-1,2,3-TRIOL. D.L. Dorset¹, W.A. Pangborn¹, and A.J. Hancock², Medical Fdn. of Buffalo, Buffalo, NY 14203¹, and University of Missouri, Kansas City 64110²

Diffraction investigations have been carried out on racemic dipalmitoyl phosphatidic acid (DPPA) and cyclitol analogs. In the three of the four possible 1,2-acylated DPPA analogs examined, only the isomer with the fatty acid chains *cis* substituted to the cyclitol ring and with the phosphate esterified *trans* to these (1,2/3, 3P) gives both a high resolution hexagonal electron diffraction pattern and an X-ray long spacing similar to racemic DPPA, when these are crystallized from $CHCl_3$. The free acid 1,2/3, 3P analog also gives a tilted chain polymorph (from alcohols) which apparently has chain packing similar to C-form fatty acids; its dipotassium salt gives a chain packing with untitled chains and 0.4 methylene packing. Results of this study suggest that the acyl chain conformation is the hairpin found in a recent crystal structure reported for a racemic phosphatidyl ethanolamine. [Supported by NIH grant GM21047 and a Grant in Aid from Missouri Heart Association].

TU-POS-H3 MACROMOLECULAR STRUCTURE ANALYSIS WITH AN ATOMIC RESOLUTION STEM. L.T. Germinario, Dept. Biophys. The Johns Hopkins University, Baltimore, Md. 21218

A serious impediment to high resolution electron microscopy of biomacromolecules is the specimen damage due to the inelastic scattering of the incident electrons. The general consensus is that organic molecules can tolerate an electron dose of 10^{-3} Coul/cm² before gross structural alterations occur. Furthermore, amino acids and proteins lose from 50-90% of their mass (Lin, 1974, Radiat. Res. 59:521), thus further decreasing the possibility of recording information on the secondary structure with reasonable statistical accuracy. STEM of derivatized ribonuclease (RNase) carrying three molecules of glycyl-L-methioninato platinumum (II) at methionine residues 13, 29, and 79, indicates that the situation is not as bleak as it appears. STEM images of derivatized RNase molecules recorded on the first scan, when compared to x-ray radiographs of a 6Å resolution balsam wood scale model of RNase-S containing glass marbles at methionines 13, 29, and 79, revealed unexpected similarities in the heavy atom positions and the unstained portions of the RNase polypeptide chain. These results suggest that the STEM's unique detector and data system may extend the spatial resolution in biological objects. Was supported by NIH GM08968 and NIH FOGM57395.

TU-POS-H4 ISOLATION OF LENS GAP JUNCTIONS. D. Goodenough, Dept. Anatomy, Harvard Medical School, Boston, MA.

Mammalian lenses are comprised of a solid cyst of cells, encased in a connective tissue capsule. The lens has no blood supply and receives all its nutrients from the aqueous humor. Cells in the center of the lens are joined by, and may receive their nutrients via numerous gap junctions with cells at the periphery. Lenticular gap junctions between lens fibers (cells) are remarkable in that the junctional subunits (connexons) are arranged in a non-crystalline, disordered state. Lens junctions are isolated by dounce homogenization of 40 fresh calf lenses in 5mM tris buffer, pH 9.0 with 2mM EDTA, 10^{-4} M phenylmethylsulfonyl fluoride and 10^{-5} M p-chloromercuribenzoate added to control proteolysis. The homogenate is pelleted three times at 8K for 20 m. Following a wash in 5×10^{-4} M CaCl₂ in 1mM bicarbonate buffer pH 8.0 the pellet is then resuspended in 7M urea, buffered with 1mM NaHCO₃ pH 8.0 and pelleted at 8K x 20 m. The junctions are floated at a 41/30% sucrose interface at 100,000g x 2 hrs. The junctions are resuspended in 0.2% deoxycholate (DOC) in 5mM tris buffer, pH 9.0 and floated again at 41/30% sucrose interface. Interestingly, the lattice of connexons remains disordered following isolation and subsequent treatment with 10^{-4} M Ca⁺⁺ or pH ranges from 4-8.

TU-POS-H5 IN VITRO INDUCED AND REVERSED CATARACTS IN THE CALF LENS. E. Serrallach,* J. Clark,* Ch. Young,* L. Mengel,* T. Sauke,* G.B. Benedek, MIT, Cambridge, MA 02139 USA

We have observed that the cold cataract temperature T_c in the intact calf lens varies markedly as a function of the concentration of various ions (KCl, NaCl), D₂O, reagents (glycols) and pH-values. Reversible changes in T_c were produced by dialyzing the lens against different buffers. The values obtained were $\Delta T_c / \Delta [KCl] = +25^\circ C / Mole$ and $\Delta T_c / \Delta [glycerol] = -10^\circ C / Mole$. We can raise T_c above body temperature with ionic solutions. This opacified lens at body temperature is reversed by introducing into the ionic solution agents, e.g. glycols with negative $\Delta T_c / \Delta C$. Similar findings are obtained with lens homogenates, which have thixotropic properties as determined from viscosity measurements. Suitable cut sections of the lens show high order optical diffraction patterns, consistent with the hexagonal packing of lens fibers. The appearance of the cold cataract is related to an increase of the intensity of the diffraction spots, suggesting an increase in intercellular spacing. A physical mechanism for these microstructural changes will be presented.

CELL BIOLOGY I

TU-POS-II ³¹P NMR STUDY OF THE STATE OF Mg²⁺ IN THE HUMAN RED BLOOD CELL. R.K. Gupta, J.L. Benovic* and Z.B. Rose*, Institute for Cancer Research, Philadelphia, Pa. 19111.

The chemical shifts and the spin-spin couplings in the ³¹P NMR spectra of intracellular ATP in human blood directly reveal that 83% and 76% of the total ATP is complexed to Mg²⁺ in the aerobic and anaerobic states, resp. This determination does not differentiate between molecules free in solution and those bound to hemoglobin due to rapid exchange on the NMR time scale of free and complexed ATP. From these data the intracellular level of free Mg²⁺ is determined to be 0.22 ± 0.04 mM in the aerobic and 0.61 ± 0.08 mM in the anaerobic state of normal red cells. Knowledge of the free Mg²⁺ permitted a calculation of the distribution of ATP, ADP and 2,3-DPG among their complexes with Mg²⁺ and hemoglobin. Since the Mg²⁺ in the red cell is largely complexed, the 3-fold increase in free Mg²⁺ under anaerobic conditions may significantly affect the rates of intracellular enzymatic reactions. The ³¹P NMR spectrum of sickle cells is qualitatively similar to that of normal cells under aerobic conditions but a large broadening of the ³¹P resonances is observed anaerobically reflecting polymerization of intracellular hemoglobin. (Supported by NIH grants AM-19454, GM-19875 and USPHS RCDA AM-00231).

TU-POS-12 HIGH RESOLUTION ³¹P NMR OF HUMAN PLATELETS. K. Ugurbil*(a), R. G. Shulman(a), H. Holmsen*(b), & J. Costa (c)(x) Bell Laboratories, Murray Hill, N.J. (b) Temple University, Phila., PA., (c) NIMH, Bethesda, Md.

High Resolution ³¹P NMR spectra of human platelets measured at 145.7 MHz show well resolved peaks from ATP, NAD⁺, P_i, and phosphomonoesters. Upon hydrogen peroxide addition, the cytoplasmic ATP pool is reduced by ~90% as determined by chemical analysis. A proportionate decrease in the ATP NMR intensity is also observed indicating that there is a negligible contribution to the NMR peaks from the ATP in storage granules possibly due to association of the nucleotides in the granules. Stimulation by thrombin resulted in secretion of the granular adenine nucleotide, as determined by chemical analysis, and in corresponding increases in the NMR intensities. Taking advantage of the different chemical shifts when divalent metal bound (cytoplasm) and metal free (supernatant) we have distinguished between adenine nucleotide in the cytoplasmic and the discharged granules.

TU-POS-13 PARAMAGNETIC CHANGES IN CANCER: A STUDY OF 7-12 DIMETHYLBENZANTHRACENE (DMBA) INDUCED MAMMARY TUMORS USING FROZEN AND LYOPHILIZED TISSUES. Peter L. Gutierrez, William Antholine* and Harold M. Swartz.

Controversy exists as to whether free radical levels increase in cancer. Sample preparation techniques (lyophilization) can cause an apparent increase. We induced mammary tumors in Sprague-Dawley rats with a single dose of DMBA and examined lyophilized and non-lyophilized samples by ESR. In blood, no changes in Ceruloplasmin or Transferrin were found with either type of preparation. A free radical signal was found in blood only after lyophilization and was the same in controls and experimentals. Free radicals in livers from tumor bearing animals were indistinguishable from those of controls.

In tumor tissue, there was an increase in both free radicals and Mn^{++} using both types of preparations. To our knowledge, this is the first system in which an increase in free radicals has been demonstrated in non-lyophilized tumors.

TU-POS-14 ELECTROMOBILITY AND SURFACE CHARGE CHANGES IN ASCITIC SARCOMA 180 TUMOR CELLS TREATED WITH CIS-DIAMINO-DICHLOROPLATINUM(II). D.A. Juckett, MSU, East Lansing, MI 48824.

The inorganic platinum complex, cis-diaminodichloroplatinum(II), has proved to be a very good anti-cancer compound. Its mode of action in decreasing tumor growth is not known. This work examines the effect of this drug on the surface charge of the cell. Cells, which are grown in mice, show a 30% decrease in electromobility 24 hours after injection of the drug. Their partition in a two phase aqueous-polymer system also dramatically decreases. The isoelectric point seems however to remain constant. After treatment, these cells are smaller than control cells and a large proportion of them remain metabolically active (dye exclusion test). It appears that cis-Pt(II) internally alters the tumor cells to reduce their growth, and changes in the surface properties somewhat reflect these alterations. Further studies examining these changes will be presented.

TU-POS-15 MECHANICS OF ROULEAUX FORMATION IN VITRO FOR CELLS FROM BLOOD WITH HIGH SEDIMENTATION RATE. Martin M. Lee and Peter B. Canham, Biophysics Department, University of Western Ontario, London, Canada. N6A 5C1.

An inverted Nikon microscope was used to record (using 16mm film) red cells forming rouleaux on a glass coverslip. The cells were at a concentration of approximately 10^{-3} by volume in plasma or in Ringer solution with 3g/l of added rouleaux inducing agent (polyvinylpyrrolidone: MW 360,000). Blood was studied from a long term diabetic (erythrocyte sedimentation rate 95mm/hr, hematocrit 30%, blood sugar 287 mg/100 ml). There was no intercellular sliding when two cells came together in plasma which was the mode for normal cells in normal plasma (1). There was intercellular sliding for doublet cell formation for the diabetic cells in PVP-Ringer. The cells appeared to have a higher membrane stiffness in that the initial phase of doublet formation was greatly prolonged.

1. Fung, J.S.K. & Canham, P.B. *Biorheology* 11: 241, 1974.

Supported by the Ontario Heart Foundation.

TU-POS-16 FIBROBLAST INTERACTION WITH COPOLYPEPTIDE FILMS M.E. Soderquist*, H. Gershman* and A.G. Walton, Intr. by J. Blackwell, Department of Macromolecular Science and †Biochemistry, Case Western Reserve University, Cleveland, Ohio 44106

The attachment of Syrian Hamster Fibroblasts (NIL B) and SV40 virus transformed NIL B cells (SV-NIL) to various, neutral, acidic or basic copolypeptide films has been studied. Results show that adhesion, in a balanced salt (protein free) solution, is essentially independent of the copolypeptide composition. Attachment is first order and goes to 100% completion. Pretreatment of the polypeptide surfaces with serum albumin causes a considerable modification in behavior. Basic, lysine containing substrates cause much faster uptake and total attachment than do hydrophobic or acidic surfaces. On the non-basic surfaces attachment is reversible. Preliminary indications are that the mediation of attachment by protein does not originate in conformational changes but probably arises from the rigidity and extent of the proteinaceous interface. The effect of protein mediation noted for NIL B cells is accentuated with SV40 cells, reflecting their modified surface properties.

TU-POS-17 SEPARATION OF MOUSE PERITONEAL CELLS BY VELOCITY SEDIMENTATION. J.E. Leider* and N. Catsimpoalas, Biophysics Laboratory, MIT, Cambridge, MA 02139.

Velocity sedimentation at 1g was used to study the cell population of the mouse peritoneal cavity. This preparative method proved effective in separating the two major cell types present, macrophages and lymphocytes. Analysis of the cell distributions consisted of Coulter counting and sizing and cell smear staining for morphology or for nonspecific esterases to identify phagocyte - enriched fractions. Adult CBA/J mice were used to assess the value of the separation technique. Large cells, identified as macrophages, sedimented first, followed by smaller lymphocytes. Inter-strain variability in the sedimentation pattern was examined using cells from strains CBA/J, C57BL/6j, and CB6F₁/J. The separation profiles were similar from one strain to the next. The effect of age on the sedimentation profile was investigated using CB6F₁/J mice of ages 4, 8, and 12 weeks. Significant differences were found in the cell patterns of the various age groups. In all studies, sizing analysis correlated with cell classification from Wright's-Giemsa staining for morphology and nonspecific esterase staining for mononuclear phagocytes.

TU-POS-18 ALTERATIONS IN VELOCITY SEDIMENTATION PATTERNS OF HUMAN ERYTHROCYTES AS A FUNCTION OF STORAGE AGE. E.M. Skrabut¹, N. Catsimpoalas¹, and C.R. Valeri^{2*},

¹Biophysics Laboratory, MIT, Cambridge, MA 02139 and

²Naval Blood Research Laboratory, Boston, MA 02118

Peripheral human blood was collected in CPD and stored at 4°C under blood bank conditions for up to 30 days. Aliquots of the units were withdrawn during this storage and fixed for 10 minutes with 2.5% glutaraldehyde (final concentration). These fixed cells were then subjected to transient velocity sedimentation at unit gravity (N. Catsimpoalas, et al., *Life Sci.* 18:481, 1976). The resulting patterns indicate that blood stored from 0 to 4 days presents a bimodal distribution of low (~25% of total cells) and intermediate sedimentation rates. Blood stored from 5 to 21 days presents a unimodal pattern of intermediate velocity sedimentation rate. Out dated blood (>21 days) exhibits a bimodal distribution of intermediate and high (~30% of total cells) velocity sedimentation rate erythrocyte populations. This methodology presents a means of determining the storage age of human blood and may be of value in predicting *in vivo* survival of transfused RBC (Supported by ONR Contract No. N00014-76-C-1155).

TU-POS-19 ANALYSIS OF THE MORPHOLOGY OF SPERM CELLS USING A RESISTIVE-PULSE TECHNIQUE. R. W. DeBlois, General Electric R&D Center, Schenectady, NY, 12301

The conventional Coulter Counter has been earlier employed to determine the volume distributions of sperm.⁽¹⁾ The present study employs its resistive-pulse technique, but with pores of small diameter, made by the Nuclepore etched-particle-track process, to examine sperm of both the sea urchin and the bull. Head and tail are readily distinguished and separately measured. Preliminary measurements give the head of the sperm of the sea urchin, *Arbacia punctulata*, as $(5.5 \pm 0.5) \mu\text{m}^3$. The tail is quite uniform along its length, with a diameter of $(0.26 \pm 0.1) \mu\text{m}$. Bull sperm heads and tails show considerable variation, with a modal volume for the heads of motile sperm near $13 \mu\text{m}^3$ and tapering tails of median diameter near $0.5 \mu\text{m}$.

(1) J. Brotherton and G. Barnard, J. Reprod. Fert. **40**, 341-347 (1974).

TU-POS-110 NON LINEAR BACTERIAL GROWTH KINETICS: DRUG-CELL COUNTERINTERACTIONS. A. L. Koch, Dept. Biology, Indiana University, Bloomington, Indiana, 47401

A number of factors influence the sensitivities of bacteria to inhibitors of growth. Here, I report studies with *Escherichia coli* and rifampicin under conditions where the bacteria can grow rapidly in the absence of drug. During rapid growth, the rate of drug penetration in wild type bacteria is so slow that the balance between penetration, growth, and inducible detoxification mechanisms becomes critical. A momentary pause in growth is sufficient to cause catastrophic destruction. On the other hand, prior exposure to lower levels of rifampicin can protect cells against higher doses when high levels of cells are present in the system. Thus the drug concentration, the growth rate, and the cell concentration are critical in determining the outcome: The culture may either grow indefinitely or it may slow, stop, and lyse. Growth was followed turbidimetrically in a double beam spectrometer linked to a mini-computer. The instrumentation was adequate so that under optimal conditions the specific growth rate could be determined to less than 1% in a three-minute run. Supported by NSF under grant BMS72 01852 A03.

TU-POS-111 FAST FREEZING OF THIN TISSUES BY THERMAL CONDUCTION INTO SAPPHIRE CRYSTALS AT 77°K. J. Meisner and W. A. Hagins, LCP-NIAMDD, National Institutes of Health, Bethesda, Maryland 20014

Solutions and thin tissues such as retinas must sometimes be rapidly frozen to halt chemical reactions or immobilize diffusible constituents for microanalysis. The sample is usually compressed between polished faces of Cu or Ag blocks chilled to 77°K. Since the thermal conductivity of synthetic sapphire is several times that of these metals at 77°K, polished sapphire blocks should permit faster freezing. We have confirmed this using an automated freezer and 8% agarose gels containing embedded thermocouples. Studies of freezing by high speed photography and depth profile analysis of composition of frozen samples will be shown. No systematic variation in sample composition exceeding 5% with depth was seen when 0.5 mm thick gels containing THO and ^{14}C labeled EDTA were frozen by the sapphire block method.

TU-POS-112 THE EFFECTS OF MICROTUBULE INHIBITORS ON CONJUGATION IN THE CILIATE *STENTOR POLYMRPHUS*. D. Grandy, Department of Biology, Case Western Reserve University, Cleveland, Ohio. 44106

The microtubule inhibitors Benomyl (methyl-1-[butylcarbamoyl]-2-benzimidazole carbamate), IPC (isopropyl-N-phenyl carbamate), Trifluralin (1,1,1-trifluoro-2,6-dinitro-N,N-dipropyl-p-toluidine), and colchicine have been investigated with respect to their effect on conjugating *Stentor polymorphus*. Results to date indicate that these agents do not have any apparent effect on the event of conjugation. They do however, interfere with the normal cell surface repair process which takes place after separation at the locus of previous cell-cell fusion. This interference may be manifested as a permanent loss of cilia in the region of previous fusion as seen when the inhibitor Trifluralin is employed ($10^{-5} \mu\text{g}/\mu\text{l}$) or as a delay in the repair process such as is observed when IPC is used ($10^{-4} \mu\text{g}/\mu\text{l}$ → delay of 24 hours).

EPITHELIAL TRANSPORT I

TU-POS-11 MEMBRANE MICROVISCOSITY & ANTIDIURETIC HORMONE ACTION ON WATER PERMEABILITY. B. R. Masters, D.D. Fanestil*, J. Yguerabide, Depts. of Medicine & Biology, University of California, San Diego, La Jolla, California 92093

Previous studies on microviscosity of perylene stained cells isolated from toad bladder showed an increase in fluidity with c-AMP derivatives; intact bladder showed a similar effect with ADH with a physiological time course (1,2). The 7% increase in fluidity (a minimum value) can't account for >10-fold increase in water permeability. Laser excitation of perylene stained mucosal membrane of intact toad bladder shows a similar increase in the fluidity with ADH (100mU/ml). These results and independent studies (3) on metabolic dependence of offset of ADH action on water flow suggests that action of ADH in water regulation may involve pores. Support: NSF PCM 75-19504. References: (1) B.R. Masters, in Cellular Function and Molecular Structure, ed. P.F. Agris, Academic Press, 1977. (2) B. R. Masters et. al. Microviscosity of mucosal cellular membranes in urinary bladder of toad, J. Membrane Biol. 1978. (3) B.R. Masters & D. Fanestil Metabolic dependence of the offset of Antidiuretic Hormone induced osmotic water flow: role of endocytosis.

TU-POS-J2 TIME COURSE STUDIES SUGGEST THE EXISTENCE OF TWO WATER PATHWAYS IN FROG URINARY BLADDER. M. Parisi, J. Chevalier*, P. Ripache and J. Bourguet C.E.N. Saclay, Dept. de Biologie, 91190 Gif sur Yvette, France.

A new experimental approach allowed the time course study of unidirectional and net water fluxes in frog urinary bladder (one minute periods). It was observed that: 1) The pattern of the increase in unidirectional flux induced by ADH was not affected by unstirred layers or by the presence of an osmotic gradient. At different stirring rates, a constant factor relates the increase in net and unidirectional fluxes. 2) The response to ADH, cyclic AMP or serosal hypertonicity can be increased or decreased by modifying mucosal pH. 3) The unidirectional water flux at rest was not affected neither by the variation in mucosal pH nor by the presence of unstirred layers. These results agree with the hypothesis that the action of ADH adds a new pathway for water, superimposed to the basal one. The analysis of the time course of water fluxes suggest that this second pathway is uniformly affected by unstirred layers, even during early stages of ADH action. This could be related to the observation of membrane particle clusters after a 1 min. challenge with ADH. (see abstract by J. Chevalier et al.).

TU-POS-J3 EARLY ALTERATIONS OF MEMBRANE ULTRA-STRUCTURE DURING ANTIDIURETIC ACTION J. Chevalier*, J. Bourguet and M. Parisi C.E.N. Saclay, Dept. de Biologie, 91190 Gif sur Yvette, France.

The existence of intramembranous particle aggregates in some urinary epithelia exposed to antidiuretic hormone and their relevance to water permeability is now well established. The origin of these aggregates is however still unsettled. We now report on alterations observed in frog urinary bladders fixed one minute after their exposition to ADH, i.e. well before the maximum of the hydrosmotic response. i) Typical clusters of particles on PF face (and complementary groove arrays on the EF face) are observed after such an hormonal pulse. They are entirely comparable to those present during sustained ADH challenge, but their frequency is much lower. ii) Other formations, no longer seen in the fully developed response, are however also observed. They result from the juxtaposition on the same external leaflet (EF) of particle condensations and groove alignments, suggesting a more labile particle partition coefficient between the two membrane leaflets. Such differences indicate that cluster formation could involve a progressive anchorage of particles to some cytoplasmic components.

TU-POS-J4 NON-LINEAR OSMOSIS IN FROG SKIN. Y. T. Lau, R. H. Parsons and G. Feeney*, Dept. Biol., Rensselaer Polytechnic Inst., Troy, NY, 12181.

Osmotic water movement across poisoned frog skin was measured for various gradients (Ringer's solution containing 2 mM KCN plus sucrose or Na_2SO_4). Extracellular space and cell volume (V_c) were measured on the same skins. Previously we have shown that the osmotic permeability (L_p) decreases with an increase in osmotic gradient. At the same time there is a decrease in cell volume (Lau & Parsons, *Biophysical J.*, 17:91a, 1977). The purpose of this abstract is to present experimental data which examines the role of the cell volume in more detail. The cell volume with 100 mOsm gradient (hyper-osmotic solution in corium bath) was 2.31 ± 0.21 (9) $\mu\text{L.mg dry wt}^{-1}$. After exposing the tissue to a 500 mOsm gradient and then replacing the 100 mOsm gradient there was a drop in cell volume to 1.47 ± 0.11 (9) $\mu\text{L.mg dry wt}^{-1}$ which persisted during the water flow measurements at 100 mOsm gradient. The L_p decreased to 86 ± 8 (9) of the initial L_p , i.e. followed the cell volume and not the osmotic gradient. A second experiment was done with different gradients and the same cell volume. Here L_p remained constant.

TU-POS-J5 EFFECT OF TRANSEPITHELIAL POTENTIAL $\Delta\psi$ ON RATES OF ACTIVE NA TRANSPORT $J^a(\text{Na})$ AND CO_2 PRODUCTION $J(\text{CO}_2)$ IN TOAD BLADDER. S.J. Rosenthal*, J.G. King*, A. Essie, Dept. of Physiology, Boston U. Sch. of Med., Boston, MA 02118

A mass spectrometric molecular flux apparatus (MFA) was used to measure $J(\text{CO}_2)$ continuously, simultaneously with transepithelial current I in toad bladder. After equilibration at short-circuit for several hours, $\Delta\psi$ was clamped at 100mV to depress $J^a(\text{Na})$ for up to 50 min. The subsequent elimination of $J^a(\text{Na})$ with amiloride allowed calculation of $J^a(\text{Na})$ and suprabasal $J^{\text{SB}}(\text{CO}_2)$. In model experiments a step change in $J(\text{CO}_2)$ produced an exponential response in the MFA signal with time constants of 0.25 and 1.6 min due to the MFA and Ringer solution respectively. $J^{\text{SB}}(\text{CO}_2)$ was continuously computed from the MFA signal. On clamping $\Delta\psi$ at 100mV, $J^a(\text{Na})$ declined immediately and remained near-constant for ≥ 10 min. Within 2-4.5 min of perturbation of $\Delta\psi$, $J^{\text{SB}}(\text{CO}_2)$ became near-constant for some 3.5-10 min. During this early period the ratio $J^a(\text{Na})/J^{\text{SB}}(\text{CO}_2)$ declined $46 \pm 13\%$ ($n=11$) from its value at $\Delta\psi=0$; during the final 30 min it approached its initial value. The data are consistent with an incompletely coupled active Na transport system, capable of regulating the metabolic cost of transport on prolonged perturbation of $\Delta\psi$.

TU-POS-J6 APICAL SODIUM CONDUCTION IN FROG SKIN IS A MULTISTATE MECHANISM. T. Hoshiko, Physiology Dept., Case Western Res. Univ. Sch. Med., Cleveland, Ohio 44106.

Voltage clamp current fluctuations of isolated frog skin are attributable to the sodium selective apical membrane and appears to be a channel-mediated mechanism. Total current noise is a function of the clamp voltage or the clamp current. A test for a multistate versus a single state mechanism for ion conduction proposed by Y. Chen (*Biophys. J.* 16:965, 1976) was applied to low frequency data obtained previously from a 0.071 cm^2 area of frog skin. The test is to calculate a function $E(V)$ over a range of clamp voltages (v):

$E(V) = \sigma^2 / (1 - \bar{a} \cdot (V - V_{\text{Na}}))$; where \bar{a} is a mean coefficient over all conduction states such that $\bar{a}\bar{g}$ gives the mean conductance. $E(V)$ is an estimator of single channel conductance, γ , and is equal to γ for a single state mechanism. In frog skin, $E(V)$ varied from 0.22 to 75.0 pmho for clamp potentials from -35 to +80 mV (for a spontaneous potential of about +35 mV). Thus apical sodium conduction appears to be a multistate mechanism. (supported by USPHS grant AM05865)

TU-POS-J7 MICROELECTRODE STUDIES OF THE ACTIVE SODIUM TRANSPORT PATHWAY IN LARVAL SALAMANDER. R. Hudson,* and L. B. Kirschner, Pullman, Washington 99164.

In vivo microelectrode studies on larval salamander skins showed the apical membrane potential difference (APD) to be 40mV in 1mM NaCl (inside cell negative). The APD depolarizes logarithmically in the range 0.1-100mM NaCl by 11.2mV/decade.

The *in vivo* transepithelial potential difference (TEP) is 10mV in 1mM NaCl (serosal side positive). In the range 0.1-100mM NaCl the TEP reaches a maximum at 10mM (+35mV) and falls between 10-100mM. In contrast, with increasing Na Gluconate the TEP displays a hyperbolic relationship approaching +50mV in 100 mM. It appears that skins are as impermeable to Cl at low concentrations (0.1-3mM) as to gluconate. Above 3mM Cl conductance develops. However, the APD was not altered by substitution of the impermeant anion gluconate. Hence, it is suggested that a paracellular shunt through the skin for Cl develops at higher concentrations.

How the TEP is effected by calcium will also be discussed.

TU-POS-J8 INTRACELLULAR LONG TIME CONSTANT TRANSIENT VOLTAGE RESPONSE TO CURRENT IN GASTRIC MUCOSA. L. Villegas, Centro de Biofísica y Bioquímica, IVIC, Caracas, Venezuela.

Intracellular potential changes induced by the passage of step ($45 \mu\text{A}/\text{cm}^2$) current pulses across isolated frog gastric mucosae were measured. Potential changes, in mV, measured in the initial 0.4 sec ($n=76$) were:

	Mucosal-cell	Cell-serosal	Transmucosal
Epithelial cells	9.21 ± 0.63	4.92 ± 0.53	12.68 ± 0.88
Oxyntic cells	13.09 ± 0.86	1.43 ± 0.13	16.58 ± 0.83

Between 0.4 and 4.0 sec the potential changes were:

Epithelial cells	9.33 ± 1.03	3.30 ± 0.83	9.63 ± 1.02
Oxyntic cells	9.54 ± 1.15	1.25 ± 0.18	6.68 ± 1.04

Summatory of the mucosal-cell plus cell-serosal measurements is not significantly different ($P>0.05$) from the transmucosal changes in both cells when $t=0.4$ sec, or in the epithelial cells when $t=4.0$ sec, while in oxyntic cells the summatory of the changes measured between 0.4 and 4.0 sec is significantly different ($P<0.005$) from the measured transmucosal change. This suggests that the long time constant transient voltage response is related to the net ion transport and spontaneous transmucosal potential difference originated in oxyntic cells.

TU-POS-J9 Na^+ -DEPENDENT Cl^- TRANSPORT BY RESTING FROG GASTRIC MUCOSA. T.E. Machen, Physiology-Anatomy Dept., Univ. of Calif., Berkeley, Ca. 94720

Standard Ussing chambers were used to measure, in $\mu\text{eq}/\text{cm}^2\cdot\text{h}$, short circuit current (I_{sc}) and fluxes of $^{36}\text{Cl}^-$ (J_{Cl}) in metiamide-treated tissues (H^+ secretion = 0). During control conditions $I_{\text{sc}} = J_{\text{net}}^{\text{Cl}} = 3.15$. While Na^+ -free (choline replaced) mucosal solution had no effect on I_{sc} , Na^+ -free serosal (S) solution caused a rapid decrease in I_{sc} and $J_{\text{net}}^{\text{Cl}}$ to zero ($t_{1/2} = 3$ mins.). When $[\text{Na}^+]$ was increased in steps from 0 back to 105 mM, I_{sc} also increased in steps back to control levels. I_{sc} was measured at different $[\text{Cl}^-]$ between 2 and 95 mM, first with $[\text{Na}^+] = 105$ mM; Lineweaver-Burk (LB) plot ($1/I_{\text{sc}}$ vs $1/[\text{Cl}^-]$) gave a straight line with $K_m = 4$ mM; when $\text{Na}^+ = 50$ mM (choline methyl sulfate to maintain osmolality), LB plot showed $K_m = 8$ mM. It was also observed that when $[\text{K}^+]$ was increased from 5 to 55 mM (this is expected to depolarize the p.d. across the S membrane of the cells), $I_{\text{sc}} = 0.17$. We propose: (1) Active Cl^- secretion is mediated by a Na^+ -coupled step at the S membrane; the electrochemical gradient for Na^+ between S and cell may be important for Cl^- entry into the cell. (2) Na^+ increases affinity of this mechanism for Cl^- . Supported by NIH grant AM19520.

TU-POS-J10 2,4,6 TRIAMINOPYRIMIDINE (TAP) INHIBITION OF ACTIVE NA TRANSPORT IN FROG SKIN. R.S. Balaban* and L.J. Mandel (Intr. by F. Ramon). Dept. of Physiology, Duke Univ., Durham, N.C. 27710

The monovalent cationic form of TAP has been previously shown by others to inhibit passive junctional Na permeation in leaky epithelia. In the present work, we have shown that TAP also inhibits the active transcellular movement of Na in the frog skin, a tight epithelium, by apparently blocking the entry of Na at the outer membrane. TAP inhibition was found to: a) be completely reversible, b) increase the electrical resistance of the tissue, c) occur only from the outer side, d) be dependent on the protonated form, e) exhibit saturation kinetics ($K_I = 0.8\text{mM}$), f) be apparently non-competitive with Na, g) be independent of external Ca, and h) be dependent on the buffering capacity of the external medium. Conversely, amiloride, an inhibitor of Na entry in the frog skin, was also found to decrease the electrical conductance of the gallbladder at $> 10^{-4}\text{M}$, which is similar to TAP's previously reported effect on the gallbladder. Thus, it appears that both the Na entry sites in the frog skin and the cationic junctional permeation sites in the gallbladder have similar reactive groups. (Supported by NIH grant AM-17876).

TU-POS-J11 NATURE OF ELECTRICAL POTENTIAL DIFFERENCE ACROSS THE GILL OF A MARINE TELEOST. D. Howe,* (Intr. by M. E. Browne), Duke U. Marine Lab, Beaufort, N. C. 28516

The transepithelial potential (PD) across the gill of a marine (SW) teleost, *Opsanus tau*, was studied. The PD in SW was -2.9 mV (blood neg.), different from the 19 mV found in other SW teleosts. Respective Nernst potentials for Na, K, and Cl were 26.5, 25, -32.5 mV. The assumption was made that the PD was a diffusion potential which could be described by the Goldman voltage equation and that Na, Cl, and K carried all transgill current. On this basis, paired values of $P_{\text{K}}/P_{\text{Na}}$ (α) and $P_{\text{Cl}}/P_{\text{Na}}$ (β) were calculated. O. *tau* were then transferred to Na- and Cl-substituted sea waters and for each set of α and β the PD expected of a diffusion potential was calculated with the Goldman equation. In no case did calculated and measured PDs agree. In addition, calculation of transport numbers showed that the Cl conductance was 1.6 times the Na conductance. Possible explanations include: 1) conductances for Mg, Ca, and SO_4 in SW were not accounted for, 2) the ion substitutes, choline and isethionate, have finite conductances, and 3) the salt excretory pump(s) is electrogenic. (Supported in part by USPHS grant HL 12157)

TU-POS-J12 MICROELECTRODE AND NYSTATIN STUDIES OF RABBIT DESCENDING COLON. N.K. Wills, S.A. Lewis, and D.C. Eaton. Dept. of Physiology, Yale Univ., New Haven, CT. 06510 and Univ. Texas Med. Br., Galveston, Tx. 77550.

We used microelectrode methods in conjunction with nystatin and amiloride to study the cellular and tight junctional resistances of colon epithelial cells. K^+ -selective microelectrodes and bi-ionic potentials were also used to assess the source of the basolateral membrane potential (V_{bl}). Analysis of the relationships between transepithelial resistance (R_T) and short circuit current (I_{sc}) and the ratio of apical to basolateral resistance (R_a/R_{bl}) yielded the following values: 1) Nystatin estimates: junctional resistance (R_s) = 730 ± 150 (S.E.M.) Ωcm^2 . Native R_a was 705 ± 123 Ωcm^2 and $R_{bl} = 95 \pm 14$ Ωcm^2 . 2) Amiloride results: $R_s = 481 \pm 70$ Ωcm^2 , native $R_a = 644 \pm 225$ Ωcm^2 and $R_{bl} = 161 \pm 31$ Ωcm^2 . Intracellular K^+ activity was 72 ± 8 mM. $P_{\text{Na}}/P_{\text{K}}$ and $P_{\text{Cl}}/P_{\text{K}}$ estimated as .02 and .04, respectively. We conclude that V_{bl} is primarily a K^+ diffusion potential, although a small electrogenic component may be present. An equivalent circuit of the colon is presented.

TU-POS-J13 ELECTRICAL PROPERTIES OF THE BASOLATERAL MEMBRANE OF THE RABBIT URINARY BLADDER. S.A. Lewis, N.K. Wills, and D.C. Eaton*. Dept. of Physiology, Yale Medical School, New Haven, Connecticut 06510. Dept. of Physiology and Biophysics, University of Texas Medical Branch, Galveston, Texas 77550.

To determine the electrical properties of the basolateral membrane of the rabbit urinary bladder we measured: i. intracellular K^+ and Cl^- activities; ii. sodium/potassium and chloride/potassium permeability ratios; and iii. the magnitude of an electrogenic pump. An intracellular K^+ activity of 72 mM and Cl^- activity of 16 mM was measured using intracellular ion-exchange microelectrodes. The $P_{\text{Na}}/P_{\text{K}}$ and $P_{\text{Cl}}/P_{\text{K}}$ of the basolateral membrane were calculated by using the Hodgkin-Katz, Goldman equation. The best fit $P_{\text{Na}}/P_{\text{K}}$ was 0.044 and $P_{\text{Cl}}/P_{\text{K}}$ was 1.17. A Na^+ electrogenic pump which hyperpolarized the basolateral membrane by up to 20 mV was measured in the absence of chemical gradients. Ouabain rapidly reduced this potential to zero. We conclude: i. the basolateral potential is a diffusion potential with K^+ and Cl^- the most permeable ions; ii. there is a ouabain sensitive, Na^+ dependent, potential generating active transport system located at the basolateral membrane.

TU-POS-J14 EFFECT OF MEMBRANE POTENTIAL ON THE D-GLUCOSE TRANSPORTER IN RENAL BRUSH BORDER MEMBRANE VESICLES,
R. J. Turner* and M. Silverman, Toronto, Ontario.

Considerable evidence now indicates that D-glucose and Na⁺ are co-transported across the renal brush border membrane (BBM) and that a high affinity phlorizin binding site is identical to that part of the carrier exposed at the external face of the BBM. We have studied the effect of membrane potential on this transporter using a BBM vesicle preparation. The intravesicular electrical potential (membrane potential) was varied by imposing ion gradients across the vesicular membrane and/or by employing ionophores such as valinomycin. Experimental maneuvers which made the intravesicular membrane potential more negative enhanced both Na⁺-dependent D-glucose uptake and the initial rate of high affinity phlorizin binding. Similar results were recently reported by Aronson (A.S.N. Fall Meeting, 1977). These data are compatible with a model in which the free D-glucose transporter carries a net negative charge. In parallel with the experimental data we will present the results of a mathematical model of the simultaneous movement of D-glucose, Na⁺ and its corresponding anion into the intravesicular space.

SUBGROUP MEETING

TU-SUB-A1 SOCIOBIOLOGY: HEREDITARY, HUMAN NATURE AND THE BIOLOGICAL SCIENCES. M.D. Rosenthal*, Norfolk, Va 23501

Sociobiologists claim to be fashioning a "new synthesis" which explains the behavior of all organisms, including humans, in terms of evolutionary selection. All human behavior is thereby reduced to the survival and propagation of genes. E.O. Wilson asserts that the "human biogram" includes such genetic traits as male dominance, female subordination and inferiority, competitiveness, aggression, and territoriality. Biological science has shown that human genes transmit biochemical and physiological potentials, but that all complex behavioral patterns are learned. Thus, there is no such thing as "human nature." The AAAS has actively promoted this biological determinism. It has elected Arthur Jensen a Fellow, featured Sociobiology at its meetings, and attacked the political motivations of Wilson's critics. Wilson was recently awarded a Presidential Medal of Science. Furthermore, Sociobiology has already inspired a rapid increase in biomedical literature purporting to find a genetic (or familial) component for everything from alcoholism and schizophrenia to atherosclerosis and cancer. Biological scientists can play an important role in opposing the new Social Darwinism.

TU-SUB-A2 SOCIOBIOLOGY: THE NEW SOCIAL DARWINISM AND THE SOCIAL SCIENCES. S.J. Rosenthal*, Norfolk, Va. 23508.

Sociobiologists have advocated the "biologizing" of the social sciences. That is, they want social scientists to retreat to biological and hereditary explanations for everything from racism, xenophobia, and religious fanaticism to warfare and genocide. Social scientists would thereby absolve those groups and institutions in contemporary societies which foment racial, national, and religious hatred of responsibility for their actions. Even warfare and Nazi genocide would be removed from their sociocultural, economic, and political roots and be transformed into part of "human nature." Sociobiology has been prominently featured at professional meetings, favorably reviewed in prestigious journals, and lavishly promoted in popular media. Nevertheless, only a few social scientists have become crusaders for sociobiology, while an increasing number of social scientists and organizations such as the International Committee Against Racism have begun to criticize Sociobiology and oppose its spread. Out of these efforts has come an increased awareness of how social science has been misused to serve regressive ends in the past and of the threat that this could happen again in the future:

SYMPOSIUM

TRANSDUCTION OF IONS IN CELLS AND ORGANELLES

W-AM-1S LIGHT REGULATED PERMEABILITY OF RHODOPSIN-PHOSPHOLIPID MEMBRANE VESICLES
D. F. O'Brien, Eastman Kodak, Research Laboratories, Rochester, NY 14650

Light absorption by rhodopsin in receptor cell membranes initiates the excitation of the receptor cell. Rhodopsin-phospholipid membrane vesicles have been studied in order to localize initial transduction events. Rhodopsin vesicles prepared from unsaturated phosphatidylcholines (PC) or PC and phosphatidylethanolamines display kinetics for the metarhodopsin I to II transition comparable to those of receptor cell membranes. NMR spectroscopy has been utilized to examine the structural organization of the vesicles. Briefly, the proton, ^{31}P , and ^{13}C -NMR data show homogeneous broadening of the phospholipid resonances due to the methyl, methylene, phosphate groups as well as the carbons of the glycerol backbone. Experiments with added shift or relaxation reagents demonstrate the rhodopsin vesicles are sealed in the dark, and permeable after light exposure. Selected ions (Ca^{2+} , Mn^{2+} , Co^{2+}) are photoreleased from the interior of the vesicles. The quantity released is proportional to the initial ionic concentration. The ions released/rhodopsin bleached is dependent on the light intensity, and high yields (40-200) of Ca^{2+} /rhodopsin bleached are observed at low levels of rhodopsin bleaching.

The present results indicate rhodopsin spans the phospholipid bilayer membrane, and are consistent with an increase in the permeability of membrane vesicles initiated by light excitation of rhodopsin.

Collaborators include: N. Zumbulyadis, L. F. Costa, F. M. Michaels, R. S. Miller, and R. A. Ott.

W-AM-2S THE MOLECULAR STRUCTURE OF A PROTEIN INVOLVED IN ACTIVE TRANSPORT. J. E. Kyte,*
Department of Chemistry, University of California, San Diego, La Jolla, California 92093

($\text{Na}^+ + \text{K}^+$)Adenosine triphosphatase is the enzyme responsible for the active transport of sodium and potassium across the plasma membrane of animal cells. It is proposed that the enzyme, spanning the membrane, forms a channel across it through which the cations pass, in and out of the cell. This channel passes through the center of the enzyme molecule, is formed by the juxtaposition of two identical subunits which are related by a twofold symmetry axis normal to the plane of the membrane and is located between them along that symmetry axis much like the channel which runs along the twofold axis in the hemoglobin molecule. Experimental observations of the structure of the enzyme which are consistent with this hypothesis will be presented.

W-AM-3S ^{31}P AND ^{13}C NMR STUDIES OF METABOLISM AND BIOENERGETICS IN SUSPENSIONS OF LIVING CELLS. R. G. Shulman, K. Ugurbil, T. R. Brown, H. Rottenberg, S. Ogawa, T. Yamane, G. Navon, J. A. den Hollander and S. M. Cohen, Bell Laboratories, Murray Hill, N.J. 07974

High Resolution ^{31}P NMR studies of intact cells are capable of measuring intracellular and extra-cellular pH and their differences, ΔpH , because many phosphate metabolites have pH sensitive chemical shifts. In addition it is possible to follow intracellular metabolism by measuring the time course of resolved ^{31}P peaks. By feeding glucose to anaerobic *E. coli* and accumulating NMR spectra for two minutes we followed the rates of Fructose 1,6 diphosphate formation, the conversion of ADP to ATP, the changing inorganic phosphate concentrations and the time dependence of ΔpH . The time sequences indicate that under these conditions ATP hydrolysis generates a ΔpH . Under anaerobic conditions inhibiting ATPase activity by DCCD or by the use of ATPase⁻ mutants maintains $\Delta\text{pH}=0$ and extends the ATP lifetime. It is possible to show that the rate of glycolysis is pH dependent decreasing sharply as the pH drops below 7. In aerobic *E. coli* it has been possible to saturate the nuclear spin of the terminal phosphate of ATP and to watch this saturated spin appear at the intracellular inorganic phosphate peak. This saturation transfer is eliminated by 1mM DCCD showing that the dominant pathway is through ATPase. T_1 measurements coupled with these saturation transfer results enable us to determine the *in vivo* unidirectional rate constants for the ATPase reaction. Glycolysis has been followed in more detail in *E. coli* and brewers yeast by ^{13}C NMR studies of labelled glucose metabolism. Many of intermediates and end products of glycolysis have been identified in one minute accumulations, and the end products evolve into intermediates of the citric acid cycle upon introducing oxygen. Selected applications of these techniques to mutants of glycolysis in micro-organisms, long lived lymphoid line cells, HeLa cells, Friend erythroleukemic cells and rat liver mitochondria will also be discussed.

W-AM-4S HOW DO NEUROTRANSMITTERS CONTROL ION CHANNELS IN BIOLOGICAL MEMBRANES? H. A. Lester, Division of Biology, Caltech, Pasadena, CA 91125

This problem is studied at the acetylcholine (ACh) receptor of nerve-muscle and nerve-electroplaque synapses. Fluctuation analysis and single-channel recordings reveal a unique open conductance of the channel; with present techniques one can detect no intermediate steps in the transitions between open and closed states. Transition rates are revealed by relaxation experiments. One may exploit (a) brief pulses of ACh itself, released in response to presynaptic impulses; (b) sustained jumps of agonist concentration, produced by *cis-trans* photoisomerization of Bis-Q; or (c) jumps of membrane voltage. Opening rates increase linearly with agonist concentration, at a rate of 10^7 M sec^{-1} for ACh itself and 4-30 times higher for some *bis*-quaternary compounds with hydrophobic groups. Perhaps the channel opens as the receptor binds an agonist molecule (or the second in a sequence of two molecules). Closing rates (10^2 - 10^4 sec^{-1}) also vary among agonists, but apparently not with agonist concentration. Perhaps the channel-closes as the bound agonist molecule leaves the receptor (or as either of two molecules leave). Channels close more rapidly, and agonist binds less tightly, as the membrane is depolarized; both effects occur at a rate of e-fold per 85 mV. What role does this voltage sensitivity play in the functioning synapse? It allows receptors both (a) to bind ACh tightly at the resting potential ($K_D \sim 50 \mu\text{M}$); and (b) to release ACh quickly if the transmitter-receptor interaction leads to a postsynaptic impulse. Thus an efficient response to transmitter is reconciled with rapid, repetitive transmission. In recent experiments we probe the agonist-receptor-channel complex with photochemistry. A brief flash photoisomerizes a bound molecule of *trans*-Bis-Q, which is a good agonist, to the *cis* form, which is a poor agonist. As a result the channel closes within 100 μsec —at least two orders of magnitude faster than with unperturbed *trans*-Bis-Q. This observation, like the other facts presented, emphasizes the tight and rapid coupling between the binding site and the channel.

MINISYMPOSIUM

ULTRAHIGH RESOLUTION ELECTRON MICROSCOPY

W-AM-1M VISUALIZATION OF ISOLATED HEAVY ATOMS WITH THE STEM AND THE CTEM. Joseph S. Wall, Biology Department, Brookhaven National Laboratory, Upton, New York 11973.

Visualization of isolated heavy atoms has been demonstrated with both the Scanning Transmission Electron Microscope (STEM) and the Conventional Transmission Electron Microscope (CTEM). Application of heavy atom specific labels to biological systems has been limited by radiation damage induced in the imaging process. Radiation damage can be reduced by imaging ordered arrays at low dose and employing spatial filtering techniques. Use of heavy atom labels to analyze arrays of less than $\sim 10^4$ elements will require improved imaging techniques and/or improved techniques for specimen preservation. Theoretical calculations can give estimates of heavy atom signals and of the efficiency of utilization of available information, but only crude estimates of image noise and the physical effects of (chemical) radiation damage. The STEM is uniquely suited to measure experimentally such parameters on the same specimen since, as stated by the reciprocity theorem, the operating modes of the CTEM can be simulated with a STEM (with known changes in detector efficiency). The reverse is not practical with currently available CTEM's. Atom signals calculated theoretically for various instrumental operating modes are in good agreement with experimental measurements. Background noise consists of two components: quantum counting noise and spatial fluctuation in substrate signal. At low dose, quantum noise predominates. Substrate noise from the thin ($\sim 20\text{\AA}$) amorphous carbon films commonly employed, is poorly understood theoretically, and few experimental measurements are available from either instrument. The dose dependence of single atom signal to noise ratio is a distinctive feature of each imaging system.

With either instrument it appears that a significant advance in specimen preservation will be necessary for application of heavy atom labeling to randomly distributed biological molecules. Significant reduction in atom motion and in mass loss has been demonstrated for cooled specimens, and improved preservation has been obtained for frozen hydrated specimens. Now that the practical problems involved in building vibration free cold stages have been essentially solved, it appears that low temperature techniques will offer the next important advance in the practical utilization of heavy atom labels. (Supported by the U.S. D.O.E. and Biotechnology, Resource Branch, NIH).

W-AM-2M STRUCTURAL STUDIES OF NUCLEOPROTEIN COMPLEXES. Michael Beer*, Department of Biophysics, Johns Hopkins University, Baltimore, MD 21218

The structure of macromolecular complexes can be illuminated by following their assembly in the electron microscope. Thus complexes between one or more ribosomal proteins and r-RNA reveal the protein binding sites and the constraints put on the RNA by the bound proteins. To pursue such studies at high resolution we use heavy atom labels and a STEM which can image them. That atomic labels allow the deduction of structure is indicated by studies of Osmium reacted polynucleotides which show atom distributions constant to better than 10\AA and consistent with the known structure. Protein labeling similarly suggests that susceptible groups can be demonstrated. Thus using RNase as a test system it was shown that three atoms of Pt[Gly-L-Met]Cl bind to one molecule of protein and the STEM reveals three heavy atoms within images of the enzyme. When 4-Mercaptobutyrimidate binding to lysines is followed by Pt attachment to the SH groups so coupled again the heavy atoms can be observed coupled to the protein molecules.

Such labeling techniques are being used to localize proteins or nucleic acids in nucleoprotein complexes, to establish precise binding sites and to indicate shapes and sizes of proteins.

W-AM-3M PHYSICAL LIMITATIONS CONFRONTING STRUCTURE ANALYSIS AT ATOMIC RESOLUTION. R.M. Glaeser, Division of Medical Physics and Donner Laboratory, University of California, Berkeley, CA 94720

Structure analysis of complex biological materials at atomic resolution by electron microscopy and electron diffraction is confronted by four major difficulties. (1) The problem of maintaining the needed degree of specimen hydration within the vacuum of the microscope can now be overcome by differential pumping, by glucose embedding or by the use of frozen specimens. These three methods are to some degree complementary, and each suffers from one or another drawback. (2) The problem of electron-beam induced radiation damage can only be overcome by spatial averaging of low-dose, statistically noisy images. New work by Saxton and Frank indicates that this principle can be extended to small arrays of particles and even, in favorable cases, to individual particles. The use of low specimen temperatures seems to give a 3- to 6- fold enhancement of the allowable electron dose for macromolecular specimens. Improved vibrational stability and stage-tilting capabilities must be made available in order to take advantage of this effect. Numerous other technical advances, including improved detector devices, are also needed. (3) The failure of the first Born approximation in the theory of electron scattering is known as the "dynamical effect" in diffraction theory. Theoretical calculations indicate that dynamical scattering of high energy electrons may introduce complications in structure analysis for a specimen thickness greater than 200Å to 300Å. (4) The contrast transfer performance of the best present-day instruments is limited at about 3.5Å resolution. Improved spatial and temporal coherence, the use of shorter wavelength electrons, and the use of spherical and chromatic aberration correctors are among the possible solutions to the problem of getting an instrumental resolution of 2Å or better. The recent progress of N. Uyeda and his colleagues in imaging the chlorinated phthalocyanine molecule with 500 keV electrons clearly demonstrates the advantages that higher resolution would give in electron microscope structure analysis of biological materials.

W-AM-4M STRUCTURE ANALYSIS OF MOLECULES IN CRYSTALLINE ARRAYS. P. N. T. Unwin, MRC Laboratory of Molecular Biology, Hills Road, Cambridge CB2 2QH, England

The three-dimensional structures of ordered assemblies of biological molecules can be obtained electron microscopically by methods similar to those used in X-ray diffraction analysis of protein crystals. The structure factor phases are obtained by calculation from Fourier transforms of the images, and the amplitudes are obtained by direct measurement of electron diffraction intensities (or by calculation from the images). This approach avoids the subjective element involved in the selection of isolated particles, and overcomes, to an extent, the limitations in visualizing them at high resolution brought about by radiation damage. The applications and prospects of the method will be discussed, using recent structure determinations as illustrations.

W-AM-5M IMAGE PROCESSING AT ULTRAHIGH RESOLUTION. J. Frank*, New York State Department of Health, Division of Laboratories and Research, Albany, New York 12201

With the advent of new methods of structural investigation combining specimen preserving preparation techniques, low dose electron microscopy and computer averaging /1/, the resolving capability of the electron microscope can now be fully utilized in the study of biological objects that occur in flat, ordered arrangements. As the electron optical resolution limit is approached, the instrument aberrations increasingly prohibit a naive interpretation of the electron micrograph in terms of a shadowgraph of the object's mass density distribution. Under the regime of phase contrast theory, the projection of the potential distribution of the object is imaged with a defocus dependent distortion which can be characterized by a transfer function. Deconvolution becomes a necessary step in the reconstruction of the true object projection. The influence of instrument factors such as defocusing, illumination aperture, energy spread and electrical instabilities on the transfer function are now well understood. This knowledge can be used to optimize the information yield contained in the electron micrograph.

Attempts to extend averaging methods to non-periodic objects with specific attachment to the supporting film lead to the application of correlation and signal detection methods to electron micrographs. It has recently been shown /2/ that subminimum exposure versions of a biological particle although invisible to the eye can be detected by the aid of correlation functions. First reconstructions from sets of arbitrarily oriented and translated particles obtained with computer alignment techniques have been reported /3/.

The value of point mapping operations dependent on local or global statistics in preprocessing and interpretation of electron micrographs is currently being assessed systematically. Experience in other fields has shown that these operations are very effective in discriminating between areas with different texture. In the context of low dose microscopy of non-periodic objects, it may be expected that they can be used to aid the search for particle boundaries.

/1/ Unwin, P.N.T. and Henderson, R. (1975), *J. Mol. Biol.* 94, 425-440

/2/ Saxton, W.O. and Frank J. (1977), *Ultramicroscopy* 2, 219-227

/3/ Frank, J., Goldfarb, W., Eisenberg, D., and Kessel, M., these proceedings

W-AM-6M HIGH-RESOLUTION CELL ARCHITECTURE BY HIGH-VOLTAGE ELECTRON MICROSCOPY.* Mircea Fotino, University of Colorado, Boulder, Colorado 80309.

Improved resolving power is one of the important features of transmission electron microscopy at higher accelerating voltages. Other consequences of high-voltage operation will also be briefly reviewed as background of interest in ultrastructure research.

The effectiveness of high-voltage electron microscopy in biological research has been explored and improved over the last few years. It is increasingly being recognized as a powerful and productive tool for the study of macromolecular and cellular systems. Areas of applicability include the fine structure and organization of organelles, the identification of global features in cells and tissues, the assembly and evolution of viruses within host cells, the role of fibers and microtubules in cell motility, the localization of specific proteins by antibodies, the evolution of chromosomes and of the entire mitotic apparatus, the identification by autoradiography of extended transport patterns of small RNA within the cell, the role of specific drugs and other agents in the transformation of normal cells to malignancy, and others.

Many of these applications leading to new perspectives of global cell architecture are carried out through extensive use of stereoscopic imaging, particularly suitable to the exploration of three-dimensional configurations.

*Supported by NIH Division of Research Resources under Grant No. RR00592.

RADIATION BIOLOGY

W-AM-A2 PHOTOLYSIS OF IODINATED CYTOSINE IN DNA. R. O. Rahn and R. S. Stafford, Biology Division, Oak Ridge National Laboratory, Oak Ridge, Tennessee 37830

The photochemistry of iodocytosine (IC) containing DNA was examined for possible evidence of excitation energy transfer. *E. coli* DNA was iodinated with ^{125}I using the Commerford method and samples containing from 1 to 84% IC were irradiated at either 254 nm or 313 nm. At 313 nm, a fluence of $3 \times 10^4 \text{ J/m}^2$ removed 20% of the iodine. Sedimentation analysis showed that the initial molecular weight was $>10^6$ daltons and that 1 chain break and 1 alkali labile bond were formed for every 10 iodines lost. The presence of ethanol or cysteamine reduced the number of breaks 2-fold. The rate of iodine loss at 254 nm was the same for the 1% and 84% substituted samples and equivalent to that for IdCMP. Hence, long range energy transfer to IC traps in DNA is not a likely event. (Operated by the Union Carbide Corp. for the Department of Energy.)

W-AM-A1 RADIATION EFFECTS ON 5-BROMOURACIL-SUBSTITUTED DNA IN VITRO AND IN VIVO. J. D. Zimbrick and C. M. Beach,* University of Kansas, Lawrence, Kansas 66045

It is a general phenomenon that living cells containing DNA in which thymine (T) is replaced by 5-bromouracil (BU) are more radiosensitive than their unsubstituted counterparts. The radiation chemical basis for this sensitization is hypothesized to involve negative charge transfer to BU followed by dissociation to form uracil-5-yl radicals and Br^- . In vitro studies on gamma-irradiated aqueous solutions show that T^- , O_2^- , CO_2^- and certain other anions transfer charge to BU which then dissociates as hypothesized. These in vitro studies have been extended to BU-substituted *E. coli* DNA (BU-DNA). It has been found that e^- plus either OH^- or CO_2^- are able to destroy essentially all of the BU bases in the DNA and that CO_2^- is more effective than OH^- in destroying BU. These data present strong evidence for support of the hypothesis that negative charge is transported along DNA chains. O_2^- anions are not able to transfer charge to DNA. BU destruction in the DNA of gamma-irradiated *E. coli* in vivo has been determined to be approximately 50 bases/100eV. (Supported by NIH-NIGMS grant GM-18927.)

W-AM-A3 Effective LET for DNA incorporated ^{125}I and Size of Sensitive Target for Inactivation of Cultured Mammalian Cells. K.S.R. SASTRY*, U. of Mass., Amherst, and D.V. RAO, N.J. Med. School, Newark. Recent experiments¹ have shown that DNA incorporated ^{125}I is about 6 times more effective than DNA incorporated ^3H or ^{131}I in killing cultured mammalian cells. The observed high LET behavior of ^{125}I is qualitatively ascribed to influence of low energy Auger electrons emitted in the electron capture decay of ^{125}I . We have evaluated the Auger and Coster-Kronig electron spectra in ^{125}I decay using McGuire's theoretical rates², and calculated the effective LET, \bar{L} , of these electrons as a function of the distance r from the disintegration site. \bar{L} is very sensitive to r , varying from about 130 KeV/ μ at $r = 10 \text{ A.U.}$ to 1 KeV/ μ at $r = 5 \mu$. If we use recent RBE vs LET data of Cox et al.³, we find that the observed RBE for ^{125}I indicates a sensitive target size of about 40-50 A.U. with $\bar{L} \sim 100 \text{ KeV}/\mu$. For the same value of r , we obtain RBE ~ 1 for ^3H and ^{131}I .
*Supported by Grant BRSG RR07048-09 to U.Mass.
¹K.G. Hofer and W.L. Hughes, *Rad. Res.* **47**(1971)94
²E.J. McGuire, *Phys. Rev. A* **5**(1972)1043, 1052; **9**(1974)1840
³R. Cox et al. *Nature* **267**(1977)425

W-AM-A4 ESR-ENDOR STUDIES OF RADIATION DAMAGE TO NUCLEOSIDES AND SUGAR-PHOSPHATE MODEL COMPOUNDS S.E. Locher* and H.C. Box (Intr. by R. Fiel). Roswell Park Memorial Inst., Buffalo, NY 14263

Low temperature ESR-ENDOR studies of radiation damage to single crystals of nucleosides and sugar-phosphate compounds have been undertaken. A carbon-centered radical with two non-exchangeable β couplings has been identified after X-irradiation of 6-azauridine at 4°K. Abstraction of hydrogen from C₄ of the ribose is a probable explanation. Irradiation of glucose-1-phosphate at 4°K yields several radical species. One species has an anisotropic g value indicative of an oxygen-centered radical. ENDOR studies indicate at least three different overlapping carbon-centered radicals. One of the carbon-centered radicals contain two protons weakly interacting with the unpaired electron. A second radical exhibits two proton hyperfine couplings, one of which is markedly anisotropic. Rather poor ENDOR signals from the third carbon-centered radical indicate at least five proton couplings.

W-AM-A5 ESR-ENDOR STUDY OF RADIATION DAMAGE IN ZINC ACETATE. R. LoBrutto* and H.C. Box, Roswell Park Memorial Institute, Buffalo, NY 14263

Zinc acetate dihydrate is a useful model compound for studying radiation damage processes. Several steps in the radiation damage mechanism have been determined through use of ESR-ENDOR spectroscopy at 4.2°K. ENDOR measurements have provided accurate determinations of proton hyperfine couplings in the radical species CH₃ and H₂C-CO₂. Further, the primary reduction product, H₃C-CO₂, was found to decay into a secondary radical, probably CO₂, upon warming the sample. The species CO₂ is produced with much greater yield, by irradiation at room temperature. The ¹³C hyperfine coupling tensor and g-tensor for this secondary species were measured. Comparison with similar data from other studies of irradiated carboxylic acids and salts suggests that, in the former, the primary reduction product decays to form a radical of the type R-C=O (where R is an aliphatic group), while CO₂ is the main secondary reduction product in salts of carboxylic acids.

W-AM-A6 OPTIMUM ALPHA PARTICLE CROSS-SECTIONS FOR INDUCTION OF CELL LETHALITY, DIVISION DELAY, DNA DAMAGE, AND MUTATION. A. Cole, The University of Texas System Cancer Center, Houston, Texas 77030

Am-241 alpha particles of 2 to 24 μ m penetrations have been utilized to induce various forms of damage in mammalian cells. Optimum cross-sections in μ m², which were observed for 2 to 3 MeV particles which deposited energy at the rate of 200 KeV/ μ m within the cell, were 4,400 for DNA single strand breaks, 900 for DNA double strand breaks, 200 for division delay, 65 for lethality, about 0.16 for cell transformation (indirect estimate based on data reported in the literature), and 10⁻³ for mutation (6-thioguanine resistance). Since an alpha particle which deposits 200 KeV/ μ m will damage any susceptible site that it traverses, optimum cross-sections can be taken to correspond to the total projected areas of the affected sites. For example, actual projected areas in μ m² were 3,200 for the DNA, 330 for the cell, 160 for the nucleus, and about 10 for a chromosome, 1 for a centriole, and 10⁻³ for a gene. In this way optimum cross-sections, combined with other data, were utilized to specify likely susceptible targets. (Supported by DOE Contract EY-76-S-05-2832.)

W-AM-A7 HEAVY PARTICLE TRACKS IN RADIOBIOLOGY.

A. Chatterjee*, J.L. Magee, and C.A. Tobias* Lawrence Berkeley Laboratory, Berkeley, California 94720

A theoretical model will be presented to correlate the microscopic distribution of energy around the trajectory of a penetrating heavy particle with the production of chemically reactive species in water. Because of glancing collisional losses, a heavy particle develops a cylindrical region of very high energy density called the "core." Outside the core there are numerous tracks of energetic electrons produced in knock-on collisions and this region is called the "penumbra." It is generally believed that in about 10⁻¹⁰ sec reactive species are most likely to have reacted with various biological molecules. In view of the short time involved, we have assumed that the electron tracks are chemically isolated from each other. As the chemical reaction in the core progresses the size of the core also increases because of diffusion. This core expansion leads to engulfing of radicals present in the penumbra region. With the help of a differential equation these processes have been described and evaluated quantitatively. Results of this model have been applied to the Fricke dosimeter system. These results and their relevance to radiobiology will be discussed.

W-AM-A8 DETERMINATION OF THE ATOMIC NUMBER AND ELECTRON DENSITY OF BIOMATERIALS BY DUAL-ENERGY TOMOGRAPHY. F. L. Roder, H. K. Huang, and M. Cerroni, The Aerospace Corp., Georgetown Univ. Med. Center, Washington, D.C., 20007.

By appropriate filtration and selection of tube potential, X-ray beams were obtained at two effective energies, which demonstrated minimal beam hardening in passing through up to ten mean free paths in copper. *In vivo* CT cross sections were then obtained at these two effective energies, and the data thus obtained were deconvolved to construct electron-density and average-atomic-number mappings, using the Klein-Nishina cross section and assuming an analytical expression for the atomic photoelectric cross section of the form $T_{P.E.} = \text{const.} \cdot Z^{4.5}/E^3$. No prior assumptions concerning the composition of the biomaterials were made. Agreement between the computed and published values for the electron density and average atomic number was within ten per cent.

W-AM-A9 RADIOPROTECTION OF PHOSPHOLIPID MEMBRANES IN TRITIATED WATER BY SUPEROXIDE DISMUTASE. A. Petkau Medical Biophysics Branch, Whiteshell Nuclear Research Establishment, Atomic Energy of Canada Limited, Pinawa, Manitoba, Canada R0E 1L0.

Phospholipid membranes, prepared in distilled water as previously described (Biochim. Biophys. Acta 433 (1976) 445) were exposed at 25° in darkness to different dose rates from ³H with addition of 0-10⁸ pCi/ml of tritiated water (NEN, Specific activity 25.0 mCi/g). Dose rates* were calculated from the ³H concentrations and its mean energy per disintegration of 0.0057 MeV. Samples were halved with one portion receiving superoxide dismutase (1 μ g/ml) and the other serving as the untreated control. Hydroperoxide formation in the two series was periodically monitored as an increase in absorbance (ΔA) at 232 nm. Radiation doses were derived from the calculated dose rates and elapsed time. The relationship between the accumulated dose (y) and dose rate (x) is of the form $y = a(\Delta A)x^b$, where $b = 0.78 \pm 0.02$ and $a(\Delta A)$ depends on the value of ΔA . Superoxide dismutase does not change the exponent b but increases the value of $a(\Delta A)$.

*Dose rate for samples without tritiated water was estimated with LiF chips, courtesy Dr. H. M. Johnson.

W-AM-A10 DRY ELECTRONS AND HOLES IN RADIOBIOLOGICAL DAMAGE. G. Bakale* and E.C. Gregg, Case Western Reserve University, Radiology Department, Division of Radiation Biology, Cleveland, Ohio 44106

A model of cellular radiation damage in the sub-nanosecond time regime that involves dry electrons and holes is presented. The physico-chemical properties of these species are extrapolated from studies of charges in non-polar liquids and applied to the quasi-structured environment of the target biomolecule, which is assumed to be DNA. Target theory is used to demonstrate the enhancement of the radiation sensitive volume due to the large diffusion coefficients of the dry charges. The mechanism of biological damage resulting directly from these species and implications to carcinogenesis will also be discussed.

W-AM-B2 Quasi-elastic Light Scattering and Microscopic Model of Motions of E-Coli Bacteria in Solution. S.-H. CHEN and M. HOLZ, Mass. Inst. of Tech.--Extensive light scattering experiments have been done to test the current models of motion of E-Coli suspended in chemotactic media. We consider contributions of the structural effects,¹ translation-rotational motions² and "twiddles"³ in the measured photon correlation function. We demonstrated that only when all these effects are taken into account, can the angular dependence of the measured correlation function be satisfactorily explained by the theory.

¹S.-H. Chen, M. Holz and P. Tartaglia, Appl. Opt. **16**, 187(1977); M. Holz and S.-H. Chen, Appl. Opt. (to be published in May 1978).

²M. Holz and S.-H. Chen, Appl. Opt. (to be published).

³M. Holz and S.-H. Chen, (to be published).

W-AM-B3 TRACKING OF BACTERIA WITH A LDV-TECHNIQUE. M. Holz and S.-H. Chen, Massachusetts Institute of Technology, Cambridge, MA 02139

The quantitative analysis of the movements of micro-organisms has received considerable interest. A light scattering instrument based on the laser Doppler difference method has been constructed to record the motion of individual bacteria. The data are collected in a rapid, automated, and unbiased fashion and can be processed by computer directly. Application of the instrument is illustrated with measurements on E. coli bacteria.

INSTRUMENTATION TECHNIQUES II

W-AM-B1 MEASUREMENT OF SWIMMING SPEED DISTRIBUTIONS OF BACTERIA USING PHOTON CORRELATION SPECTROSCOPY (P.C.S.). Gregory E. Stock, Baltimore, Md. 21218

Low-angle autocorrelation functions of laser light scattered from enteric bacteria have been analyzed to determine translational swimming speed distributions. Data were collected under a variety of conditions from several bacterial strains and were analyzed by a least-squares fitting technique. The fitting technique approximates the actual speed distribution by a linear spline (smooth and piecewise linear) function. The first and second moments of the distribution subsequently can be calculated to facilitate comparison of the motility of different preparations. Strong verification of the P.C.S. assay is provided by the excellent agreement between the results of concurrent measurements of translation by the methods of P.C.S. and microcinematography, performed on the same bacterial sample. Coupled with the analysis of synthetically generated data, this has allowed a clear determination of the actual capabilities and limitations of the light scattering assay.

W-AM-B4 ISOELECTRIC FOCUSING OF LIVING MAMMALIAN CELLS. Robert C. Boltz, Jr.*, Paul Todd, and W. C. Hymer (Intr. by A. D. Keith). The Pennsylvania State University, University Park, PA 16802

Successful cell separations have been achieved by whole cell isoelectric focusing in a preformed natural pH gradient in a vertical ficoll-sucrose density gradient. However, the conditions are outside the limits of pH and ionic strength normally tolerated by viable cells, and the carrier ampholytes are mildly toxic. Three cell types were tested in separation experiments lasting 0.4 to 2.5 hr. Freshly-dispersed rat pituitary cells retained their normal Herlant's tetrachrome staining characteristics. Rat mammary ascites tumor cells, strain 13762, formed tumors upon reinjection. Cultured Chinese hamster cells, line M3-1F3, formed colonies with greater than 10% efficiency. The fact that isoelectric focusing allows significant cell viability indicates that it can be developed into a usable living cell purification method. Work supported by USPHS contracts N01-CB-43984 and N01-CB-23863.

W-AM-B5 NMR Relaxation Times Study in Newts and Human

Blood.* H.S. SANDHU and G.B. FRIEDMANN, *Physics Dept., University of Victoria, Victoria, B.C., Canada V8W 2Y2.*
 --Measurements of the proton spin-lattice relaxation time (T_1) in whole blood, plasma, blood cells, *in vitro* liver, live and necrotic tail samples of adult newts and spin-spin relaxation time (T_2) in human whole blood, plasma and blood cells samples have been carried out using nuclear magnetic resonance pulse techniques. The measurements have been made at a frequency of 20 MHz at room temperature. The results show a single T_1 in necrotic liver samples of newts. Live and dead tail samples shows two T_1 values: a short T_1 remaining essentially constant and a long T_1 gradually increasing as a function of time measured from the instant of killing the newt. Measurements of T_2 in human plasma, whole blood and blood cells as a function of hemoglobin concentration will also be presented.

*Work supported by research grants from the University of Victoria, B.C. Department of Labour and the National Research Council of Canada.

W-AM-B6 NMR STUDY OF PHOSPHORUS-31 IN BONE. A. A. Silvidi, D. Todoroff*, S. N. Narra*, *Biophysics Lab., Physics Dept., Kent State Univ., Kent, Ohio, 44242.*

A CW magnetic resonance study of phosphorus-31 was made in samples of bone from humans and various animals. A broad-line spectrometer was used at 7.8 MHz and room temperature. Data were taken for bone of different age, and intact, powdered, and ashed bone. Line widths of the derivative curves have been measured and the second moments determined by a computer program which fit the experimental points to a Gaussian curve. While there are little changes in the line widths, the significant changes in the second moments indicate that the spin-lattice relaxation time of phosphorus may be changing. These results will be interpreted in terms of the dynamics and nearest neighbors of the phosphorus.

W-AM-B7 Magnetic Susceptibility Studies of Static and Kinetic Properties of Biomolecules. J.S. PHILLO, *Stanford U.*

--A new high sensitivity magnetic susceptometer employing superconducting technology has been used for measuring the magnetic properties of biomolecules in solution at physiological temperatures. The millisecond time resolution of this instrument has permitted its use to follow the kinetics of reactions between hemoglobin and carbon monoxide. The forward rate constant for this reaction was obtained, and the magnetic moment of the short-lived species $Hb_4(CO)_3$ was measured for the first time. Static measurements of the temperature dependence of the diamagnetism of dispersions of phospholipid bilayers show changes in diamagnetism at the gel-liquid crystal phase transition of the bilayers. This represents the first observation of diamagnetic changes during a biomolecular conformation transition.

W-AM-B8 FIELD FOCUSING NMR (FONAR) AND THE FORMATION OF IN VIVO CHEMICAL IMAGES IN HUMANS. R. Damadian, L. Minkoff*, and M. Goldsmith, *State University of New York at Brooklyn.*

In 1971 Damadian introduced the concept of whole body NMR scanning and provided the first experimental evidence of its feasibility (R. Damadian, *Science* 171, 1151, 1971). In 1972 he developed the focusing NMR (FONAR) technique to achieve the whole body scan (R. Damadian, U.S. Patent 3,789,832, filed 17 March 1972). Others followed (P. Mansfield and P.K. Grannel, 1973; P.C. Lauterbur, 1973; W.S. Hinshaw, 1974; and A. Kumar et al., 1975). We wish now to report the final materialization of this concept with the successful accomplishment of the first whole body NMR scan of a live human. The forced precessions of a nuclear magnetization under an r.f. driving field provided the basis for obtaining spatial resolution of the signal producing domains of a nuclear resonance sample. Construction of a small aperture within the D.C. field that satisfies this condition permits full-body scanning. Chemical images of the live human body will be shown.

W-AM-B9 CHEMICAL KINETICS FORMATTED DATA AS OUTPUT: TOTALLY AUTOMATED MICROCALORIMETRY OF LIPASE AND OXIDASE REACTIONS. H. D. Brown, S. K. Chattopadhyay, N.J.A.E.S., *Rutgers University, New Brunswick, New Jersey 08903.*

Automation of reaction microcalorimetry requires not only programming and implementation of mechanical aspects of instrument operation but also specification of data output in a format appropriate to the research design. Lipases (from fungal and mammalian sources) and cholesterol oxidases vary in their substrate specificity and in kinetics of reactions they catalyze. Activity using standard systems (synthetic substrates) have been compared with reactions in which human serum has been the source of substrate (levels > 10 μ l serum for cholesterol oxidase; > 20 μ l for lipases). Calvet's geometric correction for heat flow characteristics, curve fitting, and chemical kinetic analyses have been resolved to a computer operating system and then implemented in a M6800-based dedicated microcalorimeter controller (NIH GM-22679; NJ00840).

W-AM-B10 MICROPROCESSOR BASED ANALYSIS SYSTEM FOR SINGLE CARDIAC ACTION POTENTIALS. W. Thies*, L. Dooley*, M. Moloney*, and K. Greenspan, *Indiana University School of Medicine and Rose-Hulman Institute of Technology, Terre Haute, IN.*

The application of electrophysiological techniques to a systematic study of the mechanisms of arrhythmias associated with hypoxia and acute myocardial infarction is beginning to reach a feasible stage as many of the basic principles of automaticity and conduction are being defined. To more clearly define one major determinant of conduction, namely rate of rise of phase 0, an automated system has been developed. Algorithms for the detection and determination of the first derivative of phase 0 have been implemented on a small, inexpensive microprocessor (KIM-1, MOS Technology, Inc.). The system requires less than 1024 bytes (8 bits per byte) of RAM and provides a dynamic range of 48 dB with a resolution of 1 part in 256. The system has been tested on isolated canine cardiac Purkinje fibers.

W-AM-B11 TEXAC: A SPECIAL PURPOSE PICTURE PROCESSING TEXTURE ANALYSIS COMPUTER. R.S. Ledley, Georgetown Univ. Med. Centr., Washington, D.C.

Many of the most important potential applications of computer pattern recognition, particularly in the field of clinical medicine, have not yet been successfully carried out on a feasible basis because of one fundamental difficulty. Applications such as the analysis of chest X-rays, Papanicolaou smears, and other histologic analyses, require a rapid evaluation of the texture of the objects in the picture as essential parameters for successful pattern recognition. However, current computers are particularly slow at such whole picture analyses, and current techniques of curvilinear boundary analysis, determination of grey-level histograms, etc., are not sufficient. The TEXAC instrument is a special purpose computer especially designed for rapid texture analysis and is used in conjunction with a conventional computer. The TEXAC computer is capable of performing whole picture texture analysis operations very rapidly and economically.

W-AM-C2 STRUCTURAL CHARACTERIZATION OF BOVINE NASAL PROTEOGLYCAN SUBUNIT IN AQUEOUS SOLUTION BY QUASIELASTIC LASER LIGHT SCATTERING. H. Reihanian and A. M. Jamieson, Department of Macromolecular Science, Case Western Reserve University, Cleveland, Ohio 44106 and L. Rosenberg, Connective Tissue Research Laboratory, Montefiore Hospital, The Bronx, New York, N. Y. 10467.

Measurements by quasielastic laser light scattering of the translational diffusion coefficients D_t of aqueous solutions of purified proteoglycan subunit (PGS) isolated from bovine nasal septa are reported. Extrapolation to the limit of infinite dilution leads to values D_0^0 which are slightly larger than expected on the basis of the structural models previously proposed. Comparison of the concentration dependence of D_t in the presence of NaCl and GuHCl leads to the conclusion that significant self-association behavior of PGS subunit occurs in the absence of GuHCl. In solutions of low ionic strength unusual non-linear concentration dependence of the translational diffusion coefficients was observed. This phenomenon is interpreted in terms of the perturbation of 'free' translational diffusion by strong intermolecular excluded volume interactions.

W-AM-C3 ACID-BASE AND CHIROOPTICAL PROPERTIES OF CARBOXYL GROUPS IN GLYCOSAMINOGLYCANS, J.W. Park, and B. Chakrabarti, Eye Research Institute of Retina Foundation, Boston, Mass. 02114

The apparent pKa values of carboxyl groups in glycosaminoglycans have been determined by circular dichroic titration. The pKa value of iduronic acid moiety in heparin and dermatan sulfate is ca. 5; of glucuronic acid in chondroitin sulfate is ca. 4. Both N-desulfation and N-acetylation of heparin show a large effect on the pKa value of the carboxyl group of the molecule. The variations of CD properties of glycosaminoglycans with pH agreed well with those of uronic acid component; upon decreasing pH, iduronic acid shows increased negative ellipticity centered near 220 nm, while glucuronic acid appears as increased negative ellipticity ca. 230 nm and positive ellipticity near 210 nm. These differences were also observed in heparan sulfate. The different CD behaviors of iduronic acid in heparin and dermatan sulfate are attributed to the different conformation of the uronic acid moiety. (Supported by PHS Grant EY-01760 and RCDA IK04EY-00070 to B.C.)

PROTEINS AND POLYSACCHARIDES

W-AM-C1 PREPARATION OF PROTEOGLYCAN CORE PROTEIN FOR SEQUENTIAL ANALYSIS. E.N. Jaynes, Jr.,* H.G. Volger* and A.G. Walton, Intr. by D.C. Brooks, Department of Macromolecular Science, Case Western Reserve University, Cleveland, Ohio 44106

The sequence and structure of proteoglycan core protein has been of interest for many years. To evaluate the homogeneity and determine the sequence of core protein, the polysaccharide chains must first be removed without damage to the protein. This has been accomplished by a method previously used for removal of polysaccharide from glycoproteins. Treatment of proteoglycan with hydrofluoric acid in pyridine results in a high molecular weight protein containing negligible amounts of polysaccharide. Stripped core protein from bovine nasal septum proteoglycan and from other proteoglycans has been examined for homogeneity by means of SDS - polyacrylamide gel electrophoresis and other methods, and a study of the solution conformation by circular dichroism spectroscopy has been performed. Perhaps surprisingly the core protein appears to be of uniform molecular weight (~200,000). Selective cleavage and preliminary sequence studies are now in progress and are directed at ascertaining whether repeat peptide sequences occur.

W-AM-C4 EXCITON COUPLING IN THE CIRCULAR DICHROISM SPECTRUM OF THE GLYCOPOLYMER LINKAGE COMPOUND, β ASPARTYL GLUCOSYLAMINE. C. Allen Bush, Dept. of Chem. Ill. Inst. of Tech., Chicago, IL 60616.

The circular dichroism spectra of carbohydrates vicinally substituted by acetamido groups differ fundamentally from those of the common 2-acetamido-2-deoxy sugars as a result of mutual coupling effects. Our calculations follow a method due to Schellman and coworkers which has been widely used in peptide CD calculations and which treats both the exciton coupling and static field effects in a consistent manner. The calculations predict that the 189 nm amide $\pi-\pi^*$ transition is split into two oppositely signed CD bands of approximately equal magnitude. A small $n-\pi^*$ band is predicted near 210 nm. The sign and magnitude of the bands depends on the dihedral angles defining the orientation of the amides with respect to hexapyranose ring. Comparison of the calculated results with the experimental spectra of 2,3 diacetamido glucose and of the glycopeptide linkage compound, 2-acetamido-1-N-(4- α -aspartyl)-2-deoxy- β -D-glucopyranosyl amine, suggests that both amide protons are *trans* to their ring protons in the latter while they are *cis* in the former.

W-AM-C5 OPTICAL PROPERTIES AND STABILITY OF COMPLEXES BETWEEN Cu(II) AND HEPARIN, AND RELATED GLYCOSAMINOGLYCANS. D.C. Mukherjee, J.W. Park, and B. Chakrabarti, Eye Research Institute of Retina Foundation, Boston, Mass. 02114

Absorption and circular dichroic (CD) spectroscopy have been utilized to measure the formation constant and optical properties of complexes between Cu(II) and heparin, and Cu(II) and related glycosaminoglycans. The formation constant of Cu(II)-heparin is ca. 3×10^5 ; of Cu(II)-N-desulfated heparin, less than 100. All these complexes show a characteristic absorption band at 235 nm, which was attributed to a charge-transfer band. Cu(II)-heparin complex exhibits a negative CD band near 235 nm with concomitant decrease in its usual 210 nm negative band. No such CD change has been observed with Cu(II)-N-desulfated heparin at pH < 6. However, at higher pH values, it shows a CD band near 260 nm, presumably due mainly to the amine ligand, in addition to carboxyl group. These CD properties were compared with other Cu(II)-glycosaminoglycan complexes. The possibility of using the CD feature in the elucidation of the molecular conformation of the polymers will be discussed. (Supported by PHS grant EY-01760 and RCDA IK04EY-00070 to B.C.)

W-AM-C6 CONFORMATIONAL CHANGES IN CONCANAVALIN A (CON A) INDUCED BY METAL AND SACCHARIDE BINDING. R. D. Brown, S. H. Koenig, IBM Research Center, Yorktown Heights, NY 10598, and C. F. Brewer,* Albert Einstein College of Medicine, Bronx, NY 10461.

We have recently shown (Biochemistry, (1977), 16, 3883) that presence of Mn at the S1 and Ca at the S2 sites in Con A induces a conformational change in the protein to a "locked" state characterized by very tight binding of the metals. It was also shown that Mn could bind at S2 in the absence of Ca and that the Mn-Mn induced locked conformation was metastable on removal of Mn at low temperatures. In the present work, we investigated Ca and Cd binding to S1 and S2 in the absence of Mn. We show that each of these metals alone also induces the same conformational change as Ca-Mn and that the ternary Ca and Cd Con A complexes bind saccharides quite strongly. Further, we show that saccharide alone is sufficient to induce this conformational transition in apo-protein and that conformation is the main determinant in sugar binding. Ca-Mn-Con A in the final, locked state binds saccharides $\sim 10^4$ times better than apo-Con A in the initial, unlocked, state. About 10^3 of this factor is due to conformation. The main function of the metals appears to be to induce the correct conformation for saccharide binding.

W-AM-C8 INTERACTIONS OF MONOLAYERS OF CONCANAVALIN A WITH MONO-AND POLYSACCHARIDES: A STUDY BY MEANS OF POLARIZED INFRARED ATR SPECTROSCOPY. N. Ockman, *(Intr. by F.S. Cohen), Dept. of Neurology, Albert Einstein College of Medicine, Bronx, N.Y. 10461

Infrared spectra have been obtained for monolayers of concanavalin A spread on saline and solutions of dextran B-1355, methyl α -D mannopyranoside and D-galactose in a saline. The spectra of the films deposited on the germanium plate of the ATR assembly exhibit the amide bands characteristic of the polypeptide chains. Upon compression to surface pressures greater than about 25 dynes/cm, the concanavalin A films show a flattening of the isotherm. This indicates a transition to a predominantly β conformation as shown by the emergence of the band at 1635 cm^{-1} . When dextran is added to the subphase for these compressed films an additional absorption at about 3400 cm^{-1} is seen. The introduction of mannopyranoside eliminates this absorption, D-galactose doesn't affect it. These results agree with the specificity of concanavalin A for the α -D mannopyranosyl residue. The effect of the binding of dextran and α -D mannopyranoside to the monolayers of concanavalin A on the conformation and orientation of the polypeptide chains will be discussed.

W-AM-C9 COMPARISON OF THE INTERACTIONS OF TYPE I AND II COLLAGENS WITH CHONDROITIN 6-SULFATE. D.C. Brooks, R. Dabrowski, and J. Blackwell, Department of Macromolecular Science, Case Western Reserve University, Cleveland, Ohio 44106

C.D. studies of acid soluble calf skin collagen have shown that the thermal melting temperature, normally at $\sim 38^\circ\text{C}$, is increased to $44\text{--}45^\circ\text{C}$ in the presence of a glycosaminoglycan (GAG). All the common GAGs will produce this effect, although a different proportion of each is necessary to give maximum stabilization. We have now extended this work to compare the interactions of collagens I and II with chondroitin 6-sulfate (C6S). Type I was obtained by acid-extraction of rat tail tendon. Two specimens of type II were examined: one was isolated by papain-digestion of pig laryngeal cartilage and the other by non-enzymatic extraction of rat chondrosarcoma. For both type I and type II, the melting temperature is increased from 38 to 44°C by the addition of C6S. However, approximately three times as much GAG is necessary to effect maximum stabilization of type I as compared to type II. The two specimens of type II are identical in terms of the interaction with C6S, despite the differences in their source and preparation.

W-AM-C7 THE USE OF BJERRUM'S "OPTICAL PRINCIPLE" FOR THE RAPID MEASUREMENT OF LIGAND-PROTEIN BINDING ISOTHERMS. P. C. Keck & T. M. Schuster, Biochem. & Biophys. Section, Univ. of Conn. Storrs, CT 06268

The "Optical Principle" of J. Bjerrum, D. Kgl. Danske. Vidensk. Selskab. Mat.-fys. Medd. 21(4), 1 (1944), does not seem to have been used in the study of small molecule protein interactions despite the fact that the method is relatively fast and makes no assumptions about the mechanism of binding. It can be shown that if there exists upon binding a change in some measurable property (i.e. absorbance or fluorescence), then the change in the property normalized to the total protein concentration can be used to define (or prepare) a series of solutions of equivalent ligand saturation, "corresponding solutions". Variation of the total ligand concentration as a function of the total protein concentration across a series of "corresponding solutions" yields directly the formation function \bar{F} and the concentration of free ligand. This titration method yields data in agreement with results from equilibrium dialysis for the binding of methyl orange to bovine serum albumin.

Supported by NIH Grant #AI 11573.

W-AM-C10 RAMAN SPECTROSCOPY AS A PROBE OF MUCOPOLYSACCHARIDE STRUCTURE. R. Bansil,¹ I. V. Yannas,^{2*} H. E. Stanley,¹ ¹Department of Physics and Department of Physiology, Boston University, Boston, MA 02215 and ²Department of Mechanical Engineering, MIT, Cambridge, MA 02139.

We report the first Raman spectroscopic study of the glycosaminoglycans, chondroitin 4-sulfate, chondroitin 6-sulfate and hyaluronic acid, both in solution and in the solid state. These mucopolysaccharides form the matrix of all connective tissues. To aid in spectral identification infrared spectra were also recorded from films of these samples. Vibrational frequencies for important functional groups like the sulfate groups, glycosidic linkages, C-OH and the N-acetyl group can be identified from the Raman spectra. Certain differences in the spectra of the different glycosaminoglycans can be interpreted in terms of the geometry of the various substituents while other differences can be related to differences in chemical composition. In particular, the Raman spectrum is sensitive to whether the sulfate group is axial (as in chondroitin 4-sulfate) or equatorial (as in chondroitin 6-sulfate). Implications of this result in using Raman spectroscopy to probe glycosaminoglycan-collagen interactions, where the sulfate groups are presumed to play an important role, will be discussed.

W-AM-C11 LINEAR DICHROISM AND RADIAL FLOW BIREFRINGENCE OF STREAM ORIENTED HYALURONATE SOLUTIONS AS A FUNCTION OF SYSTEM PH. T. W. Barrett, Department of Physiology and Biophysics, University of Tennessee Center for the Health Sciences, Memphis, Tennessee 38163

The linear dichroism in the radial direction of solution flow over a velocity gradient of approximately $10\text{--}850\text{ sec}^{-1}$ has been obtained from hyaluronic acid at pHs 6.0, 6.5, 7.0, 7.5, 8.0, and 8.5, and $\nu = 0.1$. The radial flow birefringence was obtained for these solutions by a Kronig-Kramers transformation. There is change in linear dichroism and optical anisotropy as a function of pH, with most of the transition across the physiological range: 7.0-7.5. Previously reported axial flow birefringence and extinction angles indicating a similar pH-dependent structural change in hyaluronate solutions across the same pH range are thus confirmed with other instrumentation. The present data together with the axial measurements previously reported permit a complete description of the refractive index tensor for each of the six solutions. The interpretation of these tensors in terms of the Peterlin modification of the Rouse-Zimm Gaussian subchain theory results in a description of entropy production induced by changes in system pH.

W-AM-D2 IONIC CONDUCTANCES AND SURFACE POTENTIAL OF AXON MEMBRANES. S. Ohki, State University of New York at Buffalo, Buffalo, New York 14226.

Ionic currents across squid axon membranes under various clamped voltage conditions were measured with variation of extracellular Ca^{2+} concentrations. It was found that the maximum sodium conductance under voltage clamp was decreased by about 20% for four fold increase in the extracellular Ca^{2+} concentration, whereas the steady state potassium conductance was not changed appreciably. The shift of the conductance-voltage curve along the voltage axis and the observed changes in maximum sodium conductance with respect to Ca^{2+} concentrations in the extracellular bulk solution are analyzed in terms of surface potential and surface ion concentration of the axon membrane. New concepts of intrinsic and overall ionic conductances for axon membranes are introduced.

W-AM-D3 ESTIMATION OF ERROR IN SMALL SIGNAL RESPONSES OF LINEARIZED MEMBRANE EQUATIONS. R. Grisell, University of Texas Medical Branch, Galveston, Texas.

Formulas have been derived for bounds on error in responses to various stimuli, including impulses, steps and sinusoids. These can be used to compare with small signal data and to estimate intervals for fitted parameters. Assume a model $y=f(y,t)$ is linearizable, with linearized equations $\dot{y}_L = [L + L'(t)] y_L$, and that L is stable. Let \underline{a} be the minimum absolute value of real parts of eigenvalues of L , let b be the integral norm of $L'(t)$, and let $K \equiv \text{Mexp}(Mb)$ where $M \equiv n \cdot \max |t^{m_i} e^{-m_i}|$ with \max taken over t and multiplicities $m_i=0, \dots, n$ the number of model equations. By the nonlinearity condition, there is a δ such that for all y satisfying $\|y\| < \delta$, $\|f(t,y)\| < \|y\|$. Then a useful result is $\|y(t)-y_L(t)\| < \frac{1}{2} \|y_0\| \cdot \text{at} \cdot K \exp(1 - \text{at})$ if initial condition y_0 obeys $\|y_0\| < \delta/K$. As one application, a bound on absolute difference between current response I to step voltage stimuli of HH and its linearization can be calculated. For example, the error bound for a 1mV depolarizing step from rest can be as large as about .38 ($\Delta I/I_0$) or 38%. This is approached by the actual maximum difference between linear and nonlinear HH responses of 17%.

NERVES AND AXONS III

W-AM-D1A QUANTITATIVE DESCRIPTION OF THE FIRING PATTERN OF INK GLAND MOTONEURONS IN APLYSIA. J. Byrne, Dept. of Physiology, Univ. of Pittsburgh School of Medicine, Pittsburgh, PA 15261

The release of ink occurs in a relatively all-or-none fashion and responds selectively to strong and long lasting stimuli (Carew and Kandel, 1977). A 5 s train of electrical stimulation to the connectives mimics a noxious stimulus to the head producing a several s multicomponent EPSP followed by an accelerating burst of spike activity in motoneurons located in the abdominal ganglion. Voltage clamp experiments were performed to determine the quantitative extent to which the motoneuron ionic conductances account for the firing pattern and thus the behavior. Six conductance mechanisms have been analyzed: inward Na^+ and Ca^{2+} , outward fast transient K^+ (FK) and delayed K^+ (DK), leakage and synaptic currents. The total membrane current was described by: $I = \frac{C dv}{dt} + \bar{g}_{\text{Na}} A \cdot B (V - E_{\text{Na}}) + \bar{g}_{\text{Ca}} A B (V - E_{\text{Ca}}) + \bar{g}_{\text{FK}} A^2 B (V - E_{\text{FK}}) + \bar{g}_{\text{DK}} A^2 B (V - E_{\text{DK}}) + \bar{g}_l (V - E_l) + \bar{g}_{\text{syn}} (V - E_{\text{syn}})$, with 1st order activation (A) and inactivation (B) kinetics. A computer simulation revealed that the selective response to long lasting stimuli is due to the fast transient K^+ current shunting the initial excitatory input. A late facilitating EPSP contributes to the accelerating burst discharge.

W-AM-D4 ADMITTANCE OF THE Na CONDUCTION SYSTEM IN SQUID AXONS. H. Fishman, D. Poussart and L. Moore UTMB, Galveston TX 77550 and Université Laval, Québec

The small signal behavior of Na conduction was determined by measurement of the admittance (Poussart, Moore & Fishman 1977, Ann. NY Acad. Sci.) in the frequency range 4-1000Hz during suppressed K^+ conduction. At 11°C with 50mM K^+ and 50mM Cs^+ internally, an extremely sharp antiresonance occurs in $|Y|$. This antiresonance is distinguishable from the one that occurs when the K^+ system is not suppressed in that at constant temperature 1) the resonant frequency is lower; 2) the magnitude function is sharper and the phase function exceeds 90°; 3) it is eliminated by tetrodotoxin externally. However, the antiresonance disappears after internal perfusion with 290mM Cs^+ (no K^+) and the phase function exceeds 180° at low frequency which is indicative of a steady state net negative conductance. These data indicate that the admittance of the membrane during suppressed K^+ conduction depends critically on the leakage and residual K^+ conduction system (positive chord conductances) relative to the negative chord conductance produced by the Na^+ conduction system.

Aided by NS-11764, NS-13520 and CNRC A5274

W-AM-D5 SMALL SIGNAL ANALYSIS OF THE K CONDUCTION SYSTEM IN SQUID AXONS. L. Moore, D. Poussart and E. Fishman, University of Texas Medical Branch, Galveston Texas, 77550, and Université Laval, Quebec.

Small step clamp analysis of the K conductance in TTX treated squid axons was done to determine the maximum potential perturbation allowed in order to obtain a linear conductance response and to determine the order of the linearized system. Assuming the HH power (n^4) model, the linearized response occurs when the delay disappears, leaving only an exponential rise of I_K . Signal averaged voltage clamp currents showed diminishing I_K delay for all pulses down to a 1 mV step. Other tests of nonlinearity indicated that a linear response was not seen for pulses greater than 90µV. Thus, a linear response occurs in the limit of a decreasing perturbation of the order of the spontaneous voltage noise seen in the squid axon. This result, in conjunction with the known dependence of the delay on prepulse levels, suggests that the power model description of the sigmoid shape of the K current is an empirical approximation to the nonlinearity of the K conductance. The exponential response seen with small steps, as well as large step pulses after a depolarizing prepulse, indicates that the gating process is first order. Aided by NS-13520, NS-11764 and CNRC grant A5274.

W-AM-D6 TWO SITES FOR BA IONS IN K PORES. S.R. Taylor and C.M. Armstrong, Mayo Clinic, Rochester, N.Y. and University of Pennsylvania, Philadelphia, Pa.

Ba in or out blocks g_K (c.f. Eaton and Brodwick, *Biophys. J.* 15:41a). We perfused squid axons with KF and K glutamate saturated with Ba (30 µM or less free). Ba_{in} causes g_K to decay or "inactivate" when V is positive, more quickly at large V. High K_o slows decay. The V and K_o dependence of decay rate suggest that Ba transiently occupies a site at the inner end of the pore, and most ions then move to a more stable position nearer the outside. For the TEA derivative ϕC_3 , which occupies only the inner site, decay rate is independent of V and K_o . On repolarization Ba leaves pores in two phases: within a few ms, before K activation gates close, and slowly thereafter. The fast component is larger when K_o is high. Ba_{out} has a K_D of about 3mM, which is increased by high K_i or frequent pulsing. For Ba_{out} there is no fast component of recovery on repolarization. Apparently Ba_{in} can occupy a site that is not readily accessible from outside. These actions of Ba probably depend on its crystal radius (1.34 Å) which is so close to K (1.33) that Ba can penetrate a K pore. Pb (1.20) when inside also "inactivates" g_K .

W-AM-D7 BARIUM BLOCK OF POTASSIUM CURRENTS. Eaton, D. C., and Brodwick, M. S., University of Texas Medical Branch, Galveston, Texas 77550.

In perfused squid giant axon, low concentrations of internally applied barium produce a time and voltage dependent block of outward K^+ currents. The dose response curve for the blockage suggests a one site interaction whose dissociation constant is about 5×10^{-8} M. There may be a secondary interaction with an additional site whose dissociation constant is about 10^{-5} . In high external potassium concentrations, with internally applied barium, the tail currents after cessation of the command step show a characteristic "hook" that we associate with rapid unblocking of the K^+ channels prior to their time dependent decay. Experiments with Sr^{++} suggest a blockage similar to Ba⁺⁺, but an additional process manifests itself as a slow increase in K^+ current.

W-AM-D8 K CHANNELS OF NERVE AND MUSCLE: SINGLE-FILE, MULTI-ION PORES. B. Hille and W. Schwarz, *Physiol. & Biophys. U. of Washington, Seattle, WA.* 98195.

K fluxes in delayed rectifier and inward rectifier K channels deviate from independence in many ways that are explainable by a channel with multiple occupancy. The ions move in single file into vacant sites without modifying the barriers or the binding of other ions except through species-independent repulsion. Calculations are done for 2-site and 3-site channels which demonstrate:

1. multiple maxima of flux-concentration relations
2. unidirectional flux ratio exponents > 1.0
3. concentration-dependent permeability ratios
4. anomalous mole-fraction dependence of conductance and permeability ratios.

And with an internal impermeant blocking ion, they give:

5. strongly voltage-dependent block of outward current with relief of block by external K^+ , or,
6. ingoing rectification that shifts with E_K and shows crossover of the I-V relations.

K channels must be at least 3-site channels with high occupancy, with repulsion between ions, and with much lower barriers to ion movement within the channel than to exit from the channel. (Supported by NS-08174).

W-AM-D9 GATING SUBUNIT INTERACTIONS IN SQUID GIANT AXON. M.E. Starzak and R.J. Starzak, SUNY-Binghamton, NY 13901

Temporal shifts of delayed (K^+) currents produced by preconditioning potentials in voltage-clamped squid giant axon (Cole-Moore shift) have been observed for a series of depolarizing step clamp potentials. I-V curves from ascending potential ramps with slopes ranging from 1 mV/msec to 60 mV/msec also produce an anomalous delay with no preconditioning step pulse. To provide a consistent explanation for both these phenomena, the basic Hodgkin-Huxley model is modified slightly to permit a small interaction between the gating subunits in their closed configuration. Unlike earlier models which utilized modifications of the rate constants of first order kinetic equations to exclude subunit interactions, the present approach utilizes a small multimolecular kinetic component to describe the interaction process. The model describes the Cole-Moore shifts at all depolarizing step potentials, and satisfies the observed experimental constraints of both induction and superposition. No new kinetic steps are required to explain the phenomena since the magnitude of the temporal shifts is produced exclusively by a change in the initial kinetic conditions (supported by PHS Grant NS11676 & the SUNY Res. Found.)

W-AM-D10 CONDITIONING HYPERPOLARIZATION-INDUCED DELAYS IN THE POTASSIUM CHANNELS OF MYELINATED NERVE.

T. Begenisich, Univ. Rochester, Dept. Physiology, Rochester, N.Y. 14642.

Hyperpolarizing conditioning pulses delay the onset of potassium channel current in voltage clamped myelinated nerve fibers. Both the development of and recovery from this conditioning are approximately exponential functions of time; the time constants are functions of the conditioning voltage. The delay is larger and develops faster for more hyperpolarized conditioning pulses. The magnitude of the delay (but not the rate of development or recovery) depends upon the test potential - small test depolarizations produce larger delays than large depolarizations. The currents with and without the conditioning pulse cannot be made to superimpose by a simple time translation. Supported by NIH Grants NS08174, NS10981 and NS050825.

W-AM-D11 EFFECTS OF AMINOPYRIDINE DERIVATIVES ON POTASSIUM CHANNEL OF SQUID AXON. G.E. Kirsch* and T. Narahashi (Intr. by C.H. Wu), Northwestern Univ. Med. Sch., Chicago, IL 60611.

A variety of aminopyridine derivatives have been compared for their action in blocking the potassium channels of squid axons. The most effective blocker was 3,4-diaminopyridine (3,4-DAP), which was about 50 times more potent than 4-aminopyridine. 3,4-DAP blocked the channels in a manner dependent upon membrane potential, time and stimulus frequency. Compounds which also showed frequency dependent block but were much less potent included 2,6-diaminopyridine, 4-hydroxypyridine, and 3-hydroxypyridine. In general, compounds which had neither hydroxyl nor amino groups had little effect on the potassium channels, suggesting that hydrogen bonding is involved in the channel block. The high potency of 3,4-DAP suggests that two hydrogen bonds can be formed. Supported by NIH grant NS 14144.

MUSCLE PHYSIOLOGY III

W-AM-D12 RANDOM WALK ANALYSIS OF K FLUXES ASSOCIATED WITH NERVE IMPULSES. J.R. Clay and M.F. Shlesinger Dept Anatomy, Emory U, and Physics, Ga Inst Tech, Atlanta, GA

We have analyzed K fluxes associated with nerve membrane action potential by a random walk treatment of ion motion through a channel containing an arbitrary number of fully occupied K selective sites (Clay & Shlesinger, PNAS 74, 1977). Motion of the row is assumed to occur only when an ion strikes the channel from either side of the membrane. With each collision the row moves outward with probability p_+ or inward with probability p_- . Assuming $p_-/p_+ = \{K\}_e / \{K\}_i \exp(-qV/kT)$ gives $p_+ = (1 + \exp(q(v - E_K)/kT))^{-1}$ with $p_+ + p_- = 1$. Consequently, $I_K = \bar{g}_K n^4 N f \tanh(q(v - E_K)/2kT)$, where N is channel density, n is the HH K parameter, and f is the average collision frequency. A modest increase of f with increasing $|v - E_K|$ gives a linear instantaneous I-V for $|v - E_K| \leq 100$ mV. The tracer efflux θ_e of the model is $n^4 \lambda \chi_s$, where $\lambda = 4Nf / (dN_A \{K\}_i)$ (N_A = Avogadro's number, d = axon diameter) and, for example, $\chi_3 = p_+^4 / (1 - 2p_+ + 2p_+^2)$. The ratio $\theta_i / \theta_e = (p_- / p_+)^{s+1} = \exp((s+1)(v - E_K)/kT)$, which is identical to the Hodgkin-Keynes result. A comparison of fluxes during an HH AP with data indicates that $s=3$.

W-AM-E1 VOLTAGE CLAMP OF ISOLATED CARDIAC PURKINJE CELLS. T. Mehdi* and F. Sachs. Dept. Pharmacology and Therapeutics, SUNY, Buffalo, N.Y. 14214

In order to create a preparation of large cardiac cells without the problems of extracellular space restrictions and series resistance, we have isolated single cells from canine Purkinje strands using enzymes. The cells are 10-20 μ in diameter and 60-100 μ long, free of connective tissue and have clear striations. Viable cells can be maintained for weeks in tissue culture media. The isolated cells cannot be stimulated to contract with extracellular stimulation. The resting potential of the cells is about -20 mV. When hyperpolarized to -90 mV with a microelectrode clamp, large (1 μ A/ μ F) sodium currents with a reversal potential of +20 mV can be evoked by depolarization. The peak I_{Na} -V curve is sublinear. Asynchronous mechanical activity is often seen, especially when chloride is added to the current electrode. Associated with contractions are small current oscillations with a period of about 3/sec at 20°C, and a reversal potential of -30 mV. The contractions and currents can be reversibly blocked by intracellular injection of EGTA.

W-AM-E2 E-C COUPLING IN DEVELOPING CAT HEART J. Maylie* K. Thornburg, and J.J. Faber, Dept. of Physiology, Univ. of Oregon Medical School, Portland, OR 97201.

Neonatal cardiac cells are smaller in diameter than those of adult cats, lack T-tubules and do not have as much sarcoplasmic reticulum (SR). Studies performed on neonatal and adult papillary muscles show that post-extrasystolic potentiation is 6 times greater in the adults than in neonates. The rate induced inotropic response consists of a fast (first 6-8 beats) and a slow component (50-100 beats). The fast component accounts for 50% of the final twitch potentiation in neonates vs 95% in the adult. Beat constants of the decay of post-extrasystolic potentiation and the fast component of a negative rate staircase are the same in neonates and adults. The potentiation following an extrasystole induced during the slow component of a rate-induced inotropism is transient and decays back to the envelope of an undisturbed rate inotropism in both neonate and adult hearts. Studies using single sucrose gap voltage clamp technique show that post-clamp potentiation is significantly smaller in the neonate than in the adult. The results suggest that the development of a recirculating Ca^{2+} store parallels the development of the SR and T-tubular system.

W-AM-E3 PARAMETERS OF CURRENT NOISE CALCULATED FROM VOLTAGE NOISE AND IMPEDANCE OF THE HEART CELL MEMBRANE NEAR REST. J.R.Clay, L.J.DeFelice and R.L.DeHaan, Dept. Anatomy, Emory University, Atlanta, Ga. 30322

We have recorded voltage noise and impedance at low frequencies ($f < 10\text{Hz}$) from spheroidal chick embryonic heart cell aggregates impaled with two glass microelectrodes made quiescent with TTX. Input capacitance measured from the initial slopes of small ($\leq 1\text{mV}$) voltage responses to rectangular current pulses ($0.1\text{-}1\text{nA}$) is proportional to aggregate volume and to total cell surface. Input slope resistance (R_i) is inversely proportional to aggregate volume at constant membrane potential. R_i increases by a factor of 4-5 with depolarization from -70 to -60mV . These results together with the observed voltage homogeneity for $f < 200\text{Hz}$ indicate that a lumped circuit model is appropriate. An RLC model with a resonant frequency near 1Hz was used to fit the oscillatory overshoot of the measured voltage pulses. Current noise parameters were calculated from voltage noise measurements using $S_i = S_v / |Z|^2$. The principal result is that $S_i(0)$ increases 10 fold for $-70 < V < -60\text{mV}$. That is, $S_v(0)$ increases by 100 over the same voltage range. These results suggest $i = \bar{g}_K s(V - E_K)$ as a PM model where s decreases with $V > E_K$.

W-AM-E4 OUTWARD MEMBRANE CURRENT FOLLOWING RAPID SODIUM-LOADING OF CARDIAC PURKINJE FIBERS. D.C.Gadsby* & P.F.Crane, Rockefeller University, New York, 10021.

Briefly exposing canine cardiac Purkinje fibers to K-free fluid in a fast perfusion system causes a transient hyperpolarization on returning to K-containing fluid (Bio-phys.J. 17:7a, 1977). In a series of parallel experiments the membrane potential was controlled using a simple feedback circuit. With the membrane potential held at its resting level in the K-containing fluid, a steady net inward current is recorded within a few sec of switching to K-free fluid. On returning to K-containing fluid a transient net outward current is seen which reaches a peak in a few sec and then declines to zero within a few min. At a given external [K] the magnitude of the outward current peak increases with the time in K-free fluid. For a fixed time in K-free fluid both the magnitude of the peak of the outward current and rate of its subsequent decline increase with the level of external K ($[K] \leq 16\text{mM}$). The outward current is abolished by 10^{-5}M acetylcholinesterase. These observations support the earlier conclusion that the transient hyperpolarization results from a temporary increase in outward "electrogenic" membrane current reflecting a transient stimulation of the Na-K pump following its arrest in K-free fluid. (Grant:HL-14899)

W-AM-E5 K^+ EFFLUX AND UPTAKE IN FROG VENTRICULAR MUSCLE. G. Martin* and M. Morad, Department of Physiology, Univ. of Pennsylvania, Phila., PA 19104.

K^+ -selective μ -electrodes were used to monitor the uptake of K during activity in frog ventricular muscle. Step increases in the frequency of stimulation (24-72 shocks/min) result in an initial accumulation of K^+ (1-2 min) followed by a decay of K^+ activity to a steady state level above pre-stimulation values. Termination of beating results in depletion of K^+ often by 1 mM below pre-stimulation concentration. The magnitude of K depletion depends on frequency, duration of stimulation and $[\text{K}]_0$. Decreasing $[\text{K}]_0$ to 1-1.5 mM, addition of ouabain (10^{-5}M) or 70 mM LiCl (Na replaced by Li), suppressed K^+ depletion, while epinephrine enhances the rate and magnitude of K^+ depletion. Membrane depolarization and hyperpolarization accompanied K^+ accumulation and depletion. Action potential duration is shorter than control during the maximum K^+ depletion. The results suggest that significant K^+ accumulation occurs during rapid beating. K^+ is removed from the extracellular space by an active and possibly electrogenic process at the rate of $\sim 0.25\text{ mM/sec}$.

W-AM-E6 THE INWARD RECTIFYING POTASSIUM CURRENT IN VOLTAGE CLAMPED VENTRICULAR MUSCLE. L. Cleemann* and M. Morad, Dept. of Physiol., Univ. of Penna., Phila., PA.

Measurements of extracellular K accumulation indicate that a major part of the membrane current measured at potential below -20mV corresponds to the inward rectifying K^+ current, I_K . When the membrane is depolarized more than 20mV from the resting potential (-80mV) I_K exhibits negative slope conductance, and K^+ accumulates in the extracellular space thereby increasing the outward K^+ current. I_K is quantitatively described by the model which assumes that the movement of K^+ ions through a pore is rate limited only by the narrow section close to the inner membrane surface. $Y \approx 0.15$ is the fraction of the membrane potential, V_m , which subsides between the narrow section of the pore and inside of the membrane. The local K^+ concentration inside, K_i^* , and outside K_e^* , of the narrow sections are in equilibrium with K_i and K_e , respectively: $K_i^* = K_i \exp[(Y - V_m)F/RT]$, $K_e^* = K_e \exp[(Y - 1)V_m F/RT]$. It is further assumed that the fraction of open pores is proportional to K_e^* and that the K^+ flux through the open channel is proportional to the local K^+ gradient: $I_K \propto K_e^* (K_i^* - K_e^*)$. In this model all slow membrane currents more negative to -20mV can be attributed to extracellular K^+ accumulation. (HL 16152)

W-AM-E7 IONIC CURRENTS AND INTRACELLULAR POTASSIUM IN HYPOXIC MYOCARDIAL CELLS. W.G. Wier* (Intr. by J.W. Woodbury) Dept. of Physiol., U. of Utah, SLC, UT 84108.

K^+ sensitive liquid ion exchanger microelectrodes and single sucrose gap voltage clamp were used in normal and hypoxic myocardial papillary muscles to measure intracellular K^+ activity (a_K^i) and membrane ionic currents. Hypoxia caused statistically significant ($P < .05$) decreases in a_K^i , resting membrane potential (E_m) and action potential duration (a.p.d.). In 8 control muscles a_K^i was $99.7 \pm 3.9\text{ mM}$ and was $86.2 \pm 3.1\text{ mM}$ in 5 muscles after 2 hours of hypoxic incubation. The corresponding change in calculated K^+ equilibrium potential (E_K), (-102.1 mV to -98.3 mV), was paralleled in direction and magnitude by a change in E_m (-96.1 mV to -90.0 mV) (cf. McDonald et al., J. Physiol. 229:559, 1973). Voltage clamp experiments showed that hypoxia caused a decrease in slow inward current and an increase in outward current which accompanied a large decrease in a.p.d. (80%). The observed effects on a_K^i and ionic current have been incorporated into a mathematical model of the myocardial membrane action potential (Beeler et al., J. Physiol. 268: 177, 1977). The computed "hypoxic" action potential closely resembles measured hypoxic action potentials.

W-AM-E8 STEADY STATE SODIUM CURRENT IN CARDIAC PURKINJE FIBRES. I. Cohen*, M. Ohba**, C. Ojeda**, D. Eisner**, D. Attwell*, Physiology Laboratory, Oxford, and HSC Stony Brook.

In most regions of the mammalian heart, the upstroke of the action potential (AP) is produced by an influx of sodium ions through a TTX sensitive channel. In spite of the importance of this current, its magnitude and time course are uncertain because of the limitations of voltage clamp techniques. This study uses steady state currents from voltage clamp pulses to investigate the potential range over which a steady state TTX sensitive current exists. The results of the study indicate that the "window" of TTX sensitive current resides between -60 and -10mV . This current is responsible for a large proportion of the negative slope in the plateau range of potentials and thus may be an important determinant of the AP duration. This method provides a useful means of investigating the effects of pharmacologic agents on the sodium current in cardiac muscle.

+Supported by USPHS Grant 1R01HL2055801 ++Wellcome Trust Fellows +MRC Scholars.

W-AM-E9 THE RELATIONSHIP BETWEEN ACTION POTENTIAL RISE RATE AND SODIUM CONDUCTANCE IN CARDIAC MUSCLE. G.R. Strichartz & I.S. Cohen, Dept. of Physiol., SUNY Stony Brook, N.Y. 11794 (Intr. by R. Hahn).

Experiments are being performed to determine an empirical relationship between the maximum rate of rise of the action potential (\dot{V}_{max}) and the total fast sodium conductance, \bar{g}_{Na} , in rabbit cardiac muscle. Electrophysiological measurements of \dot{V}_{max} in the presence of various concentrations of saxitoxin (STX) and tetrodotoxin (TTX) are compared to direct binding studies of tritiated STX, or to competition studies between TTX and STX, on a homogenate of rabbit heart membranes. The dissociation constants from binding studies at 4°C are 2-4 nM for STX and 15 to 25 nM for TTX. At 37°C the K_D for STX is 20-25 nM, equal to the concentration of STX which reduces \dot{V}_{max} to 70% of control. An explicit relationship between \bar{g}_{Na} , estimated from binding studies, and \dot{V}_{max} will be presented. Supported by USPHS grants NS12828 and HL 20558.

W-AM-E10 4-AMINOPYRIDINE (4-AP) AND CHLORIDE SENSITIVITY OF MEMBRANE CURRENT OF SHEEP CARDIAC PURKINJE FIBERS. J.L. Kenyon* and W.R. Gibbons* (Intr. by L. Horn). Dept. of Physiol. & Biophys. Univ. of Vermont, Burlington, VT 05401.

We studied the effects of the potassium blocker 4-AP on the Purkinje fiber by recording action potentials with conventional methods and using the two microelectrode voltage clamp to obtain membrane currents. 0.5 mM 4-AP slowed the rapid repolarization (phase 1) and shifted the plateau of the action potential to less negative potentials. 4-AP did not affect the resting potential. In the presence of 4-AP, the replacement of the NaCl of the Tyrode's solution with sodium methylsulfate or methanesulfonate further slowed phase 1, even though chloride reduction had no effect on the untreated action potential. 4-AP reduced the early peak of outward current (I_{qr}) during clamp steps positive to -20 mV. 4-AP also reduced the steady outward current at the end of clamp steps positive to -40 mV. The small phasic outward current that remained in 4-AP was reduced by chloride replacement. Thus, there appear to be two components of early outward current: a 4-AP sensitive component that may be a potassium current plus a chloride sensitive component. (USPHS NIH grants HL 14614 and GM 00439)

W-AM-E11 CHARGE MOVEMENTS IN A CUT SKELETAL MUSCLE FIBER. J. Vergara and M. Cahalan, Department of Physiology, U. of Pennsylvania, UCLA, and UCI, Irvine, CA 92717.

We have measured charge movements related to sodium channel gating and to excitation-contraction coupling in a cut frog skeletal muscle fiber preparation using voltage gap voltage clamp techniques. Single fibers were allowed to relax after a potassium contracture, and then the ends were cut in solutions containing either CsF or TEA aspartate + 2 mM EGTA to prevent contraction. Ionic currents were blocked by external TTX, TEA, Rb, SO_4 Ringer. The sodium channel gating currents represent a total of approximately 7.5 nCoul/cm² and are partially immobilized by sodium inactivation (h). The e-c coupling charge movements have approximately a 25 times slower time course, equal on and off areas, and represent approximately 100 nCoul/cm². The charge vs. membrane potential relation is fitted by $Q = Q_{max}/[1 + \exp\{(65 \text{ mV} - V_m)/12\}]$, in good agreement with charge movements recorded in intact fibers by Chandler & Schneider and by Adrian & Almers. The cut fiber preparation presents new possibilities for studying effects of the myoplasmic solution on the charge movements. Supported by the MDA and by USPHS Grant No. NS08951 to Dr. C. M. Armstrong.

W-AM-E12 THE INJURY POTENTIAL OF FROG SARTORIUS MUSCLE.

R. A. Yount*, and S. Ochs. Indianapolis, Indiana 46202.

The depolarization of muscle fibers crushed at one end, the injury potential, is generally considered to follow the spatial distribution described by cable theory. We have confirmed earlier studies on frog sartorius crushed at the pelvic end (Ochs, S. J. Physiol. 182:244, 1966) showing that the injury potential has a longer length constant (λ) of 6 mm, as compared to a λ of 2 mm determined with short current pulses. To test for a loss of K^+ as the basis of depolarization, the internal K^+ activity (a_K^i) was measured with double-barrelled microelectrodes, one tip containing a K^+ ion exchanger to measure a_K^i , the other containing 2M NaCl to measure the membrane potential. We found a normal a_K^i of 98 mM all along the depolarized region. Replacing external Cl^- with the relatively impermeant anions isethionate, benzene sulfonate, or propionate did not greatly change the injury potential. Replacing Na^+ with increasing amounts of sucrose progressively diminished the injury potential. Thus, the injury potential appears to be insensitive to K^+ and Cl^- , with Na^+ entry possibly playing a role in producing the depolarization. Supported by the Muscular Dystrophy Association, Inc.

W-AM-E13 CHARGE MOVEMENT IN FROG SLOW AND TWITCH MUSCLE FIBERS. W.F. Gilly, and C.S. Hui*, Dept. Physiology, Yale Medical School, New Haven, CT 06510.

We have compared charge movement in frog slow and twitch muscle fibers using the 3-microelectrode voltage clamp technique. Pyriformis muscles from *Rana temporaria* were used for slow fibers, sartorius muscles for twitch fibers. 11.8 mM Ca^{++} was usually used to reduce leakage around the electrodes. Movement was blocked by using either Ringer + 2mM tetracaine or D₂O Ringer + 230mM sucrose. In both solutions, charge movement in slow fibers resembled that observed in twitch fibers; the on and off areas were approximately equal and the Q vs. V curve was sigmoid. High Ca^{++} simply shifted the Q-V curve to the right. In tetracaine Ringer, 4-7°C, values of \bar{V} and k in slow fibers were similar to those in twitch fibers (Almers and Best, J. Physiol. 262:583, 1976, and our results). Values of Q_{max} , however, were different, 8 vs. 29 nC/μF in the respective fiber types. In hypertonic D₂O Ringer, 7-10°C, these parameters remained the same, but the kinetics of charge movement were slowed. The charge movement in slow fibers was not totally inactivated by a 30-minute depolarization to voltages as high as 0mV.

W-AM-E14 RECOVERY OF LINEAR CAPACITANCE IN SKELETAL MUSCLE FIBERS. R.F. Rakowski, Dept. Physiol. and Biophysics, Wash. Univ. Sch. Med., St. Louis, MO 63110.

The three microelectrode voltage clamp technique was used to study the recovery of membrane charge in semitendinosus muscles of *Rana pipiens*. The experimental solution contained 40 mM Rb_2SO_4 , 55 mM tetraethylammonium sulfate, 8 mM $CaSO_4$, 350 mM sucrose and 10^{-7} M tetrodotoxin. Using this method membrane current is proportional to ΔV , the voltage difference between two equally spaced intracellular electrodes. The recovery of membrane charge following 1-100 sec duration hyperpolarizing pulses was determined by subtraction of the ΔV transients obtained for two identical voltage steps obtained before and after hyperpolarization. After hyperpolarization additional capacitative current was required. The additional charge was a linear function of membrane voltage. Reprimed membrane charge is simply the result of an increase in the linear effective capacity of the fiber. This observation is not consistent with the hypothesis that reprimed membrane charge is associated with the activation of contraction (Adrian, Chandler and Rakowski, J. Physiol. 254, 361, 1975).

W-AM-E15 SLOW Na AND Ca CURRENTS ACROSS THE MEMBRANE OF FROG SKELETAL MUSCLE FIBRES. P.T. Palade & W. Almers, Dept Physiology & Biophysics, U. of Washington, Seattle, WA.

After soaking 15-36hrs in 80mM K₂AGTA to block contraction, fibres were voltage-clamped (17-24°C) in vaseline gaps at -70 to -100mV with ends cut in 80mM (TEA)₂EGTA. The various external media contained impermeant CH₃SO₃⁻ and 1μM TTX. Having thus eliminated conventional Na⁺, K⁺ and Cl⁻ currents, we could observe two new ionic current species during step depolarization: (1) In isotonic NaCH₃SO₃, inward currents reach a peak of <0.5mA/cm² in 50-500ms and inactivate with time constants of 1-4s. Currents turn outward at -10 to 20mV. Inward (but not outward) currents vanish when TMA⁺ or TEA⁺ replace Na⁺. Ca⁺⁺ blocks; adding 1mM Ca⁺⁺ to isotonic NaCH₃SO₃ reduces inward current at least 5-fold. (2) At 10mM [Ca_o⁺⁺], a new inward current flows even in (TEA)-CH₃SO₃, reaching a peak of 0.1mA/cm² in 0.1 to 1s and partially inactivating within 1-4s. Reversal potential is >50mV. Peak amplitude, now unchanged by replacing TEA with Na⁺, decreases when [Ca_o⁺⁺] is lowered, and is diminished at least 4-fold by D-600 (10μM), nifedipine (1μM), pentobarbital (1mM), lidocaine or procaine (10mM) and Ni⁺⁺ (5mM). Ba⁺⁺, Sr⁺⁺, Mn⁺⁺ and Cd⁺⁺ but not Mg⁺⁺ can substitute for Ca⁺⁺. Supported by AM-17803 and MDAA.

EPITHELIAL TRANSPORT II

W-AM-E16 EFFECTS OF EXTERNAL [Ca²⁺] AND pH ON MUSCLE CHARGE MOVEMENT. H.H. Shlevin, Univ. Rochester, NY 14642.

Charge movement in semitendinosus muscle fibers of R. pipiens was studied using a 3-microelectrode voltage clamp. The 2-state model of Schneider & Chandler (Nature 242:244, 1973) was used to fit the charge movement parameters: Q_{max}=maximum quantity of charge moved; \bar{V} =transition potential; & k=constant determining steepness of the charge vs voltage relationship. Each fiber was its own control. \bar{V} shifted, consistent with surface charge theory, from a mean of -36.5mV at pH 7.15 to -25.8 at pH 5.5 & -42.5 at pH 9. Q_{max} (~34.0nC/μF) & k (~11.1mV) were unchanged over this pH range. But at pH 7.15 both \bar{V} & k changed with increasing [Ca²⁺]_o; Q_{max} was unchanged. Mean \bar{V} changed from -34.9mV in 1.8mM Ca²⁺ to -13.8 in 25 mM Ca²⁺, -19.3 in 50 mM Ca²⁺ & 3.3 in 100mM Ca²⁺. Changes in mean k from 8.3mV in 1.8mM Ca²⁺ to 15.3 in 25mM Ca²⁺, 14.6 in 50mM Ca²⁺ & 20.0 in 100mM Ca²⁺ reflect decreases in the valence of the mobile charged groups & suggest an interaction of Ca_o²⁺ with the groups. Shifts in \bar{V} with pH and [Ca²⁺]_o are consistent with the effects of these agents on the contraction threshold. No difference in Q_{max}, k, or \bar{V} was detected in fibers from cold (~30°) or room temperature (~20°C) adapted frogs at pH 7.15 & in 1.8mM Ca²⁺. Supported by NIH#GM00394 & Univ. Rochester.

W-AM-F1 MEMBRANE PERMEABILITY TO NONELECTROLYTES AS A FUNCTION OF CONCENTRATION: A NEW THEORY. J. S. Chen and M. Walser, Baltimore, Md.

Bulk solute permeability (P) measured as net flux/ΔC may differ from tracer permeability (P*) owing to solute-solute interaction during transport. If the ratio Q=P/P* is independent of concentration (C) and if solvent drag is absent, it can be shown theoretically that P should vary with C as follows: log(P₂/P₁)=(Q-1)log(C₂/C₁). Expressions can also be derived for P, P* and fluxes in the presence of gradients of C. To test this theory, tracer and net fluxes of 3 solutes across toad bladder were measured as C was increased both with and without concentration gradients. For urea, Q was insignificantly different from unity (1.04±0.03). Fluxes corresponded to predicted values as C₁ and/or C₂ were varied. For mannitol and thiourea, Q was < 1 (0.83±0.02 and 0.87±0.02, respectively). P fell progressively (by approximately 50%) as C was increased stepwise from 0.005 mM to 5 mM. While such data do not exclude carrier mechanisms for thiourea and mannitol, they are more consistent with this theoretical formulation based on constant interaction of solute fluxes.

W-AM-F2 MECHANISM OF TRANSEPITHELIAL HYPERPOLARIZATION PRODUCED BY AMPHOTERICIN B IN NECTURUS GALLBLADDER. L. Reuss, Washington University School of Medicine, St. Louis, Missouri 63110.

Membrane potentials and resistances, and paracellular resistance were measured in Necturus gallbladder epithelium before, during, and after exposure of the luminal side to amphotericin B (aB, 5 x 10⁻⁶ M). In standard Ringer's, mean potentials (mV) before and during aB were, respectively: transepithelial 2.4 and 7.5 (mucosa neg.); apical membrane 68.1 and 28.0 (cell neg.); basolateral membrane 70.6 and 35.6 (cell neg.). Membrane resistances fell by 85% (apical) and 60% (basolateral); shunt resistance did not change. Ionic substitutions in the mucosal medium produced changes in potentials and resistances which indicate that aB greatly increases luminal membrane g_K, g_{Na}, and g_{Cl}. Since the fractional increase of g_{Na} is larger than that of g_K, the K permeability of the membrane fell. Paracellular P_{Na}/P_{Cl} did not change. Thus, the main effect of aB is to increase apical g_{Na}, and not to reduce shunt selectivity and "unmask" a rheogenic basolateral Na pump. Supported by NIH Grant AM19580.

W-AM-F3 ANOMALOUS RESPONSE OF POTENTIAL TO STEP CHANGES IN Na^+ CONCENTRATION OF NUTRIENT FLUID OF IN VITRO FROG GASTRIC MUCOSA. W. S. Rehm, S. S. Sanders, J. A. Pirkle, and S. G. Spangler, Dept. of Physiol. and Biophys., Univ. of Alabama in Birmingham, AL 35294

Changes in K^+ or Cl^- of the nutrient fluid (NF) result in PD changes in right direction and $\Delta\text{PD}/10\text{X}$ of 37 mV and 19 mV respectively. In contrast step changes in Na^+ [choline (Ch) or Mg^{++} for Na^+] of NF produced changes in PD in opposite direction to that for Na^+ conductive pathways (a decrease of Na^+ in NF produced decreased positivity of NF) but in right direction for Ch conductive pathways. But the PD vs log Ch not compatible with Ch conductive pathways. Ch from 0 to 50 mM (Na^+ from 102 to 52 mM) results in 1 mV change and Ch from 50 to 102 mM (Na^+ from 52 to 0 mM) a change of 8 mV PD vs log Na^+ is almost linear from 6 to 102 mM ($\Delta\text{PD}/10\text{X} = 6$ mV). Time constant for the ΔPD due to ΔNa^+ is approximately that for diffusion across diffusion barrier. A basis for anomalous Na^+ -PD change is found in carrier coupled-ion transport models in which for one cycle there is a net transport of charge across nutrient membrane in direction in which increase of Na^+ in NF increases positive charge movement to NF. NIH and NSF aid.

W-AM-F6 KINETIC EVIDENCE AGAINST A REDOX PUMP IN THE

FROG GASTRIC MUCOSA. L.J. Mandel and T.G. Riddle*, Dept. Physiol., Duke Univ. Medical Center, Durham, N.C. 27710

Two main sources of energy have been considered for the process of acid secretion: ATP and redox. Evidence to date does not allow a clear selection between these two possibilities. We present herein strong evidence against the redox theory, while the same results are consistent with the ATP theory. With gastric mucosae of *R. catesbiana* bathed in sulfate media, we observed that the rate of acid secretion is linearly related to the short circuit current (I_{sc}). Therefore, it is possible to measure the kinetics of acid secretion through the I_{sc} . The redox state of all cytochromes and the I_{sc} were simultaneously measured during the transition to anoxia. All cytochromes become fully reduced at about the same rate, while the inhibition of I_{sc} displayed an average delay of 2.9 ± 0.8 minutes from the cytochrome reduction rate. This delay is clear evidence that an intermediate step exists between mitochondrial energy conversion (when cytochromes become fully reduced by anoxia all oxygen consumption ceases) and acid secretion, negating the existence of a redox pump directly communicating with the lumen. (Supported by NIH Grant AM-17876)

W-AM-F4 ELECTRICAL EVENTS THAT ACCOMPANY HCl PRODUCTION IN GASTRIC MUCOSA. C. Clausen, J.M. Diamond and T.E. Machen. UCLA Dept. of Physiology, Los Angeles, CA 90024.

We used equivalent circuit methods, described elsewhere, to study electrical events associated with HCl secretion in bullfrog gastric mucosa. Micrographs show that the epithelium is highly folded and that apical membrane area increases greatly during HCl secretion. Our method determines membrane capacitances (proportional to membrane areas) as well as conductances. We find: (1) Although transepithelial resistance (R_T) related to nominal tissue area is low ($\sim 200 \Omega\text{-cm}^2$), R_T normalized to apical capacitance (C_A) as a measure of real membrane area is high ($> 10,000 \Omega\text{-cm}^2$). Hence gastric mucosa is a tight epithelium. (2) R_T decreases during HCl secretion, due mainly to a several-fold increase in C_A . Normalized apical resistance changes minimally. That is, the fall in R_T is due mainly to an increase in membrane area, not to a change in permeability. (3) After histamine stimulation, HCl secretion begins well before C_A increases (~ 10 vs. 30 min.), suggesting an indirect link between HCl secretion and the area changes. (Supported by NIH grants GM 14772 and AM 17328)

W-AM-F7 VOLTAGE SENSITIVITY OF THE INNER BARRIER OF FROG SKIN TO CHANGES OF EXTRACELLULAR K^+ . R.S. Fisher* and S.I. Helman, Urbana, Illinois 61801

Isolated skins of *R. pipiens berlandieri* bathed with Cl-HCO_3 Ringer were studied with microelectrode impalement through their outer barriers. To remove the influence of the outer barrier on the intracellular voltage, 10^{-4} M amiloride was added to the outer solution. With 2.4 mM K inside, the voltage at the inner barrier, V_i , averaged 118.0 ± 4.3 mV (10). When K_i was increased to 4.5 and then to 8.0 and 14.4 mEq/L (in 3 skins from 2 to 8 mEq/L), the decrease of V_i with each step of increasing K concentration was exponential with a mean half time of 2.8 ± 2.5 min (20). The mean $\Delta V_i / \Delta \log K_i$ was 66.8 ± 2.5 mV (20). Treatment of the same skins with ouabain, 10^{-4} M, within 10 to 20 minutes decreased the V_i by 7.8 ± 2.8 mV (6) to a mean of 97.1 ± 5.0 mV (6). As above, the V_i decreased with a mean half time of 2.8 ± 2.2 (11) but the $\Delta V_i / \Delta \log K_i$ averaged 51.6 ± 2.6 mV (10). These data are compatible with the idea that the passive properties of the inner barrier of frog skin can be attributed to a high selectivity for K and that the V_i is influenced by a ouabain-sensitive electrogenic Na pump. (Supported by USPH AM 16663.)

W-AM-F5 CROSSOVER POINTS IN GASTRIC H^+ SECRETION: AN OSMOTIC ARTIFACT George W. Kidder III, Dept. Physiol., U. Md. Sch. Dent., Baltimore, MD 21201

Since acid secretion in frog gastric mucosa is aerobic, many have sought to identify the site(s) of energy coupling between the respiratory chain and H^+ transport by crossover point analysis. Hersey (BBA 344:157, 1974) has reported a crossover between flavoprotein and cytochrome b upon mucosal acidification, which presumably inhibited H^+ secretion. Using a new multiwavelength spectrophotometer to observe four respiratory pigments at once, this phenomenon has been reinvestigated. Adding HCl to bring the mucosal pH to 1.5 results in the changes reported, as does adding an equivalent amount of NaCl. Lowering the pH by substituting H^+ for Na^+ gives no spectroscopic changes. Since flavoprotein absorbs most strongly in its oxidized state (reversed from cytochromes) the observation of Hersey is explained by a decrease in path length due to osmotic tissue shrinkage. (Sup. by NSF PCM 73-06699)

W-AM-F8 AMILORIDE IS A NON-COMPETITIVE INHIBITOR OF NA-TRANSPORT IN ISOLATED BULLFROG SKIN. D.J. Benos and L.J. Mandel, Dept. of Physiology, Duke Univ. Medical Center, Durham, N.C. 27710

The diuretic drug amiloride is a reversible inhibitor of Na transport when applied to the external surface of isolated frog skin epithelium. Net Na-transport (equivalent to short-circuit current, I_{sc}) was measured as a function of $[\text{Na}]$ in the absence and presence of various amiloride concentrations to assess whether or not amiloride is competitive with Na. Alterations in I_{sc} produced by variations in $[\text{Na}]$ can be attributed to effects at the outer membrane, since Na-entry is rate-limiting. We found that log dose response curves of amiloride inhibition of I_{sc} at different $[\text{Na}]$ were indistinguishable, i.e., the fractional inhibition of I_{sc} at any amiloride concentration was independent of $[\text{Na}]$. Kinetic velocity plots (assuming Michaelis-Menten kinetics) were also not consistent with amiloride-Na competitive behavior. Furthermore, Hill inhibitor graphs suggest that one amiloride molecule can inhibit two transport sites. We conclude that amiloride and sodium are non-competitive, i.e., the receptor sites for these two molecules are separate. (Supported by NIH Grants AM-05624 and AM-16024).

W-AM-F9 EFFECT OF ADH UPON FROG SKIN MEMBRANES.

W. Nagel, Dept. Physiol. Univ. Munich, Germany
The effect of ADH (100 mU/ml Arginine-Vasopressin) upon intracellular potential under short circuit conditions (V_{sc}), apical and basolateral membrane resistance (R_o and R_i , respectively) and EMF at outer and inner border (E_o and E_i) were investigated in R. temp. V_{sc} decreased within 60 min after addition of ADH to ~40% of the control value (-79.14 mV). This was the consequence of a decrease of R_o to ~35% and a concomitant increase of R_i to ~160% of the respective control values ($2.6 \pm .3$ and $.7 \pm .1 \text{ K}\Omega\text{cm}^2$). Different from control conditions, R_i exceeded R_o after ADH. Applying a simple electrical equivalent circuit and using Amiloride to reverse the ADH effect, E_i was found to be about -120 mV and -compared to control skins- unchanged by ADH. This suggests that ADH has no direct effect upon the active transport step. E_o was estimated to be in the vicinity of +20 mV (referred to the outside) after ADH. This value is considerably less than feasible values of the Na equilibrium potential of the outer border which points to the possibility that potential dependent changes of g_{Na} and/or significant conductance for other ions except Na are important factors for the electrical gradient across this membrane.
Supported by the Deutsche Forschungsgemeinschaft.

W-AM-F10 EPITHELIAL CELL VOLUME AND ELECTRICAL POTENTIAL PROFILE ACROSS TOAD URINARY BLADDER. V.A. Bobrycki*, J.W. Mills*, A.D.C. MacKnight* and D.R. DiBona, Massachusetts General Hospital, Boston, MA 02114.

Using morphometric analysis of light micrographs from both snap-frozen and glutaraldehyde-fixed tissues, we find that the volume of bladder epithelial cells is not significantly altered when the spontaneous transmural PD is nullified by voltage-clamping. However, clamping at more depolarizing levels (50mV, serosa negative) results in pronounced swelling of the granular cells in tissues where current in the external circuit falls during the 30 min of clamping. These responses are exacerbated by ADH (100mU/ml) and prevented by amiloride (10^{-4}M). We conclude that: 1) the change in cell volume is dependent on increased cell- Na^+ of mucosal origin; 2) cell swelling only occurs when the rate of Na^+ entry to the cells is increased sufficiently by the imposed electrical potential profile; 3) the amplification of swelling by ADH is consistent with a decreased resistance to Na^+ at the apical plasma membrane and 4) the swelling of granular cells, supports their role as the principal participants in active Na^+ transport.

W-AM-F11 THE EFFECT OF THE TRANSEPITHELIAL VOLTAGE (V_T) ON THE E_{Na} OF SODIUM TRANSPORT IN TOAD BLADDER.

M. Canessa, P. Labarca and A. Leaf. Mass. General Hosp. and Harvard Medical School, Boston Mass. 02115.

Simultaneous measurements of the active Na current, J_{Na} , and Na-dependent respiration, J_{CO_2} , were done in toad bladders. Steady state measurements were obtained varying V_T in 10 mV/10 min. steps in the sequence (1) 70-0 and (2) 0-70 mV. At any V_T , a constant stoichiometric ratio of 20 Na^+ / CO_2 was found. Sequence (1) gave values of E_{Na} at $J_{Na}=0$ of 165+9 mV and at $J_{CO_2}=0$ of 156+10 mV; however after clamping V_T in sequence (2). E_{Na} fell to 102+6 mV at $J_{Na}=0$ and 94.4 mV at $J_{CO_2}=0$. E_{Na} was also determined from instantaneous conductance measurements using vasopressin and amiloride to vary J_{Na} ; E_{Na} at $V_T=50$ mV was 160+11 mV and fell to 110+9 mV at $V_T=0$. Since E_{Na} seems to vary inversely with the rate of transport, it can only be measured without drawing current from its battery. The fall in E_{Na} can be accounted for a fall in affinity of its tightly coupled chemical reaction and not by kinetic factors since J_{CO_2}/J_{Na} was constant at any V_T . The implications of these findings for the regulation of Na transport will be discussed. Supported by NIH-HE-0664

W-AM-F12 Cl^- PUMPING, PD, I_{sc} , AND HCO_3^- TRANSPORT IN TURTLE BLADDERS. J.H. Durham*, W.A. Brodsky, and G. Ehrenspeck, G., Mt. Sinai School of Medicine/CUNY, New York 10029

The effect of an induced chloride reabsorption on the I_{sc} , PD, and rate of mucosal acidification (J_{ac}) or alkalinization (J_{alk}) was determined in short-circuited, ouabain-treated turtle bladders (9cm^2) bathed initially in Cl^- -free choline Ringer media with 20mM HCO_3^- and 2% $\text{CO}_2 + 98\% \text{O}_2$ in S (pH 7.67) and with no exogenous HCO_3^- and 100% O_2 in M (pH 7.67). The control levels of PD and I_{sc} were 12mV and 28ua respectively (M positive to S) and that of J_{ac} , 3ua. Then, chloride (25mEq) was substituted for SO_4 in both bathing media or choline Cl^- (25mM) was added to both media without changing SO_4 concentration. After either addition, the PD and I_{sc} more than doubled (the I_{sc} reaching 65-70ua); and a net J_{alk} of 12 ua (max.) was activated. These data can be explained by assuming the activation of an electrogenic Cl^- pump together with a concomitant activation of a $\text{Cl}^-:\text{HCO}_3^-$ exchange process, the magnitude of which is one-fourth that of the concomitant increase in I_{sc} . (Supported in part by the NSF #PCM76-02344 and the NIH #AM 16928).

VISUAL PIGMENTS

W-AM-G1 PHOTOPHYSICS OF RETINALS. D. L. Narva, and R. M. Hochstrasser*, University of Pennsylvania, Department of Chemistry, Philadelphia, Pa. 19104

An understanding of the electronic states and decay pathways in retinal isomers is necessary to understand the photochemistry of 11-cis retinal in the vision process. We have obtained new results on the electronic spectrum of trans-retinal and on the electronic decay processes in trans and 11-cis retinal. We have obtained the first absorption spectrum of a single crystal of trans-retinal. At 2K this spectrum shows two highly polarized bands which may be a result of Davydov splitting. (The possibility of an anomalously intense second electronic state is also considered). We have also measured the wavelength dependence of the triplet yield in solutions and glasses. We find that the triplet yield of trans-retinal is independent of excitation wavelength at 77K but that at 300K the triplet yield increases for lower energy excitation. The triplet yield of 11-cis was found to be independent of excitation wavelength at 77K. We may report on our experiments (in collaboration with L. Halliday and M. Topp) on the fluorescence lifetimes of trans-retinal in a glass.

W-AM-G2 PRIMARY PHOTOCHEMICAL EVENT IN BACTERIORHODOPSIN VIA PICOSECOND SPECTROSCOPY. K. Peters, M. Applebury,* and P. M. Rentzepis, Bell Laboratories, Murray Hill, New Jersey 07974.

The primary photochemical event of bacteriorhodopsin has been identified as a proton transfer to form the K intermediate. The data indicates that the K intermediate is formed in 11 psec at room temperature which increased to 18 psec upon deuteration of the Schiff base proton. The kinetics were found to be virtually temperature independent from 298°K to 1.8°K. The first excited state of bacteriorhodopsin, S₁, has been identified with an absorption maximum at 640 nm.

*Department of Biochemistry, Princeton University, Princeton, New Jersey 08540.

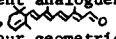
W-AM-G3 TIME-RESOLVED RESONANCE RAMAN STUDIES OF BACTERIORHODOPSIN. J. Turner*, M. A. El-Sayed*, and A. Campion* (Intr. by C. F. Brunk) University of California, Los Angeles, CA 90024

We have developed new simple time-resolved resonance Raman techniques to further characterize the intermediates of bacteriorhodopsin. In the nanosecond time scale, a pulsed N₂ pumped dye laser is used, both as the photolytic flash and the Raman probe pulse. In the microsecond and millisecond time scales, continuous wave lasers are mechanically modulated. An Optical Multichannel Analyzer with a cooled vidicon is used which enables us to obtain excellent signal to noise ratios. The aim of our research is two fold: 1) to determine the time at which the deprotonation and reprotonation of the Schiff base takes place, and 2) to determine the isomeric form of the retinal chromophore in the different intermediates formed during the photosynthetic cycle.

W-AM-G4 EXCITATION AND TEMPERATURE DEPENDENCE OF BACTERIORHODOPSIN EMISSION BAND PROFILES. G. J. Perreault* and A. Lewis (intr. by H. A. Scheraga) Cornell Univ., Ithaca, N.Y. 14853.

Laser excited emission spectra of bacteriorhodopsin have been obtained as a function of temperature and excitation frequency (ν). The spectral profiles show marked ν dependence, particularly at low temperatures. The highest -energy emission band (ca. 15000 cm⁻¹, ca. 670 nm.) is favored by low temperature and large ν . At a given ν , the 20°K and 50°K spectra are nearly superposable after scaling, but at 100°K the intensity at 15000 cm⁻¹ is considerably less. At all three temperatures, as ν decreases, the profiles vary slightly for 17600 > ν > 16800 cm⁻¹, but substantially for 16800 > ν > 16800 cm⁻¹. With similar ν -dependence, the principal emission peak (ca. 13700 cm⁻¹, ca. 725 nm.) shifts ca. 10 nm toward lower energies. The observed trend is opposite to that expected for an artifact due to re-absorption of the emission by batho-bacteriorhodopsin.

W-AM-G5 α -RHODOPSIN AND α -ISORHODOPSIN: VISUAL PIGMENTS FORMED FROM 4,5-DEHYDRORETINAL. A. Kropf and M. Sweeney Dept. of Chem., Amherst College, Amherst, MA. 01002

In order to determine the effects of a change in chromophore structure on the spectral and kinetic properties of visual pigments, we have prepared pigment analogues of rhodopsin and isorhodopsin from α -retinal, . After synthesis from α -retinyl acetate, four geometric isomers of α -retinal were purified by liquid chromatography. Contrary to an earlier report, we found that two of the *cis* isomers did combine with cattle opsin to form pigments analogous to rhodopsin and isorhodopsin. The rates of combination of the putative 11-*cis* and 9-*cis* isomers with cattle opsin in digitonin are about 1/5 the values obtained with the 11-*cis* and 9-*cis* isomers of retinal. The pigments formed have λ_{max} at 468 nm (α -rhodopsin) and 462 nm (α -isorhodopsin) and photo-bleached to the all *trans* aldehyde and opsin. Each pigment exhibits a C.D. spectrum. α -Rhodopsin has a positive C.D. peak, maximum at 463 nm, and α -isorhodopsin has its maximum at 452 nm. Each pigment has only a small C.D. absorption peak in the near UV. The binding of chromophore to protein will be discussed in light of these and other data.

W-AM-G6 THE MOLECULAR MECHANISM OF VISUAL EXCITATION A. Lewis, M. Sulkes* & M. Marcus, Cornell U., Ithaca, N. Y. 14853.

Resonance Raman spectra of squid rhodopsin have been obtained at a variety of temperature and illumination conditions. The data together with similar results on bovine rhodopsin and model system studies support a structure for bathorhodopsin proposed by Lewis*. This structure can be generated by simultaneous rotation of carbon atoms 10 and 11 out-of-plane and may be termed a di-*cisoid* configuration. It bears no resemblance to an all *trans* conformation although it can relax readily to such a configuration and can be generated by a similar motion from either rhodopsin or isorhodopsin. These results suggest that the 11-*cis*, to all *trans* isomerization is not a primary mechanism of excitation. The data support an excitation mechanism in which charge redistribution in the vertically excited state of the chromophore induces a proton translocation in the protein which is stabilized by structural alterations in the chromophore. It is interesting that such a mechanism which can explain the picosecond and photochemical data can also be restated in the terminology of allosteric mechanisms.

¹A. Lewis, PNAS (in press) Dec. 77/Jan. 78.

W-AM-G7 FURTHER EVIDENCE OF CIS-TRANS ISOMERIZATION AS THE PRIMARY PHOTOEVENT IN RHODOPSIN. B. Aton* and R.H. Callender, Physics Dept., City College, CUNY, N.Y., 10031.

Recently a number of alternative models for the primary event in vision, namely the rhodopsin to bathorhodopsin transition, have been proposed which do not involve *cis-trans* isomerization. In order to account for rhodopsin (11-*cis* chromophore), bathorhodopsin, isorhodopsin (9-*cis*) interconversion at 77°K, it was necessary to suggest that bathorhodopsin is formed photochemically from rhodopsin without isomerization followed by subsequent thermal isomerization and equilibration of 11-*cis* and 9-*cis* isomers. Here we use resonance Raman measurements to show that isorhodopsin is formed from rhodopsin at sample temperatures near liquid helium. This precludes any thermal isomerization in the ground state thus proving that *cis-trans* isomerization must occur photochemically as the primary event in vision.

W-AM-G8 KINETIC RESONANCE RAMAN STUDIES OF THE PHOTOCYCLE OF BACTERIORHODOPSIN. B. Ehrenberg and A. Lewis, Cornell Univ., Ithaca, N.Y. 14853.

The kinetic resonance Raman techniques of Marcus and Lewis¹ were employed to study the photocycle of bacteriorhodopsin. A suspension of purple membrane fragments in H₂O or D₂O was flowed through a laser beam which triggers the photoreaction and excites the Raman spectrum. To monitor the kinetics, the rate of flow and thus the average time a molecule stays within the illuminated area was adjusted. When suspended in D₂O, exchangeable protons including the one on the Schiff-base link between the retinal and the opsin are replaced by D⁺ and the rate of formation and decay of some intermediates is slowed down. This allows for better monitoring of these intermediates. There is evidence for the existence of another intermediate in the cycle following the batho product and the Schiff-base link in this new product is already unprotonated. The pH of water suspensions affects strongly the rate of deprotonation of the Schiff-base and the formation of the M⁴¹² species. This indicates the important role of the protein in modulating the changes that occur in the chromophore-protein complex during the cycle.

1. M.A. Marcus and A. Lewis, *Science* **195**, 1328 (1977).

W-AM-G9 METARHODOPSIN POTENTIAL OF DROSOPHILA: CORNEAL-POSITIVE COMPONENT DUE TO SECOND-ORDER NEURONS. R. S. Stephenson* and W. L. Pak, Purdue, W. Lafayette IN

The Drosophila ERG in response to a strobe flash shows an early biphasic potential, attributed to photostimulation of metarhodopsin and consisting of a small corneal-negative component, termed M1, followed by a predominant corneal-positive M2. It has been previously reported that M1 resembles the classical ERP whereas M2 does not: M2 disappears during anaesthesia, anoxia, or cooling to 7°C; M2 inverts deeper in the eye than M1; and only M1 has been seen intracellularly in photoreceptors. We suggest that M2 arises from second-order neurons in the lamina as a postsynaptic response to the M1 potential in the photoreceptors and we adduce the following additional evidence to support this. M2 is reduced or absent in visual mutants defective in the on-transient, which arises from laminar neurons. M2 and the on-transient invert at the same depth, and when isolated from the receptor component by recording differentially across the lamina they have similar heights at saturation. Both M2 and the on-transient are reduced under conditions which depolarize the photoreceptors, although M1 is undiminished. Thus M2 is not always a reliable metarhodopsin assay. It is a neural response triggered by a photoproduct potential.

W-AM-G10 RESONANCE RAMAN STUDIES OF BOVINE METARHODOPSINS I AND II. A.G. Doukas*, B. Aton*, R.H. Callender, and T.G. Ebrey, Physics Dept., City College of CUNY, N.Y. 10031 and Dept. of Physiology and Biophysics, U. of Ill., Urbana, 61801.

The resonance Raman spectra of bovine metarhodopsin I and II have been measured and compared to model chromophore resonance Raman data. It was found that meta I is linked to opsin via a protonated Schiff base linkage whereas meta II is linked by an unprotonated Schiff base. The suggestion of Cooper and Converse that the chromophore of meta II is retinal is explicitly disproved. The chromophores of both metarhodopsins are found to have an essentially all-trans conformation. The basic mechanism for color regulation in both forms appears to be electron delocalization. The data support the model of cis-trans isomerization as the primary mechanism for vision. Also, the conclusions and inferences of this work on energy uses and storage by rhodopsin in neural generation will be discussed.

W-AM-G11 ORIENTATION OF α -HELICAL SEGMENTS IN FROG RHODOPSIN STUDIED BY INFRA-RED LINEAR DICHROISM. H.Saibil*, M.Michel-Villaz*, and M.Chabre, Biophysique Mol. et Cell. DRF, CEN Grenoble F 38041 and (H.S.) Biophysics Depart, King's College London. WC 2B 5RL

Dark adapted frog rods, suspended in D₂O Ringer, were oriented by a magnetic field, and allowed to sediment onto a CaF₂ window. The 50 μ thick IR cell was then sealed. The oriented rods were set perpendicularly to the IR spectrometer beam, and absorption was measured with polarizers parallel and perpendicular to the rod axis. Dichroism of the peptide C=O (around 1650cm⁻¹) and N-H (around 1550cm⁻¹) vibrations were observed, as well as the dichroism of the ester carbonyl bond of the membrane phospholipids around 1730cm⁻¹. The band at 1450cm⁻¹ corresponding to exchanged N-D amide had less if any dichroism, indicating that those peptides which exchange fast are less oriented than the unexchangeable peptides. About 50% of the rhodopsin polypeptides are known to be in the α -helical conformation where the C=O and N-H bonds are nearly parallel to the helix axis. Our results indicate that in the rod disc membrane the α -helical segments of rhodopsin are preferentially oriented perpendicular to the disc membrane (supported by CNRS (ER 199) and DGRST).

W-AM-G12 METARHODOPSIN II₃₈₀ DOES NOT CONTROL RAPID DARK ADAPTATION IN VERTEBRATE PHOTORECEPTORS. Peter J. Stein* and Sanford E. Ostroy, Department of Biological Sciences, Purdue Univ., Lafayette, IN 47907.

We have studied the relationship between one of the photoproducts of vertebrate rhodopsin, Meta II₃₈₀, and rapid dark adaptation of the vertebrate photoreceptor. The time of return of rod sensitivity was measured at two different temperatures using intracellular recording in the isolated toad retina. We also measured the kinetics of the decay of Meta II₃₈₀ over the same temperature range, and at two bleaching intensities. It was found that the complete return of rod sensitivity occurred when only a small percentage of the Meta II₃₈₀ had decayed. For Meta II₃₈₀ decay to control dark adaptation, its rate constant would have to be increased by a factor of 32. It was also observed that the time of return of rod sensitivity was not altered over our temperature range, while the thermal decay of Meta II₃₈₀ exhibited a Q₁₀ of 2.2. Therefore, we conclude that Meta II₃₈₀ does not control rapid dark adaptation in vertebrate photoreceptors. A further implication of these findings is that the protein conformation, Meta II₃₈₀, cannot be responsible for the transduction process. (Supported by USPHS Grant Nos. EY413 and EY7008.)